
# Solar Eruptions

Nat Gopalswamy
NASA Goddard Space Flight Center
Greenbelt MD 20771 USA
nat.gopalswamy@nasa.gov
http://cdaw.gsfc.nasa.gov

SCOSTEP/ISWI International School on Space Science, Lima, Peru 15-25 September 2014

# The Sun-Earth System

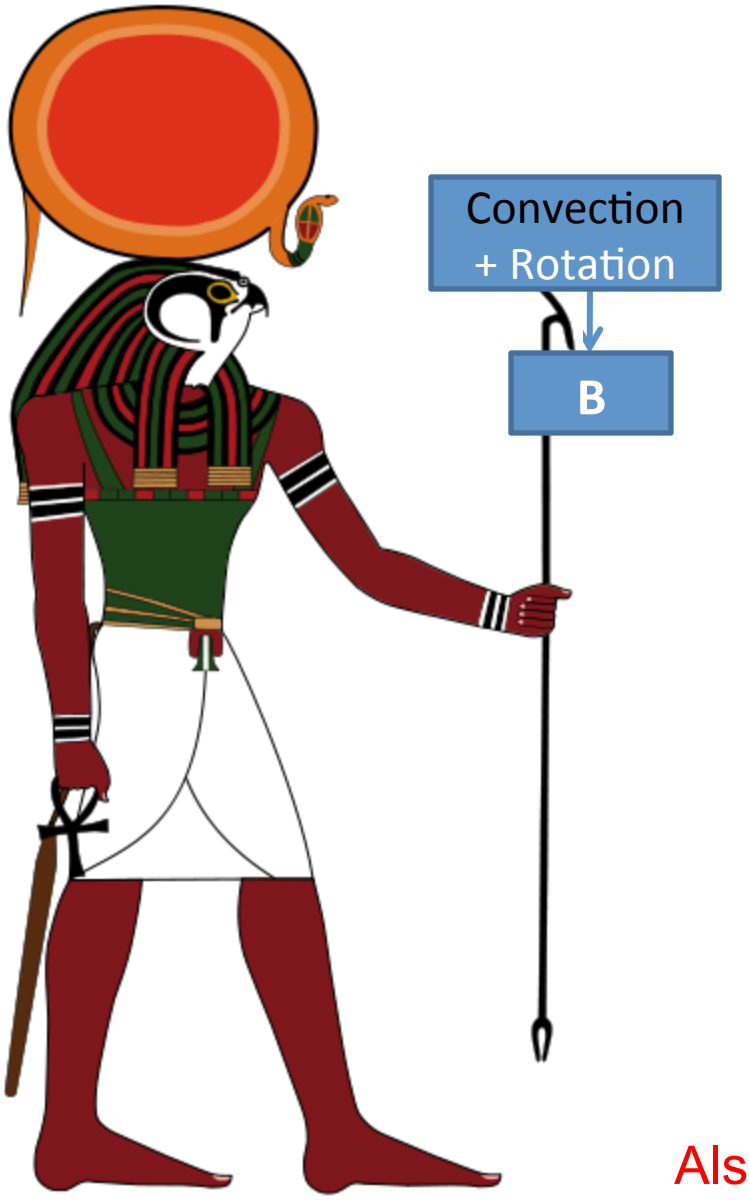


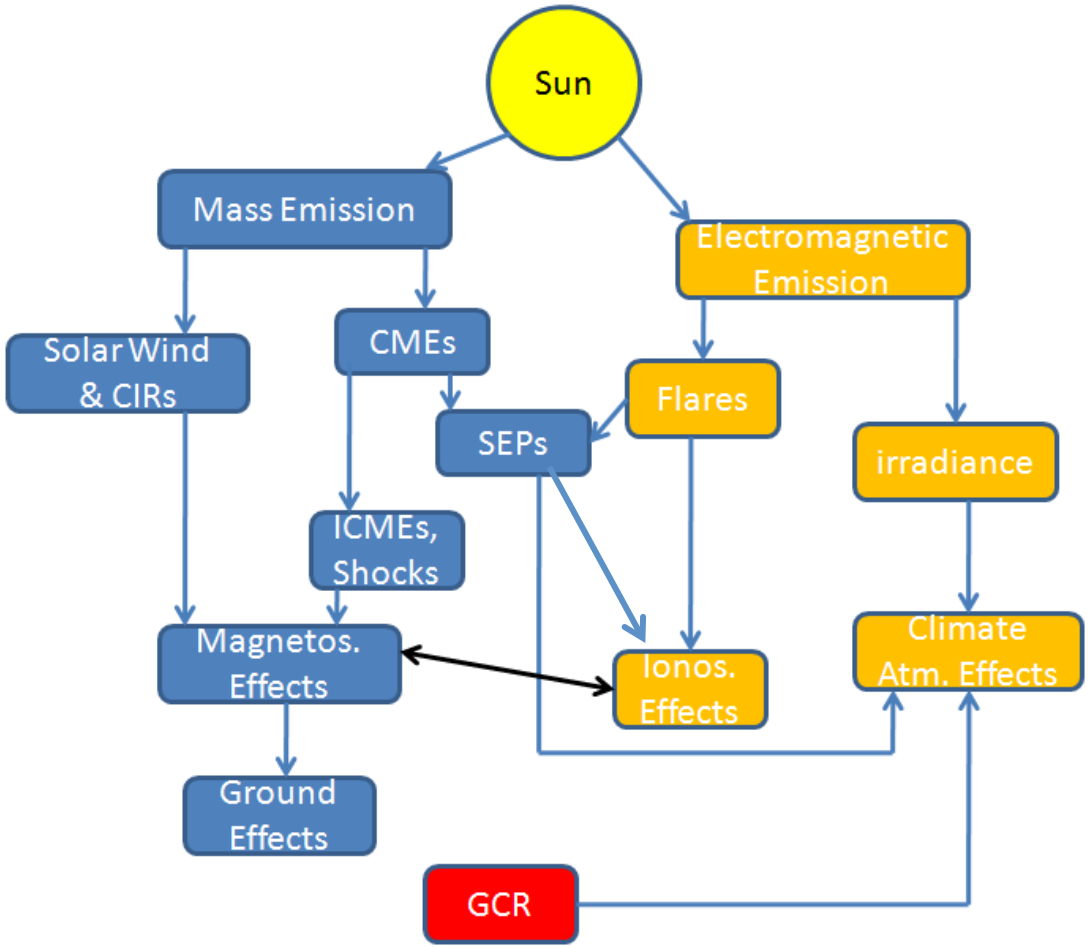


Also Earth to space coupling

# Sun is the Source of Food and Fuel

Cattle help produce food or can be food themselves; but they do graze grass as food.

courtesy: Wikipedia

Angus Red and Black Cattle

# Rice, banana, coconut, vegetables…

Ciloto area in West Java

# The “Dark Side” of the Sun

SOHO image in white light

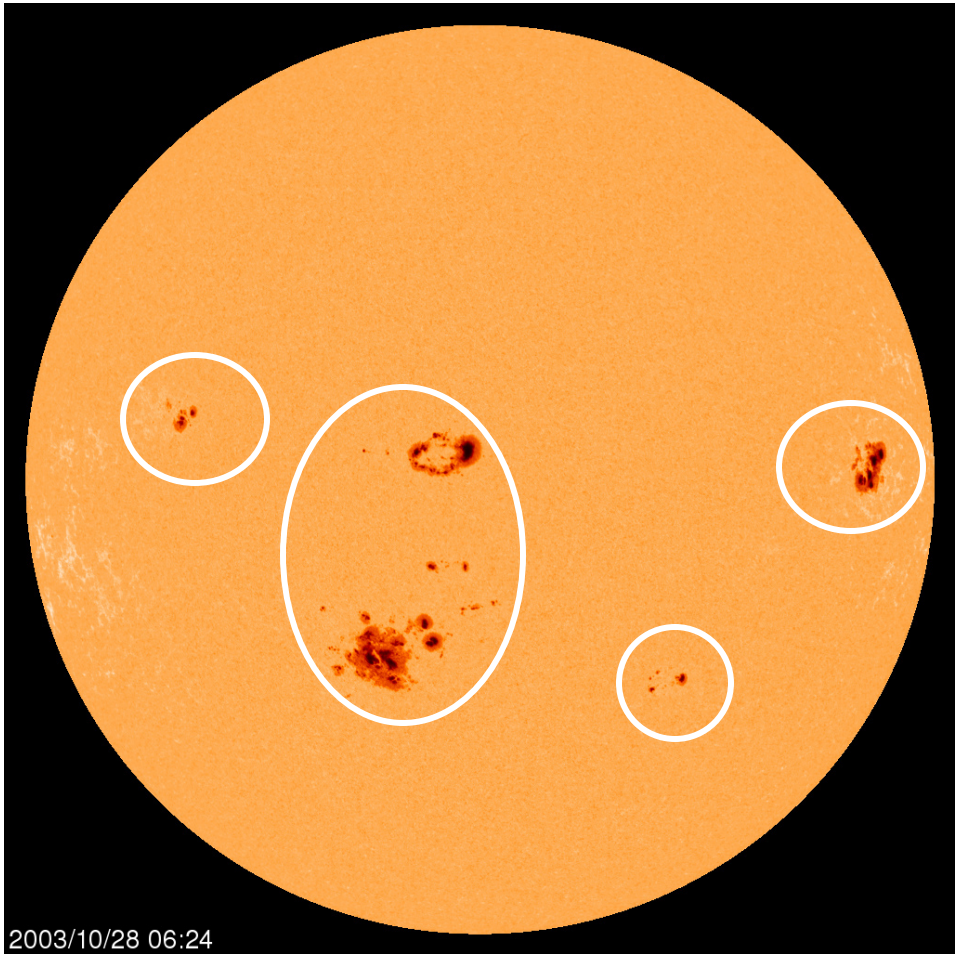


SOHO image in EUV

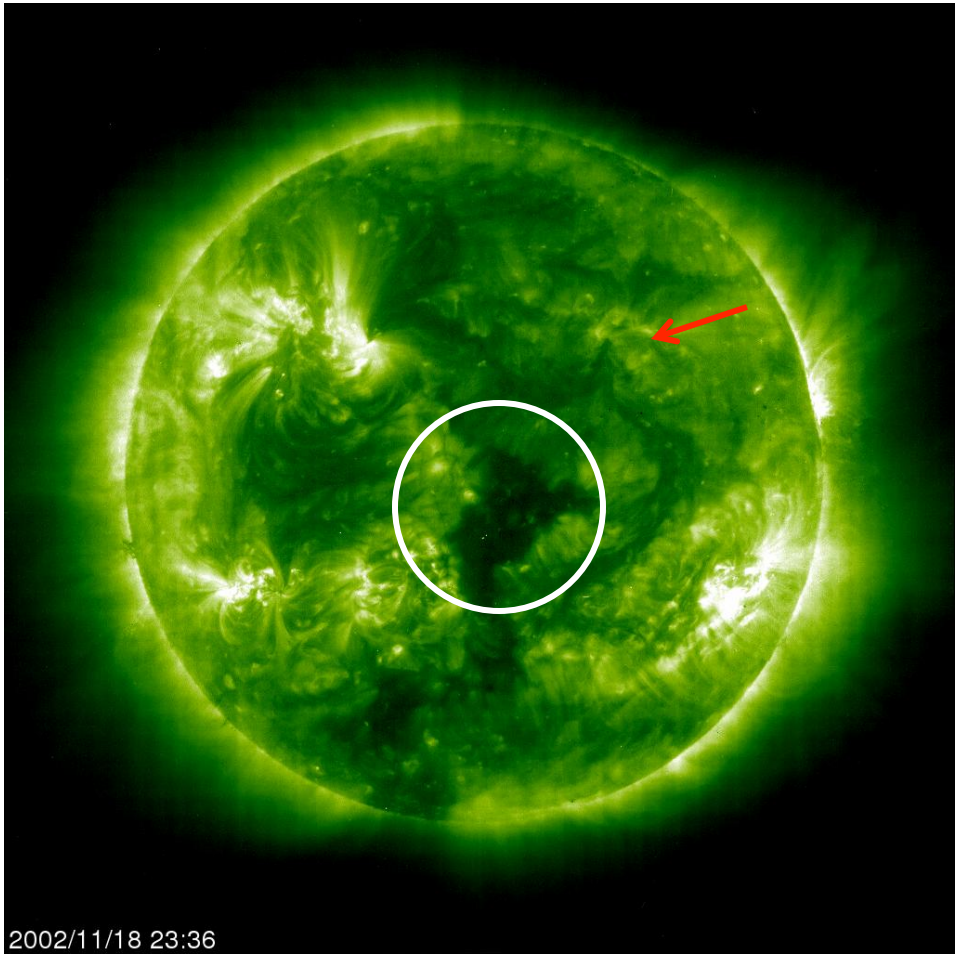


Sunspots

Coronal Hole

Filament

# Two different Magnetic Topologies

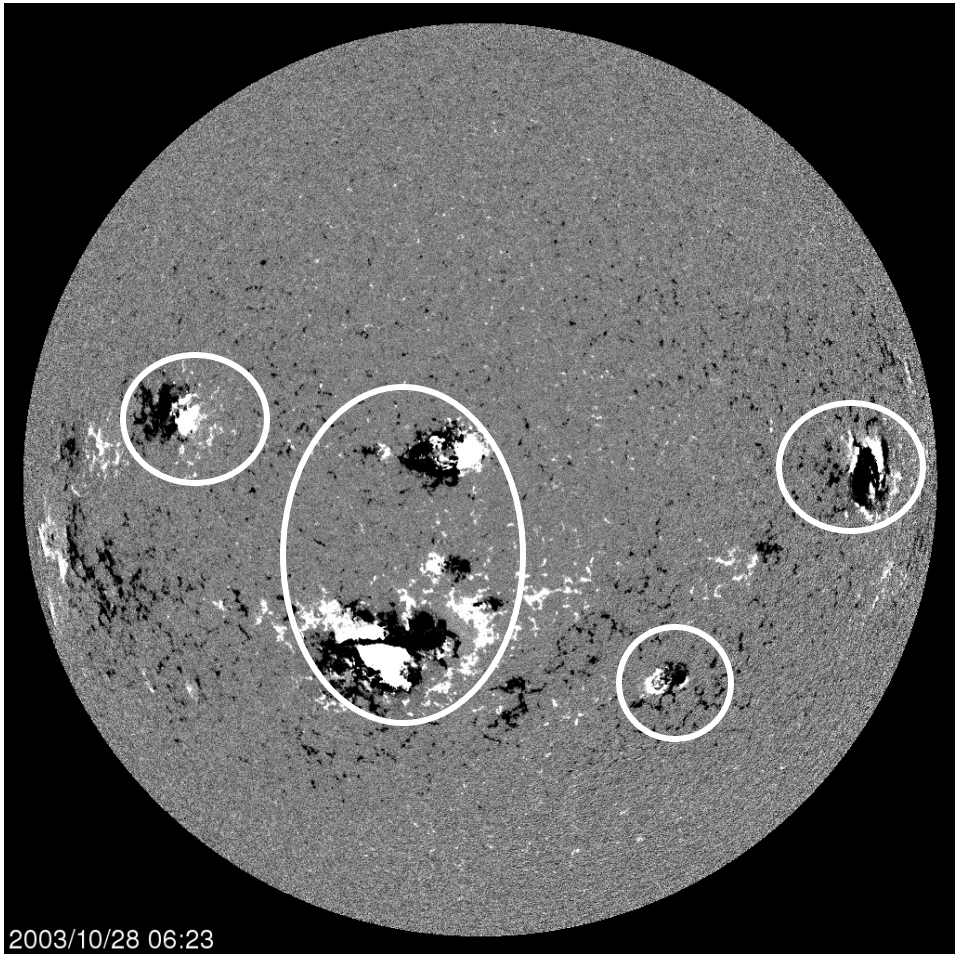


Closed and Open

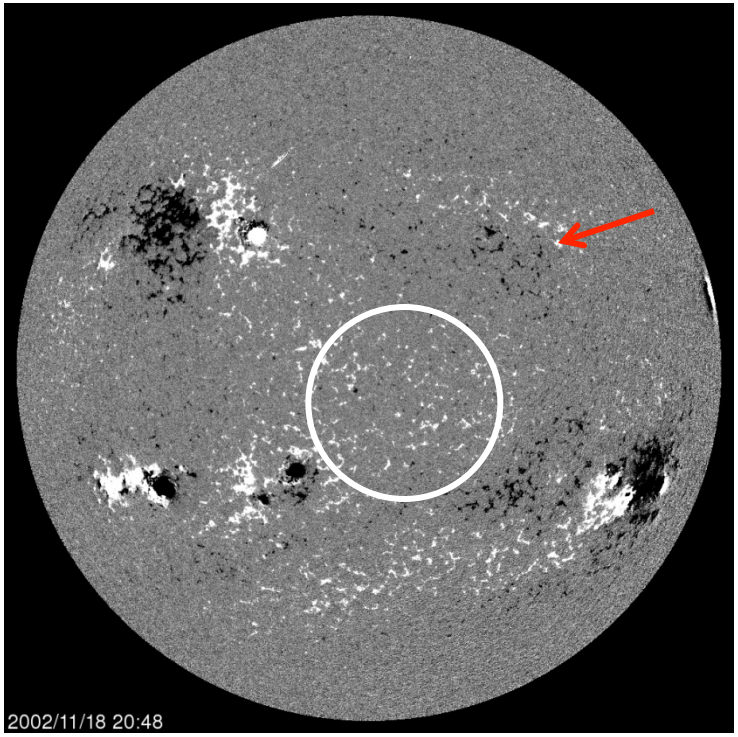


Active Region, Filament Region, and Coronal Hole

# Associated Phenomena

- Flares
- CMEs
- Prominence/Filament Eruptions
- Shocks – CMEs
- microwave bursts, hard X-rays, gamma rays
- Metric & IP Radio bursts Type III Type2
- Solar Energetic particle and GLE events
- Interplanetary CMEs and shocks
- Energetic Storm Particle Events
- Storm sudden commencement
- Geomagnetic storms
- Forbush decrease

# Wavelengths Employed

- Optical: White light, H-alpha images
- EUV images
- Infrared: He 10830 Å images
- Microwaves (mm, cm) images , light curves
- Hard X-rays images, spectra
- Soft X-rays: images
- Gamma rays
- Decimeter to km radio waves: images, spectra

Thermal & nonthermal phenomena
Ground and space-based observations

# Solar Eruptions represent…

- Flares (enhanced electromagnetic emission)
- mass motion (CMEs)
- Both are accompanied by particle acceleration
- electrons: radio emission, X-ray emission
- protons: gamma rays, neutrons (sunward)
- Solar Energetic Particles: detected in situ
- Acceleration mechanisms: reconnection (flares) & shock (CMEs)
- type III, type IV, type V: electrons from reconnection
- Type II bursts: electrons from shock acceleration
- radio bursts: diagnostic for the medium & agent

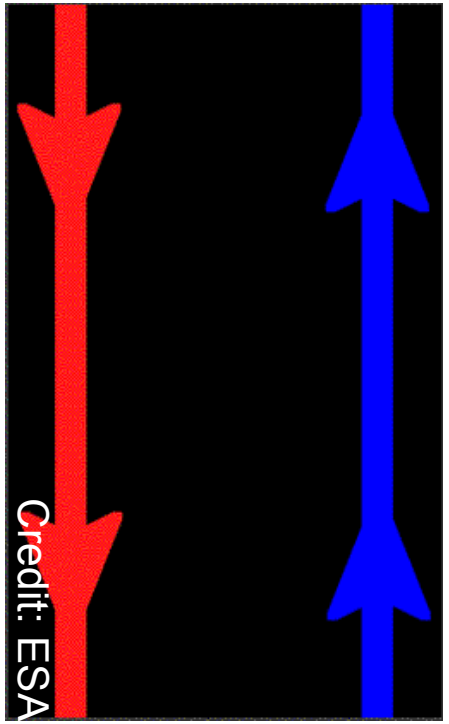

# Range of Phenomena: 2005 May 13 CME

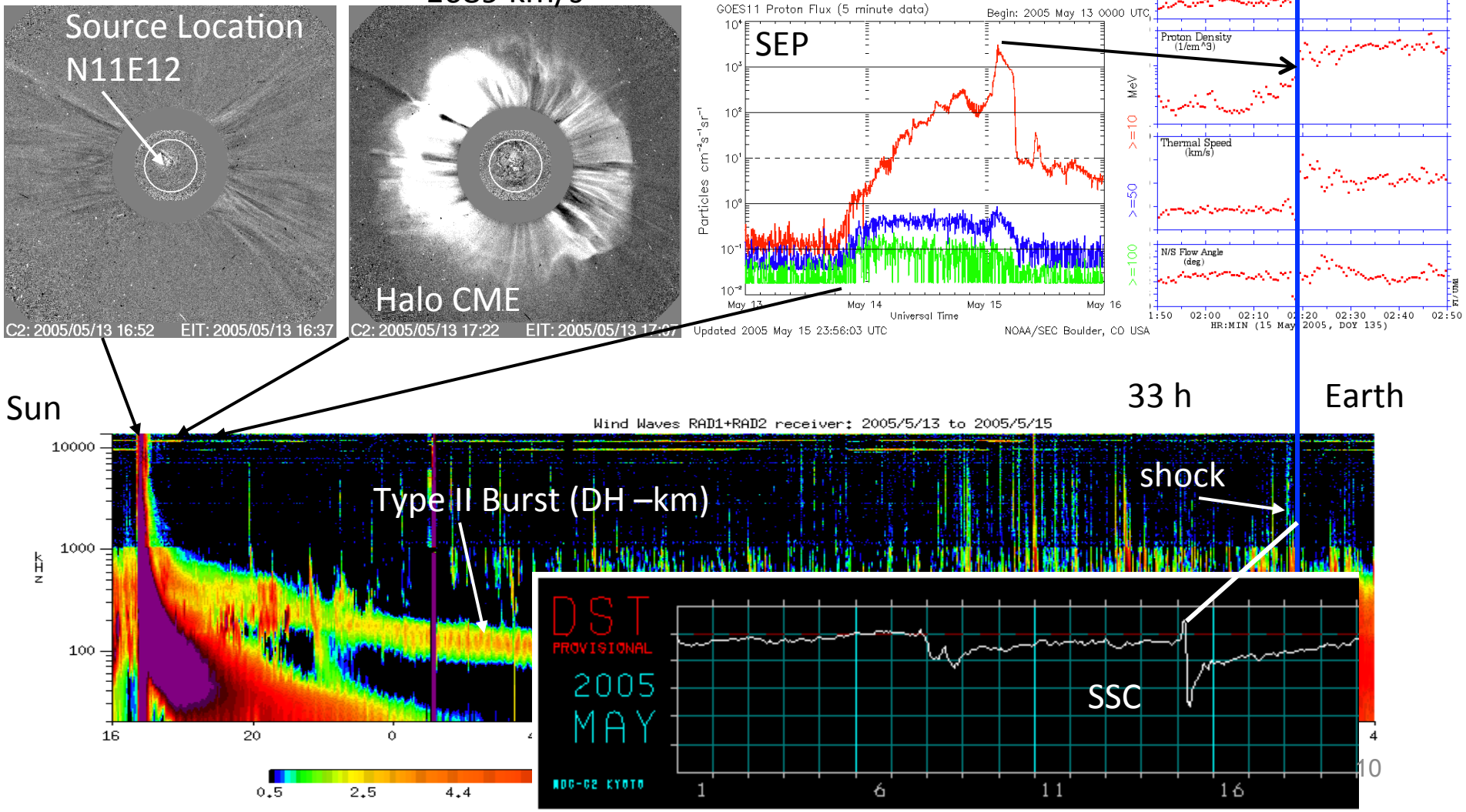

# Discovery of the Solar Flare

- September 1, 1859
- Independently observed by R. C. Carrington and R. Hodgson
- Magnetic storm on September 2

Drawing by Carrington

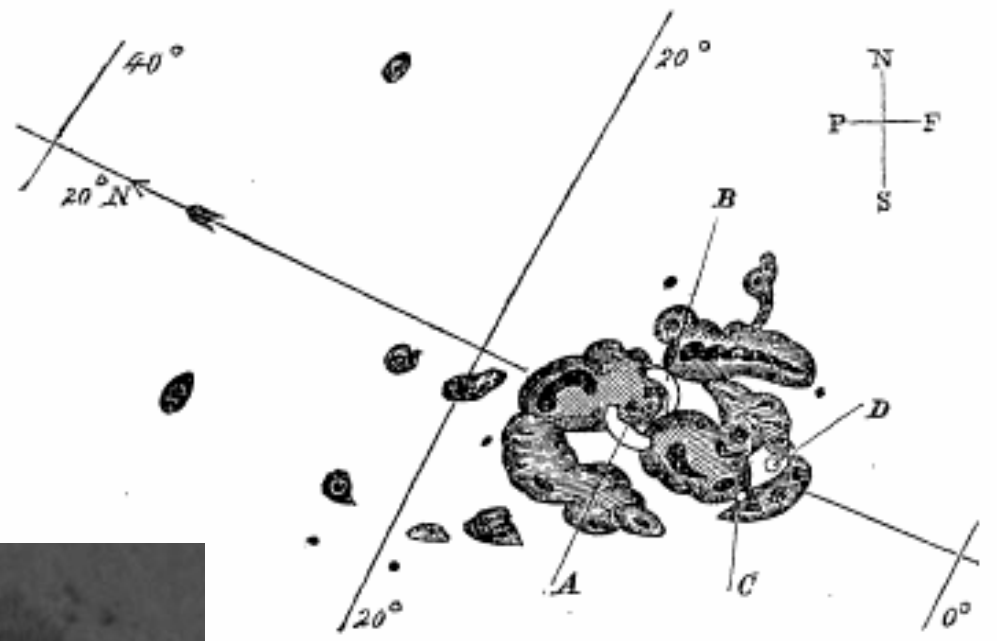


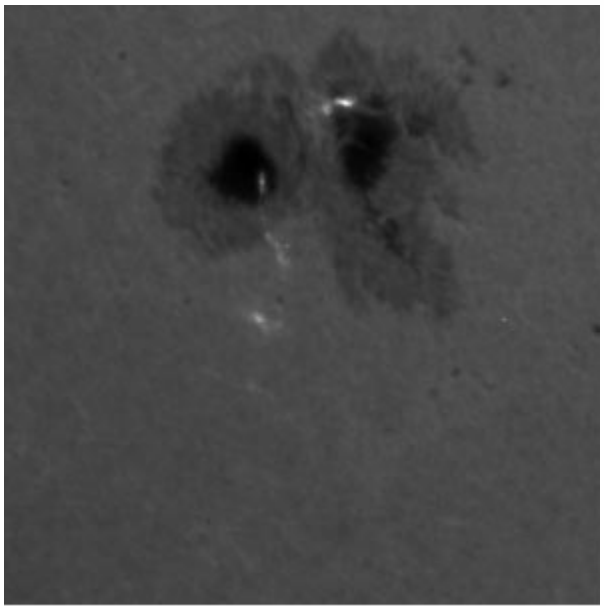

A modern white-light flare

2001 August 25

Metcalf et al. 2003

# Solar Eruption and Space Weather

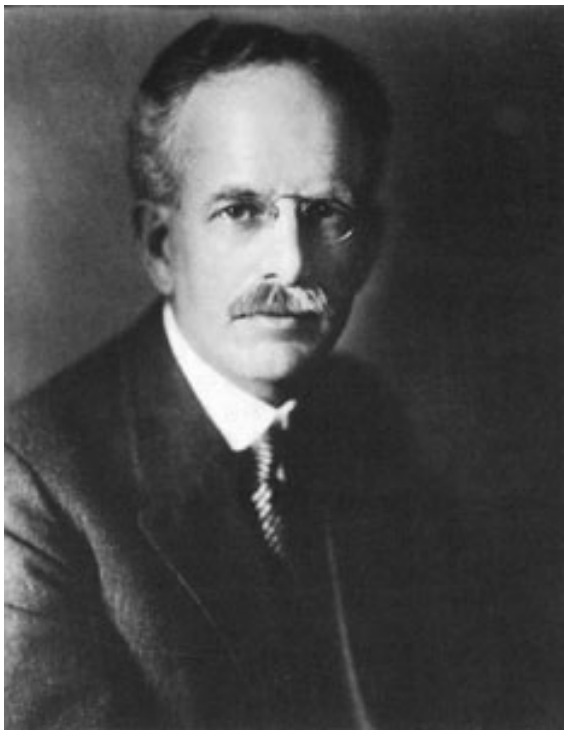

G E Hale 1868 - 1938

- Brought flares to central position via his paper in 1931:

"The spectrohelioscope and its work, Part II: Solar eruptions and their apparent terrestrial effects"

Astrophys. J. 73, 379, 1931

Big Bear Solar Observatory: 7 August 1972 Flare observed in H-alpha

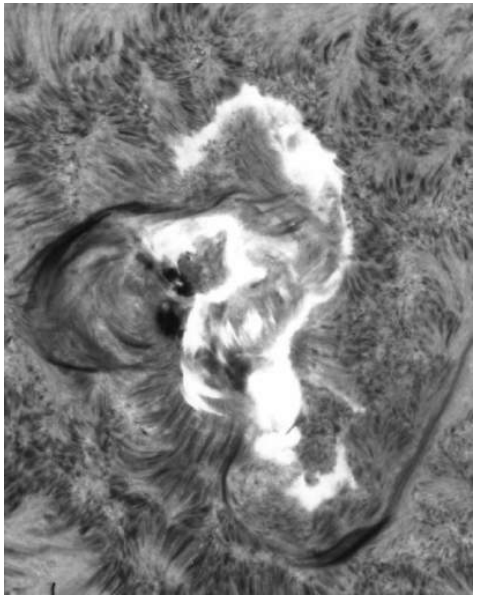

1943 Newton studied flare – geomagnetic storm connection
-estimated the angular extent of the plasma stream
to be ~90 deg (similar to modern interplanetary CME)

# H-alpha flares

- Temporary emission within dark Fraunhofer line
- In spectroheliograms, flares appear as brightening of parts of the solar disk
- Area > $10^9$ $km^2$ for large flares
- Area < $3x10^8$ $km^2$ for subflares
- H-alpha flare area has been used as the basis for optical flare importance
- Area at flare peak measured as number of square degrees (1 heliographic degree = $2\pi R/360$ = 12500 km with R = solar radius = 696000 km)
- Also measured as millionths of hemisphere (msh): $10^{-6}$ $2\pi R^2$ or ~$3x10^6$ $km^2$
- A scale of 0-4 is used with additional suffix for brightness (faint F, normal N, brilliant B)
- 4B is the highest importance; SF is the lowest

The two bright outer edges are known as H-alpha flare ribbons

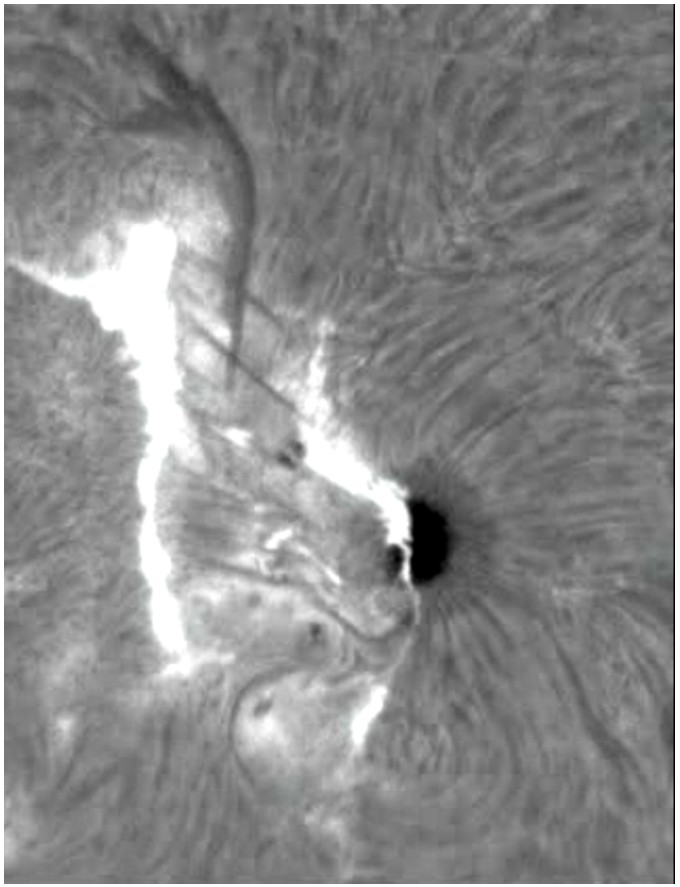

Dark loops connect the ribbons. The whole structure is referred to as flare arcade

# H-alpha Flares

| Flare Area msh (Square degree) | Faint | Normal | Brilliant |
|---|---|---|---|
| <100 (2.06) | SF | SN | SB |
| 100-250 (2.06-5.15) | 1F | 1N | 1B |
| 250-600 (5.15-12.4) | 2F | 2N | 2B |
| 600-1200 (12.4-24.7) | 3F | 3N | 3B |
| >1200 (>24.7) | 4F | 4N | 4B |

msh = millionths of solar hemisphere
Double Scale: 1-4 Area
1-3 Brightness (FNB)

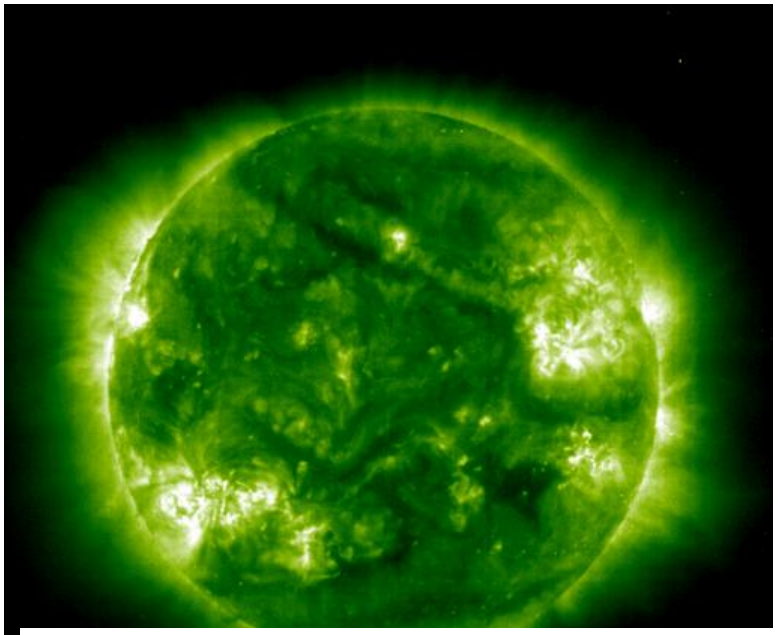

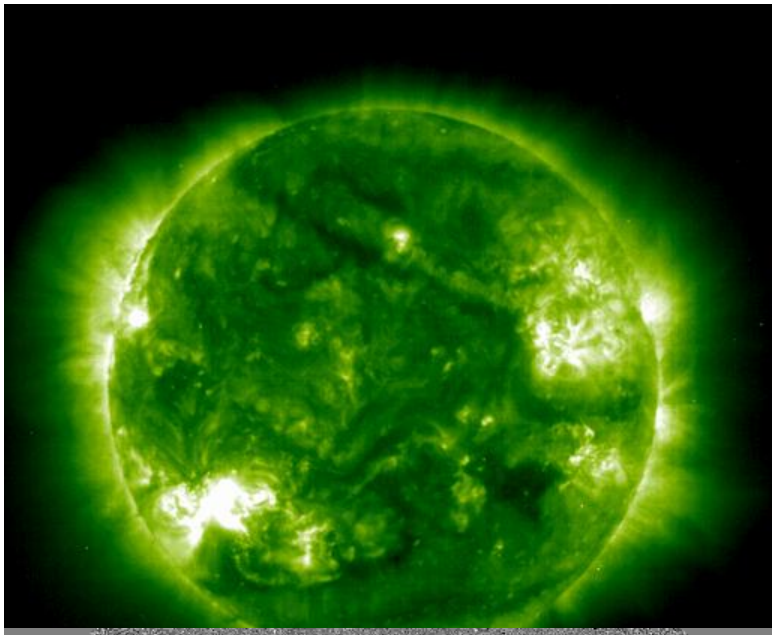

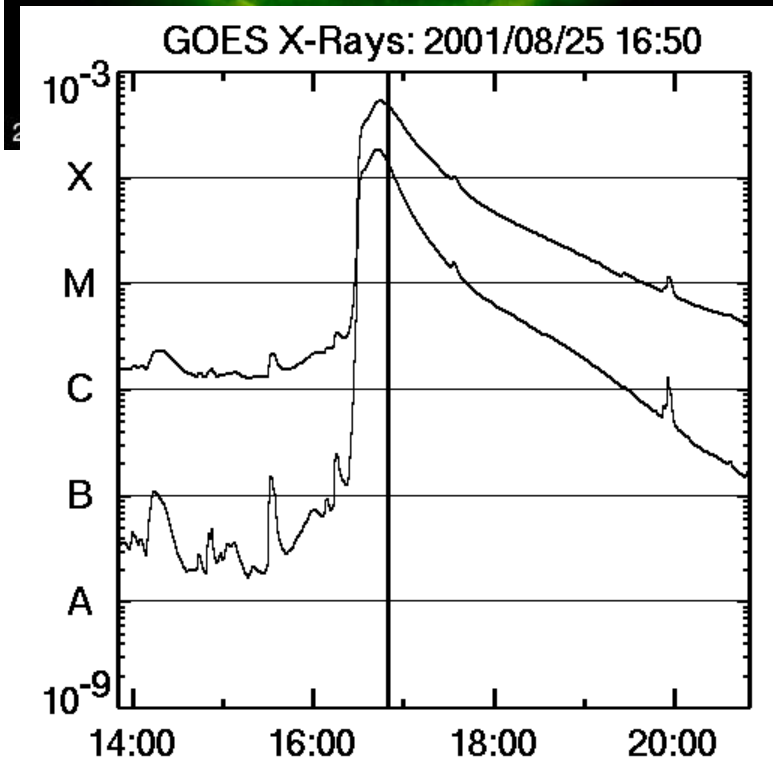
GOES X-Rays: 2001/08/25 16:50
10^-3
X
M
C
B
A
10^-9
14:00
16:00
18:00
20:00

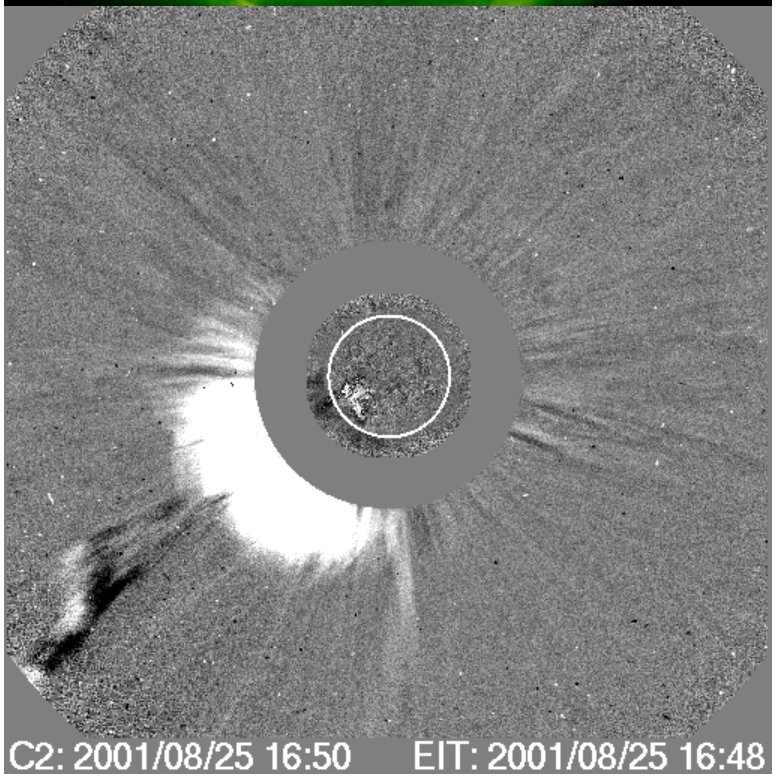
C2: 2001/08/25 16:50
EIT: 2001/08/25 16:48

# Soft X-rays

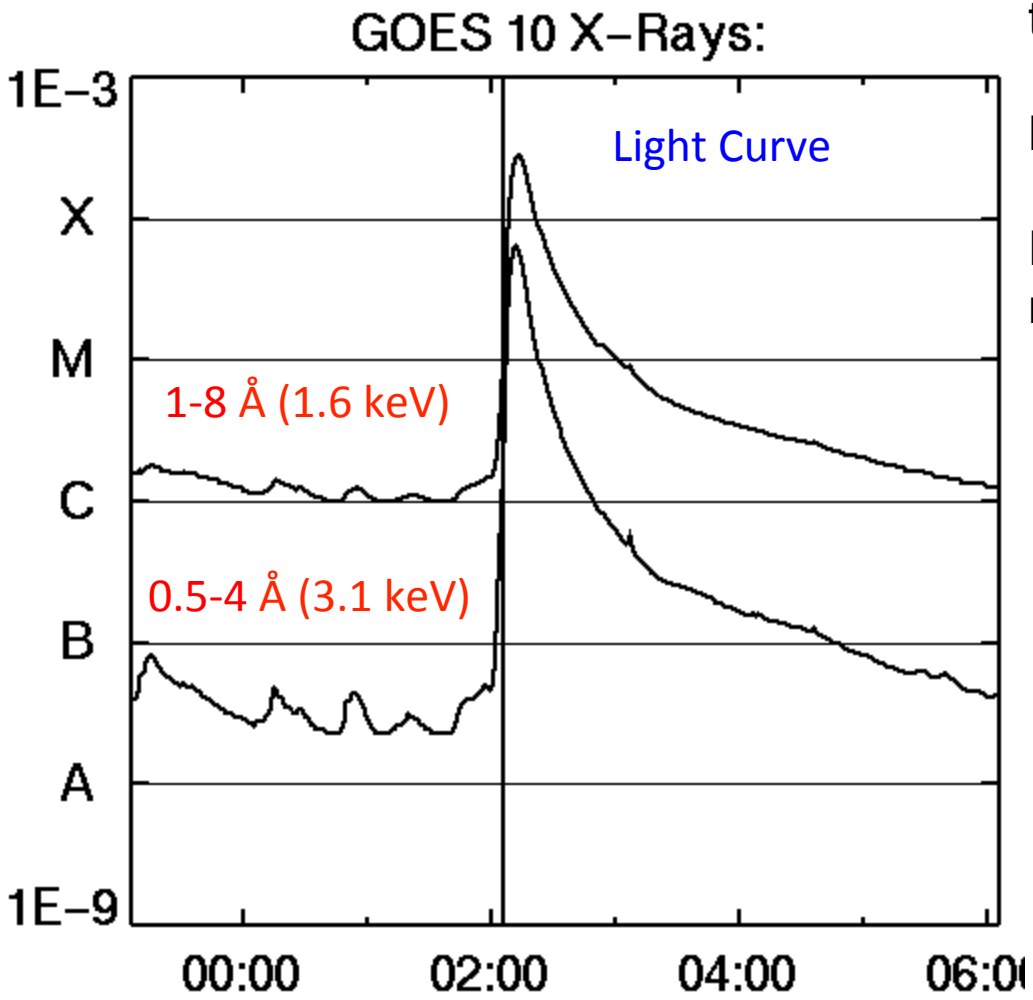


1 Å = $10^{-8}$ cm = $10^{-10}$ m = 0.1 nm

Global photon output in the 1-8 Å band
Originally C, M, X used to indicate the flare size (e.g., X2.5 = 2.5x$10^{-3}$ $wm^{-2}$)

B, A added later to denote weaker flares

Flares larger than X10 - simply state the multiplier, e.g. X28

| Importance class | Peak flux in 1-8 Å $W/m^2$ |
|---|---|
| A | $10^{-8}$ to $10^{-7}$ |
| B | $10^{-7}$ to $10^{-6}$ |
| C | $10^{-6}$ to $10^{-5}$ |
| M | $10^{-5}$ to $10^{-4}$ |
| X | >$10^{-4}$ |

# A Large Flare & its Image

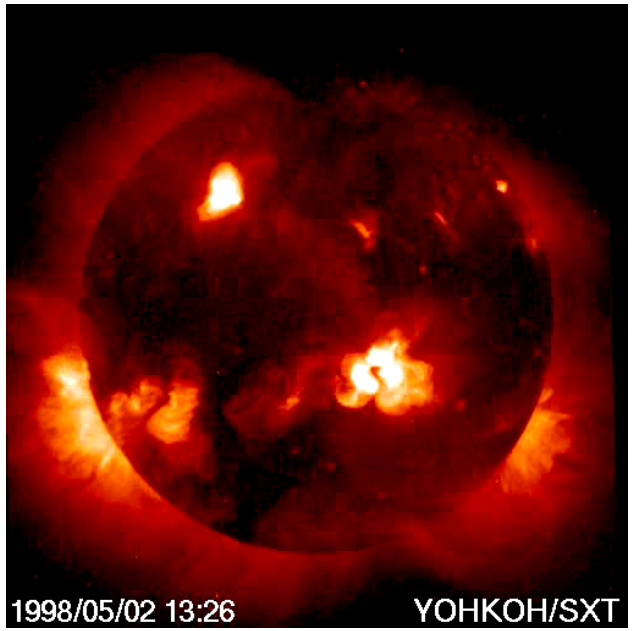


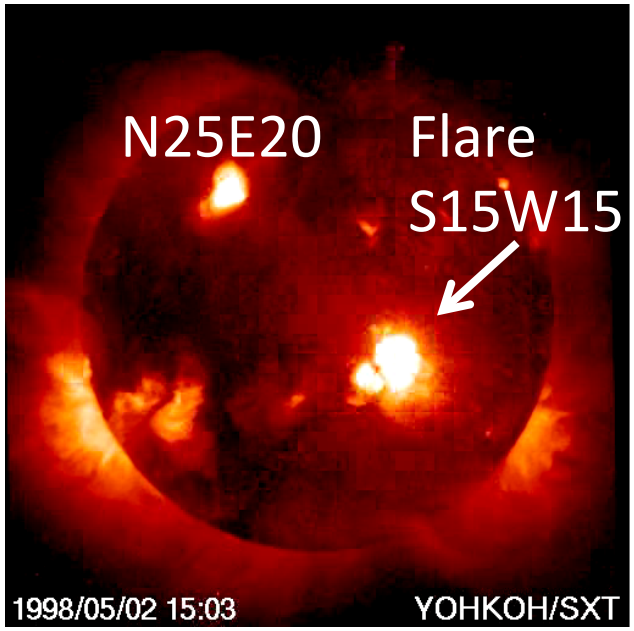


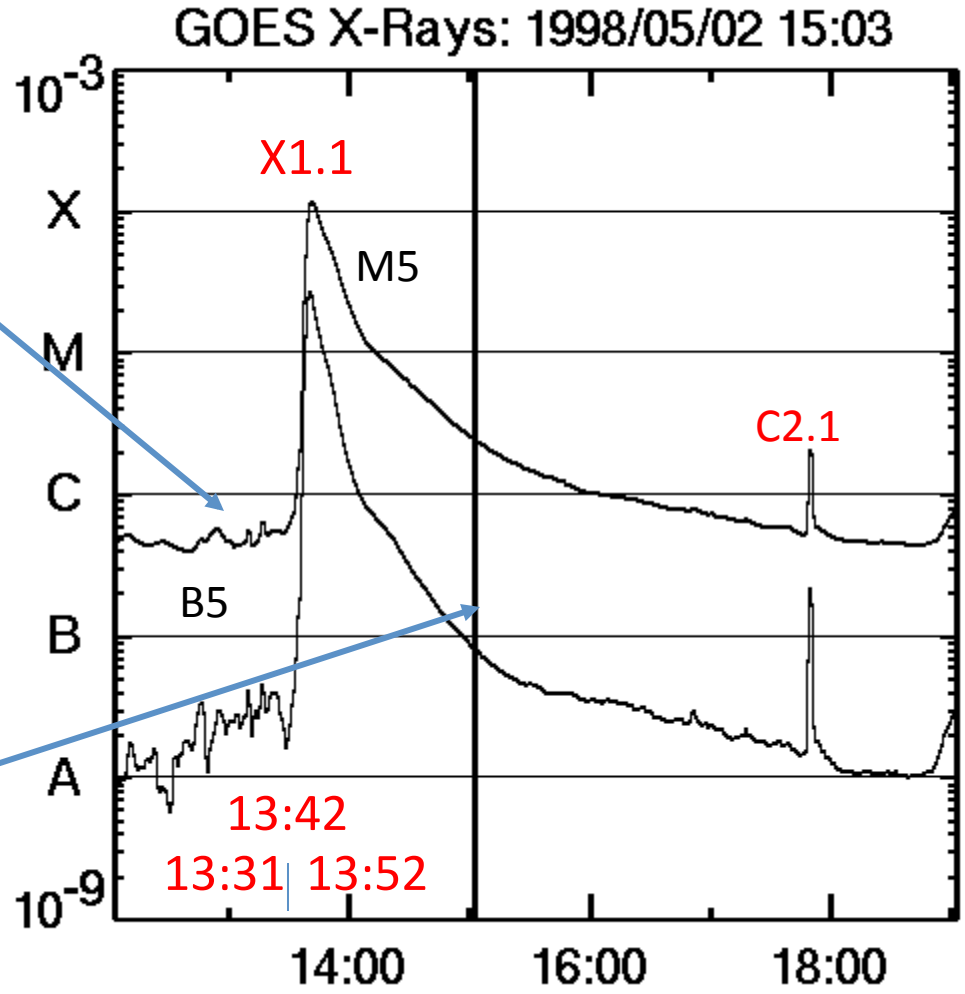


http://www.swpc.noaa.gov/ftpdir/indices/events/README

# Very weak flare

Flare seen as an extended structure in soft X-ray images. Note the brightening in the southeast quadrant

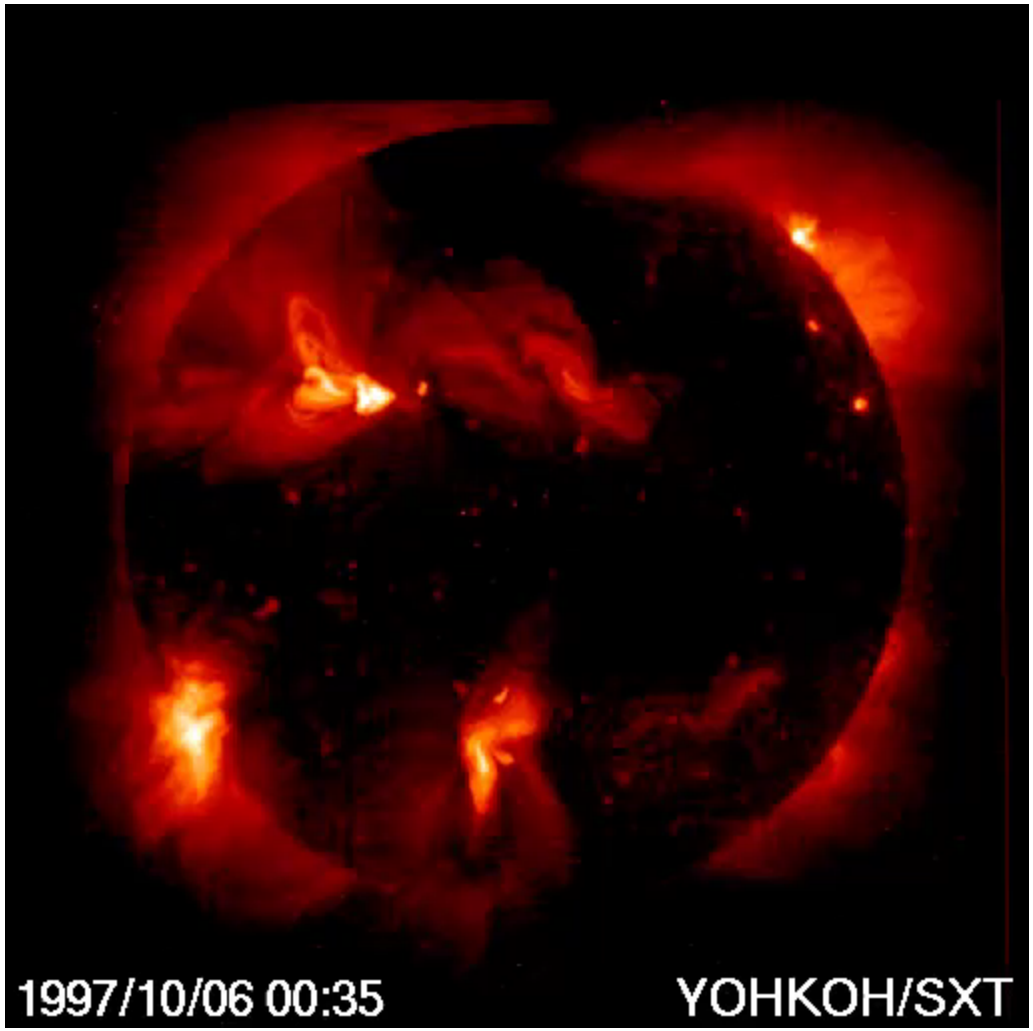


A-class flare barely seen in the soft X-ray light curve

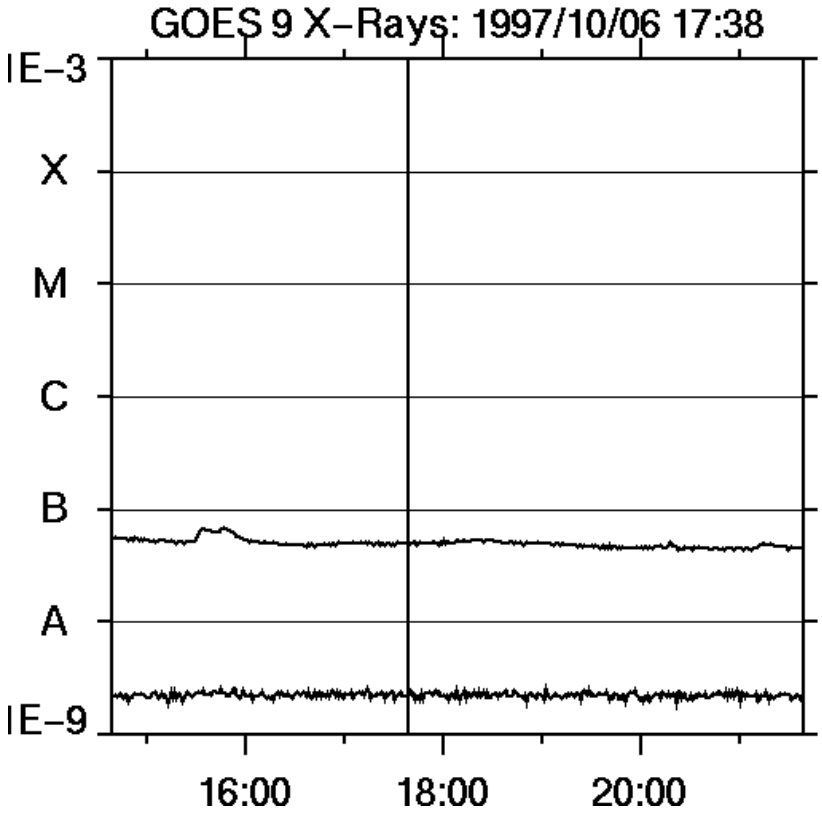


The image obtained in the energy channel 0.25 – 4 keV (2 – 50 Å)

# A Flare in Soft X-rays & Microwaves

soft X-rays: thermal emission (represents heating during the flare)
microwaves: nonthermal emission due to electrons accelerated during flare

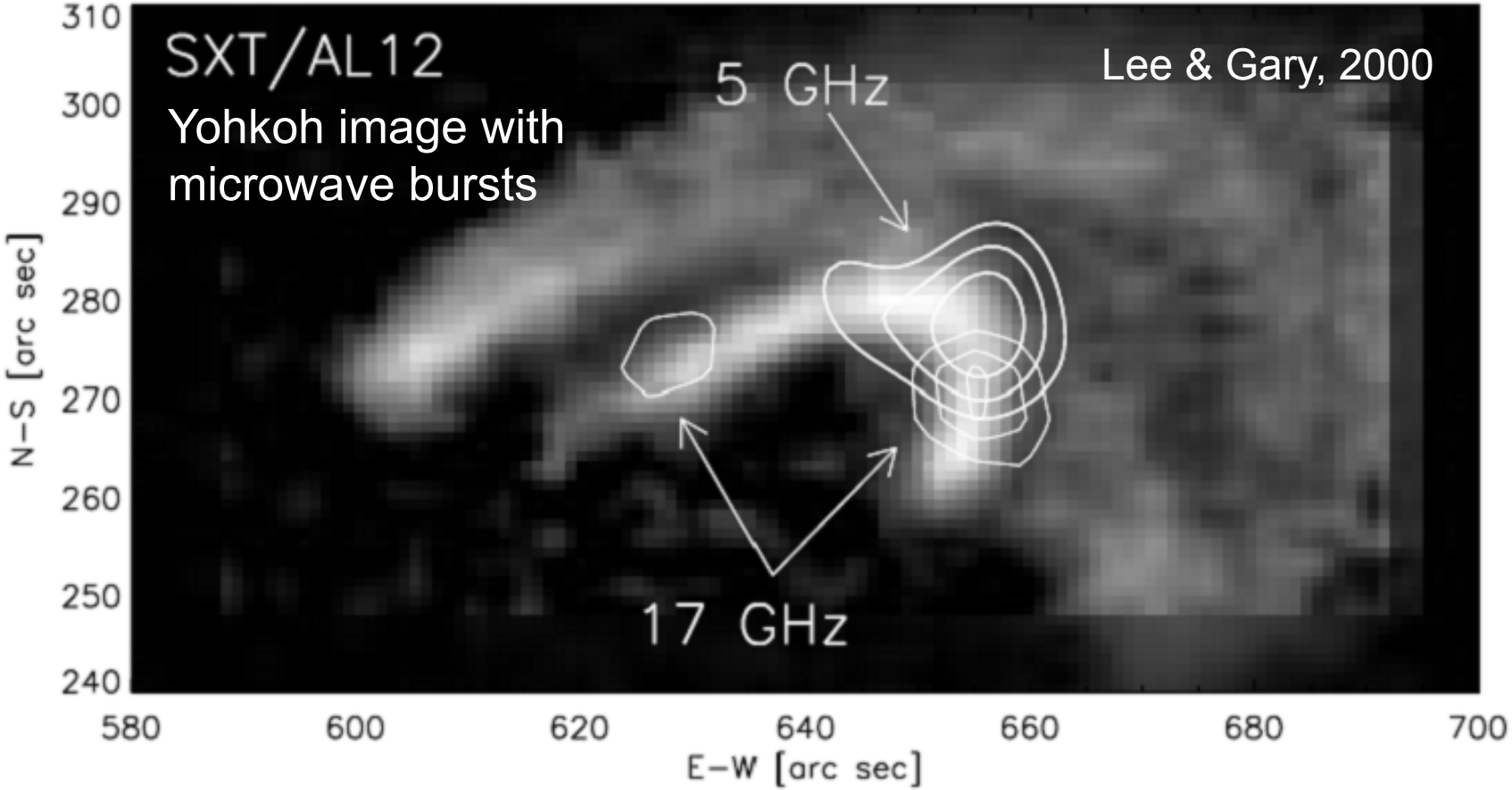


Microwave (5 GHz, 17 GHz): due to gyrosynchrotron emission from 100s of keV electrons accelerated during the flare; emission occurs at10-100 harmonics of gyro frequency ω= eB/mc. B = magnetic field, e-charge, m-mass, c-light speed

# Images of a microwave flare (17 GHz)

Nobeyama radioheliograph in Japan images the sun at 17 & 34 GHz

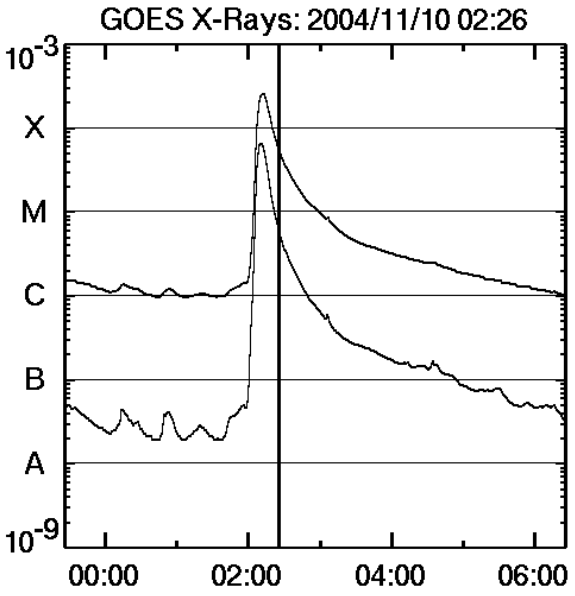


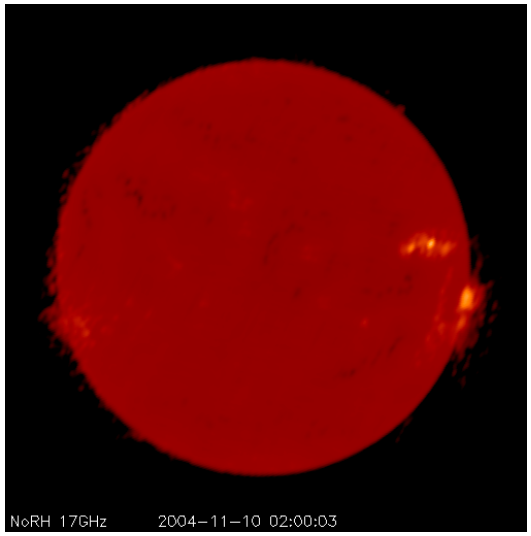


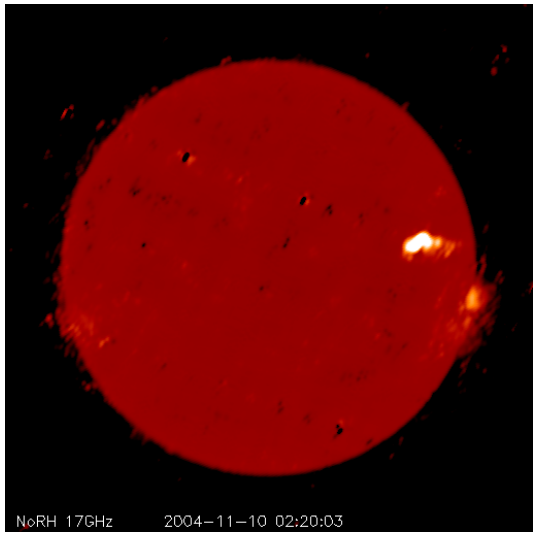


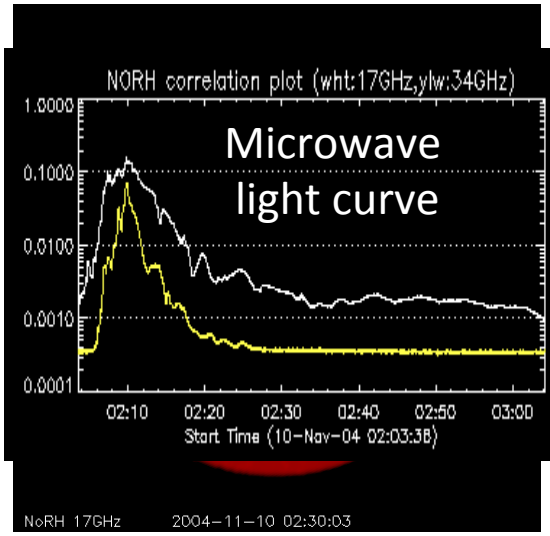


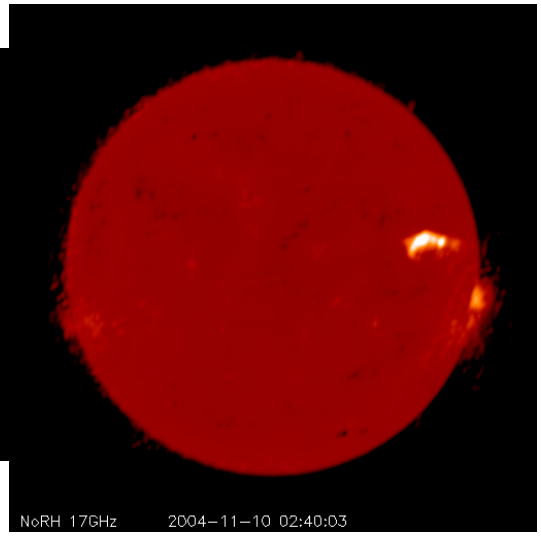


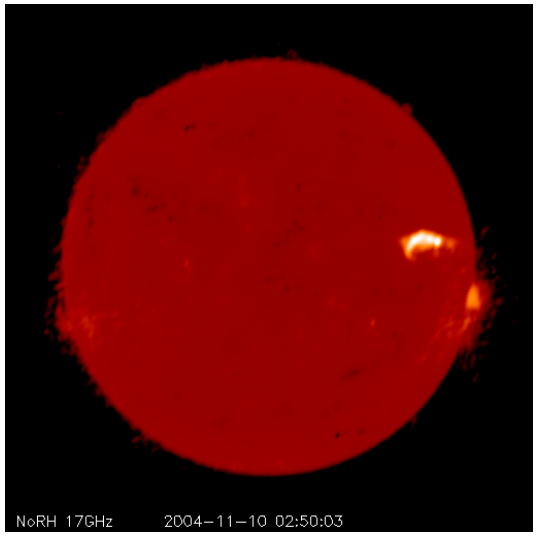

# Flare Ribbons and Hard X-Rays

Hard X-rays are photons at higher energies than soft X-rays

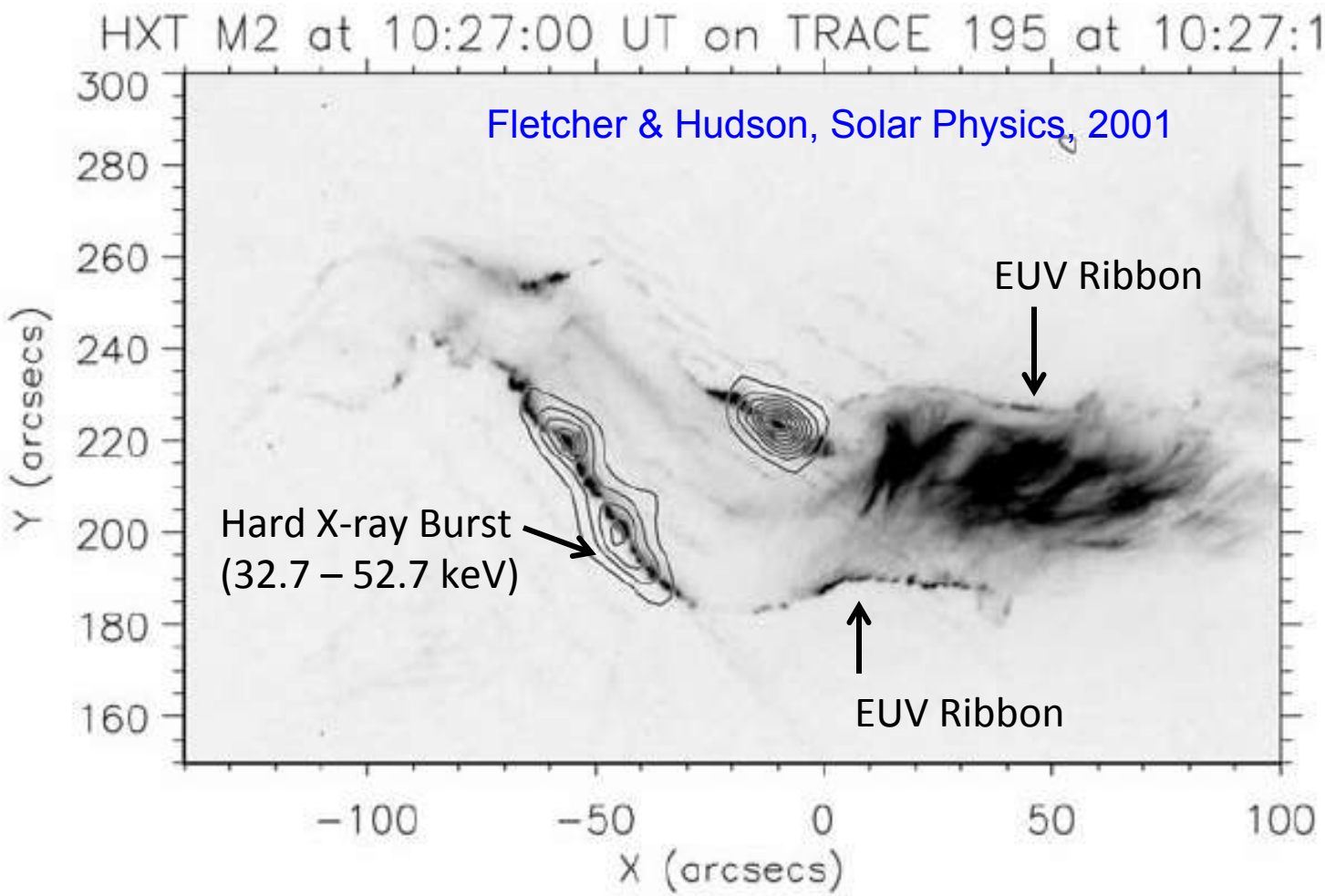


Image scale is negative: dark regions are considered more intense

Like in H-alpha, the flare arcade can also be observed in EUV. The EUV image was obtained by TRACE satellite (gray-scale image). The contours are obtained by the hard x-ray telescope (HXT) on board the Yohkoh satellite. Note that the hard X-ray bursts are located on the ribbons

# Another Hard X-ray Flare

Observations from the RHESSI satellite. Images at both soft and hard X-rays

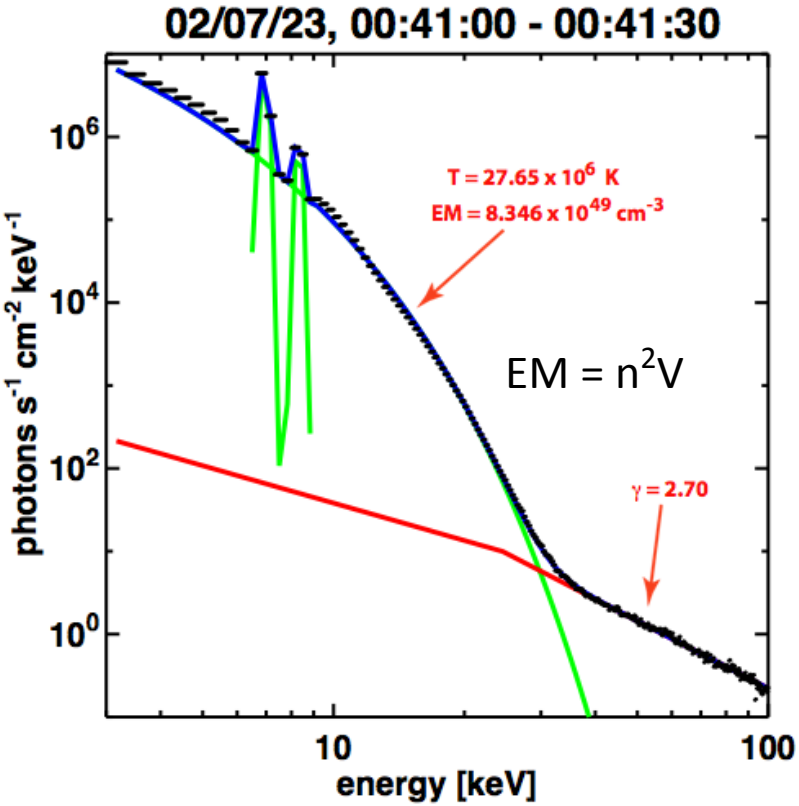


Caspi & Lin, 2005

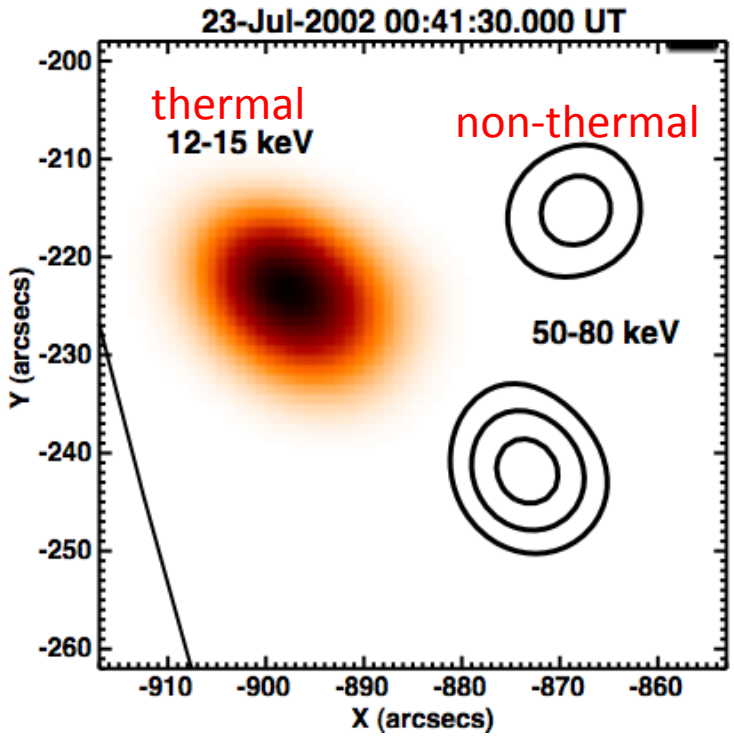


The X-ray emission can be modeled as a combination of thermal and nonthermal emissions. The thermal emission is from 27 MK plasma. The hard x-ray photons are due to energetic electrons interacting with the chromospheric protons (bremsstrahlung)

A section of the southeast quadrant of the Sun. Note that the soft X-rays (color) from higher up in the corona; hard X-rays from the surface

# Upward & Downward electrons

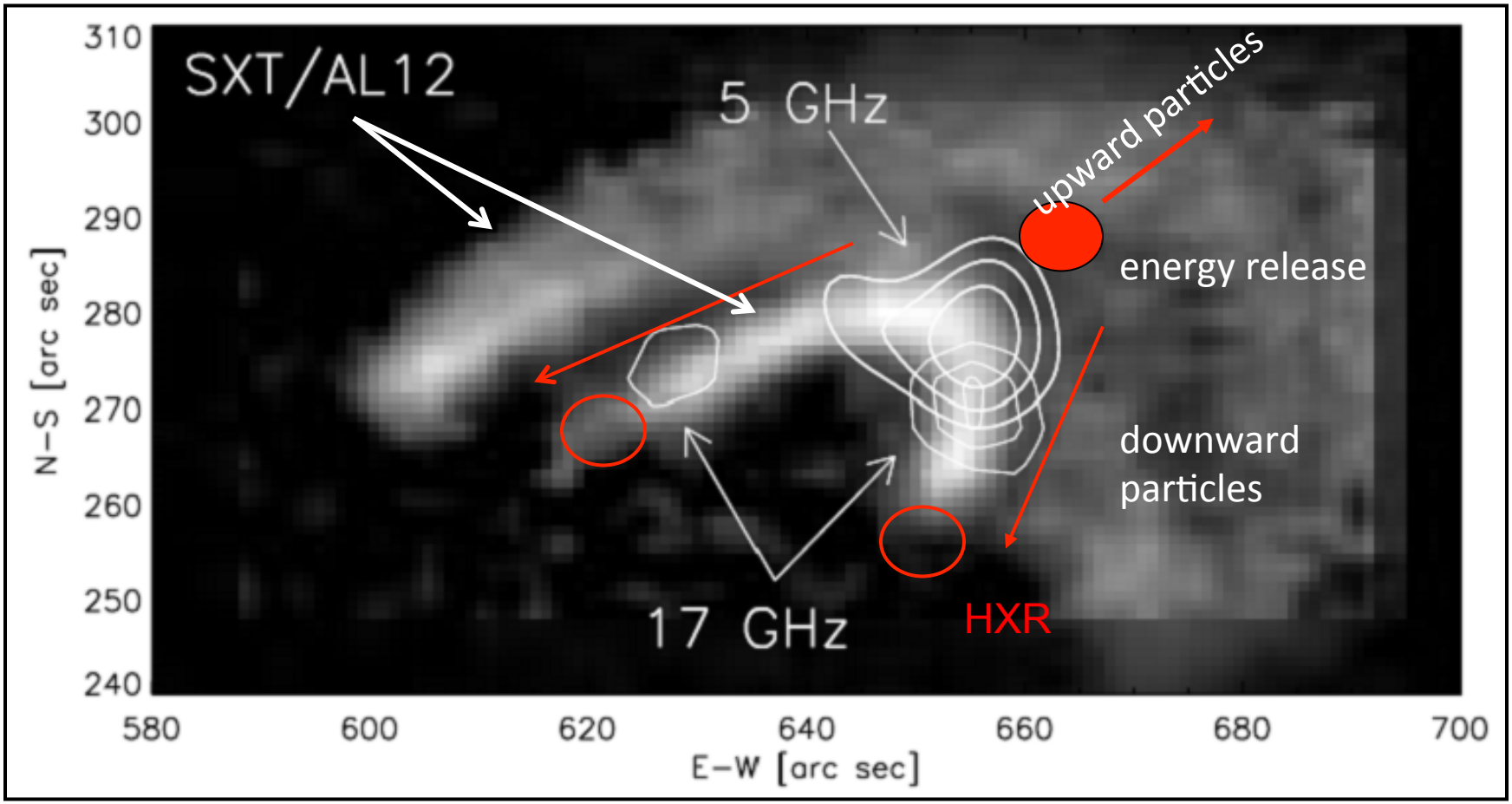


We can now understand the flare process as starting from an energy release in the corona in which the magnetic free energy goes into accelerating electrons and ions. The accelerated particles flow down magnetic loops. Higher energy electrons trapped in the loops produce microwave bursts. Lower energy electrons reach the atmosphere and produce hard-rays and excite H-alpha emission. The heated atmospheric plasma fills the loops emitting soft X-rays. Some heating also occurs at the energy release site.

# A Generic Flare

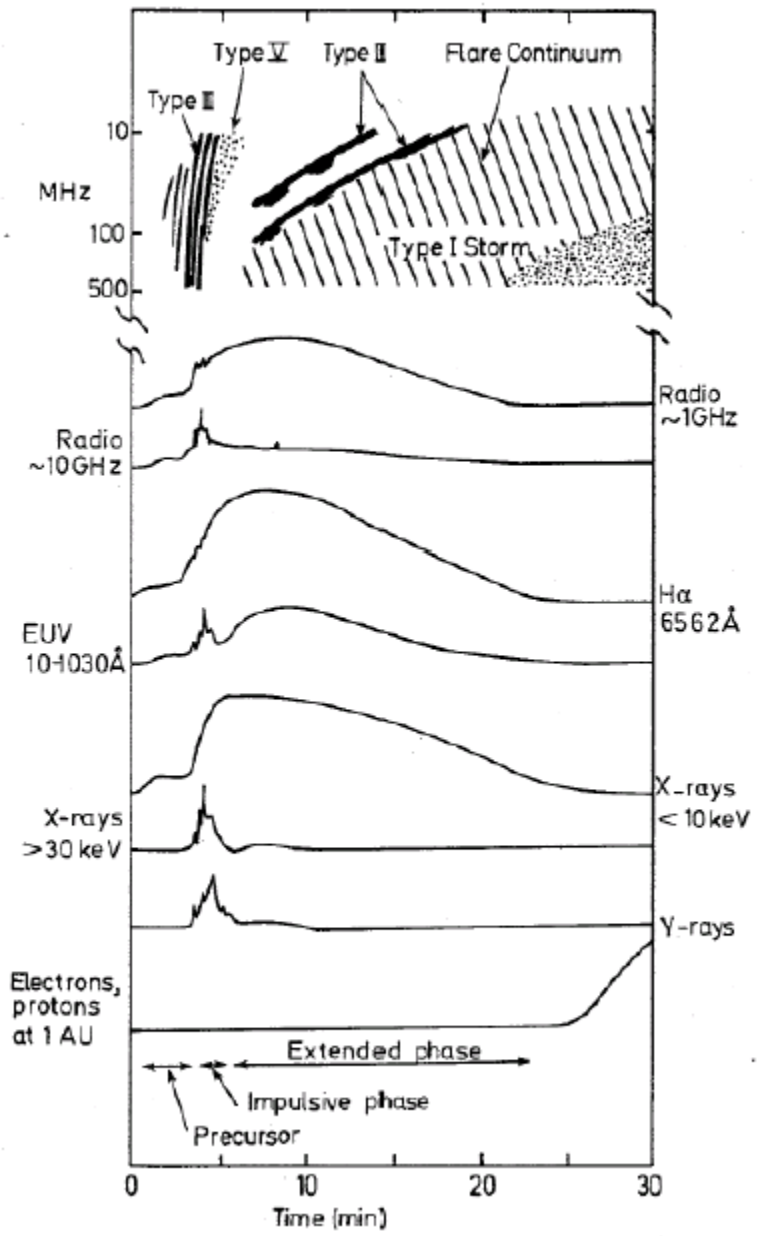


Type III – due to flare-accelerated electrons
Type II – due to shock-accelerated electrons
flare continuum – due to flare-accelerated electrons trapped in flare loops
1 GHz radio bursts – due to lower energy electrons
10 GHz radio bursts – due to higher energy electrons accelerated in the flare site
H-alpha – due to hydrogen atoms excited by particles precipitating in the chromosphere
soft X-rays, EUV – due to heated flare plasma
Hard X-rays (>30 keV) – due to accelerated electrons interacting with photospheric ions (bremsstrahlung)
gamma rays – due to particles precipitating on the Sun

electrons and ions observed in the interplanetary medium: particles escaping from the flare site, similar to the ones causing type III bursts
Some of these particles are from the CME-driven shock associated with the flare

Thermal and nonthermal emissions + energetic particles

# Composite Spectrum of a Large Flare

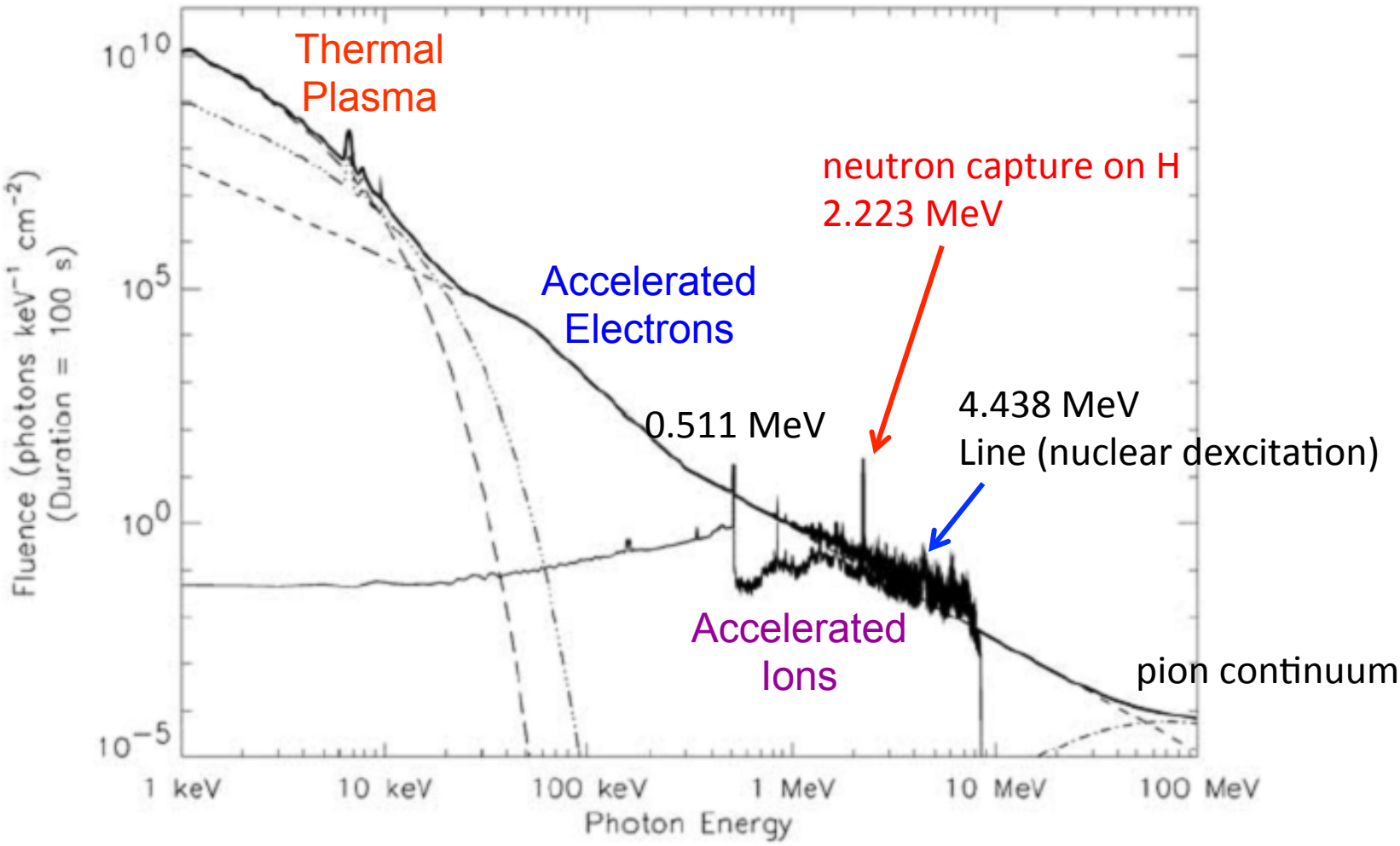


Produced by different particles from the flare site by different mechanisms

# γ -rays from Solar Flares

**γ-ray lines**

$$\left.\begin{matrix} p \\ \alpha \end{matrix}\right\} + {}^{12}C \rightarrow {}^{12}C^{*4.439}$$

$$\left.\begin{matrix} p \\ \alpha \end{matrix}\right\} + {}^{16}O \rightarrow {}^{12}C^{*4.439} + \ldots$$

$$\alpha + {}^{4}He \rightarrow {}^{7}Li^{*0.478}$$

$$\alpha + {}^{4}He \rightarrow {}^{7}Be^{*0.429}$$

Broad and narrow lines

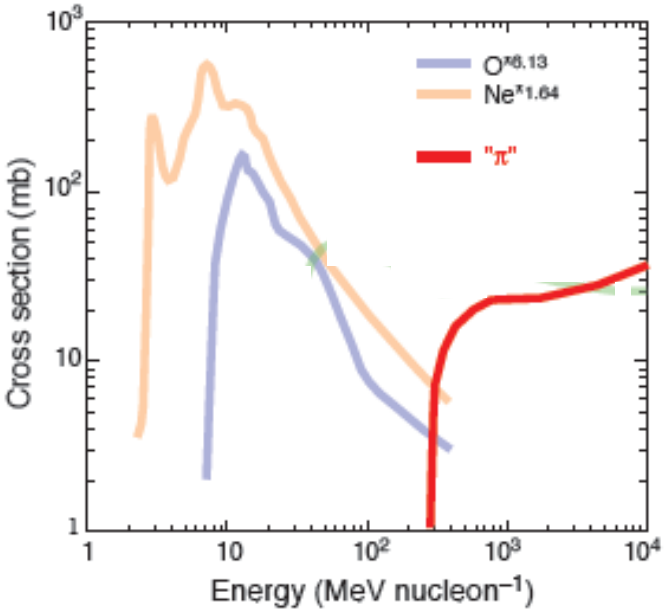


**neutrons**

$$\left.\begin{matrix} p + {}^{4}He \rightarrow n + \ldots \\ \alpha + \alpha \rightarrow n + \ldots \\ \left.\begin{matrix} p \\ \alpha \end{matrix}\right\} + {}^{12}C \rightarrow n + \ldots \end{matrix}\right\} \text{escape to Earth}$$

$$\text{capture on photospheric H} \rightarrow D + \gamma_{2.223}$$

**positrons**

$$\left.\begin{matrix} \left.\begin{matrix} p \\ \alpha \end{matrix}\right\} + {}^{12}C \rightarrow {}^{11}C \rightarrow e^{+} \\ \left.\begin{matrix} p + p \\ p + \alpha \end{matrix}\right\} \rightarrow \pi^{+} \rightarrow e^{+} \end{matrix}\right\} \gamma_{511,\ \text{cont.}}$$

**pions**

$$\left.\begin{matrix} p + p \\ p + \alpha \end{matrix}\right\} \rightarrow \left.\begin{matrix} \pi^{0} \\ \pi^{+,-} \end{matrix}\right\} \rightarrow \begin{matrix} \gamma \\ e^{+,-} \rightarrow \gamma_{511,\ \text{cont.}} \end{matrix}$$

**pions are produced in interactions of the highest-energy accelerated ions and are observable via their decay radiation**

Dermer et al. 2012

# Flare Photons in the Ionosphere

- Atmospheric Weather Electromagnetic System for Observation Modeling and Education (*AWESOME*) Monitor and Sudden Ionospheric Disturbance (SID) Monitor are ISWI instruments (radio receivers) that monitor VLF signals that bounce between Earth surface and the ionosphere
- Solar flare photons increase the ionization and hence change the conductivity of the ionosphere
- This causes change in amplitude and phase of the VLF signals

# Sudden Ionospheric Disturbance (SID) Event

Quiet Day

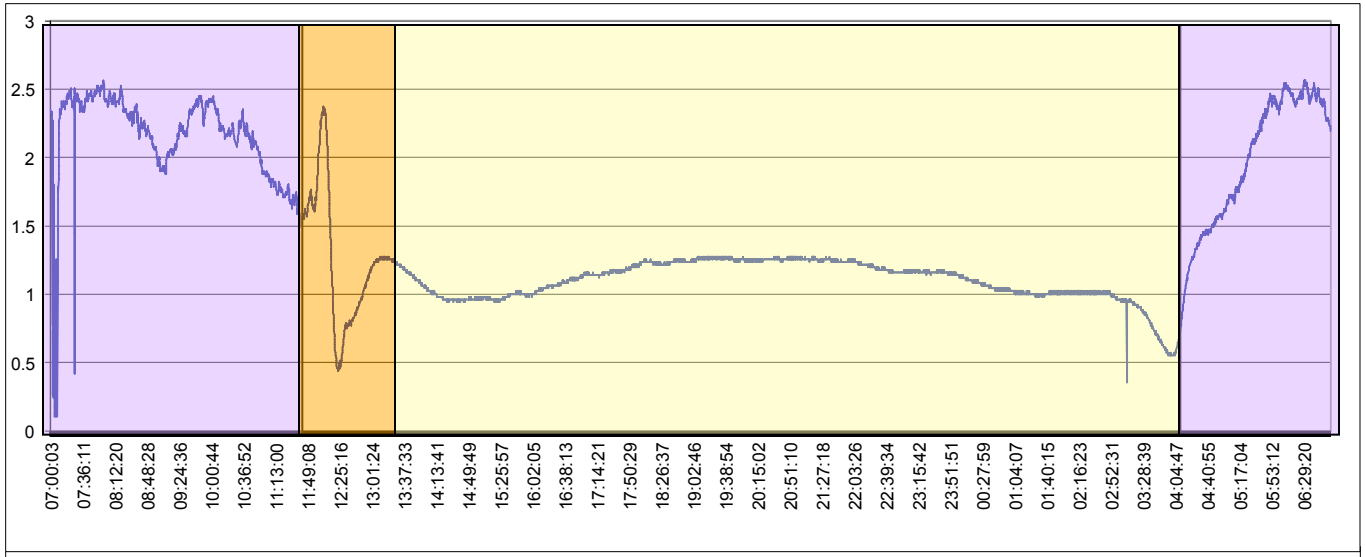


NLK
24.8 kHz

Active Day

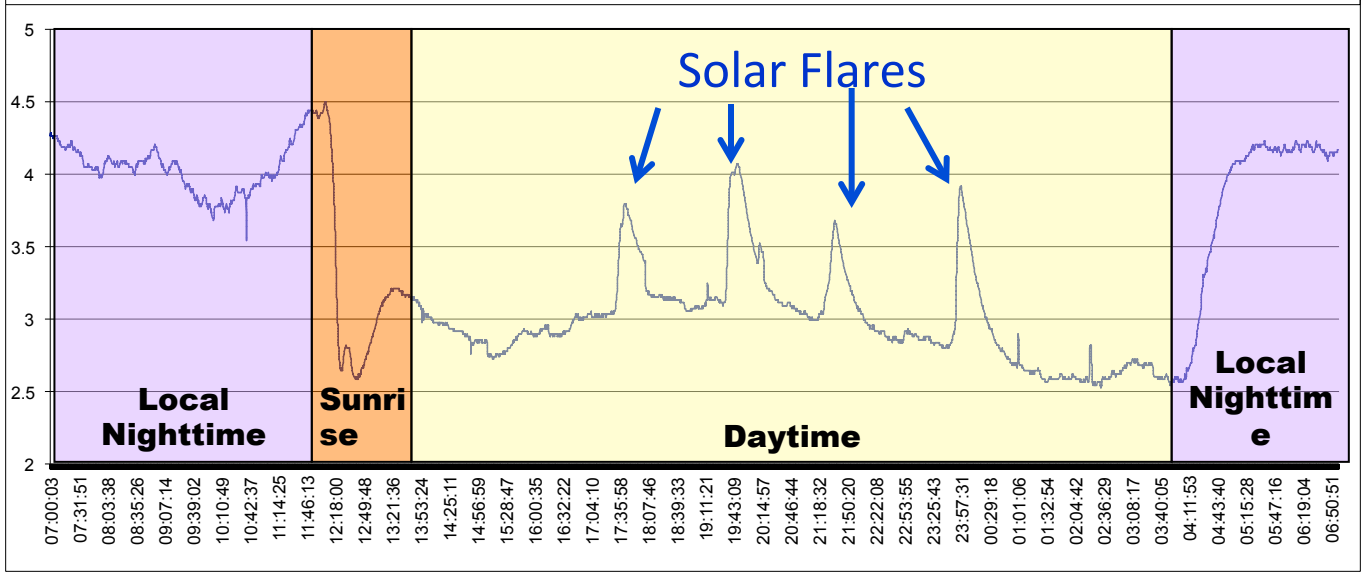


Courtesy Ray Mitchell

The VLF signal amplitude and phase are modified when flare photons modify the ionosphere

# Confined vs. Eruptive Flares

- Confined: generally a single loop
- Eruptive:
- associated with erupting prominence
- CME
- type II radio burst
- two - ribbon flares
- Post-eruption arcade

- Impulsive and gradual flares

# Confined Flares

- ~ 20% of ≥M5.0 flares are not accompanied by mass motions
- Confined flares are hotter than eruptive ones
- Both confined and eruptive flares produce hard X-ray and microwave bursts
- No EUV waves found in confined flares
- No upward energetic electrons (lack of metric or longer wavelength type III, type II bursts) in confined flares

# Confined Flare: No mass motion

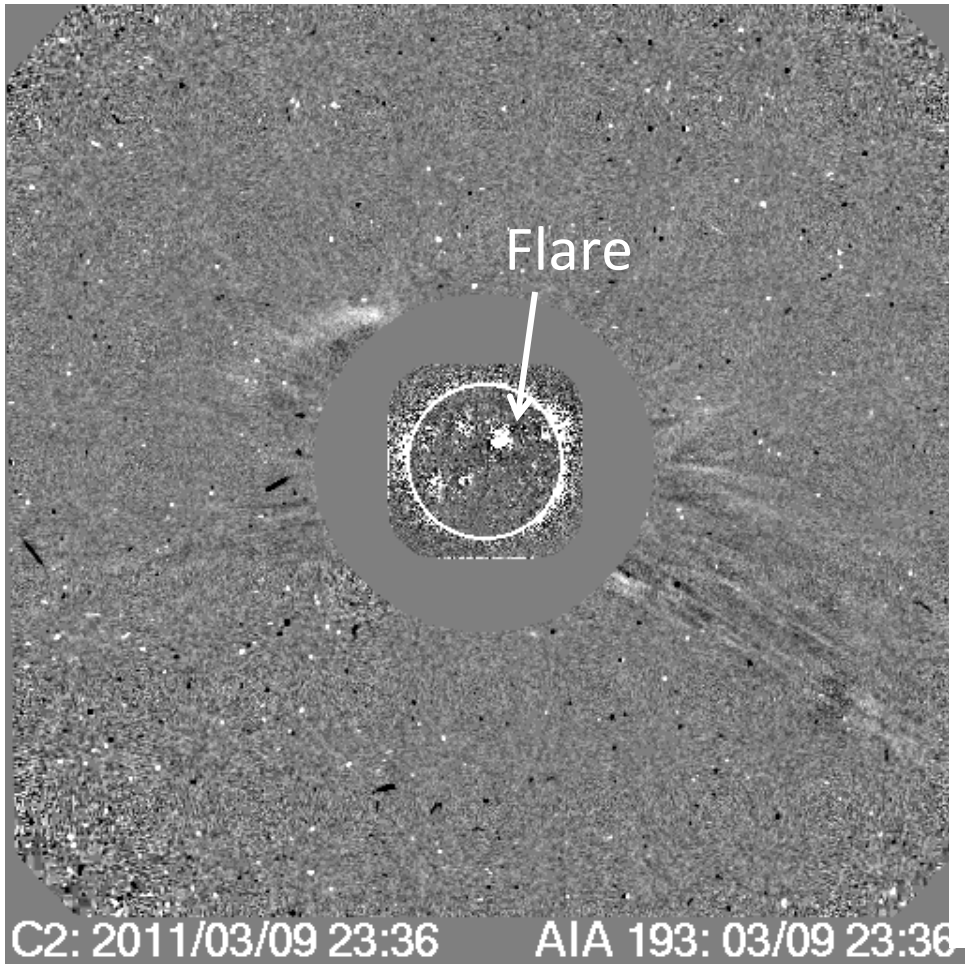


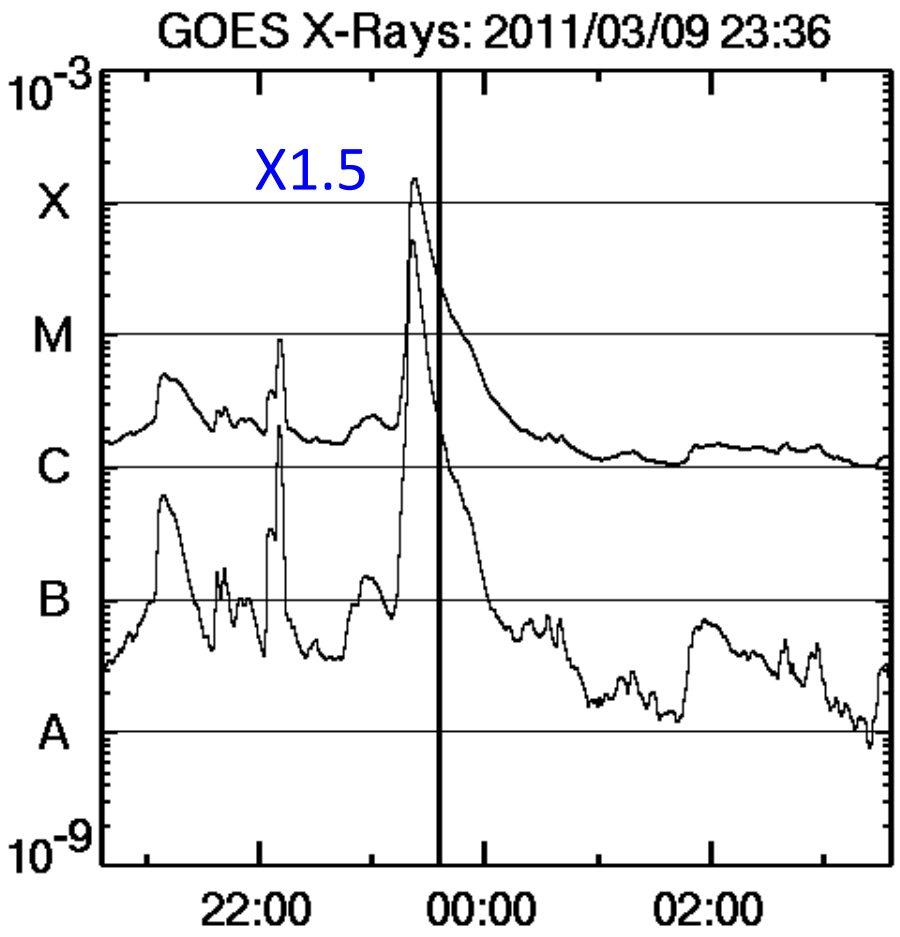


Confined flares just produce excess photons

# CME is an Eruptive Event

Flares have prompt effect on the ionosphere

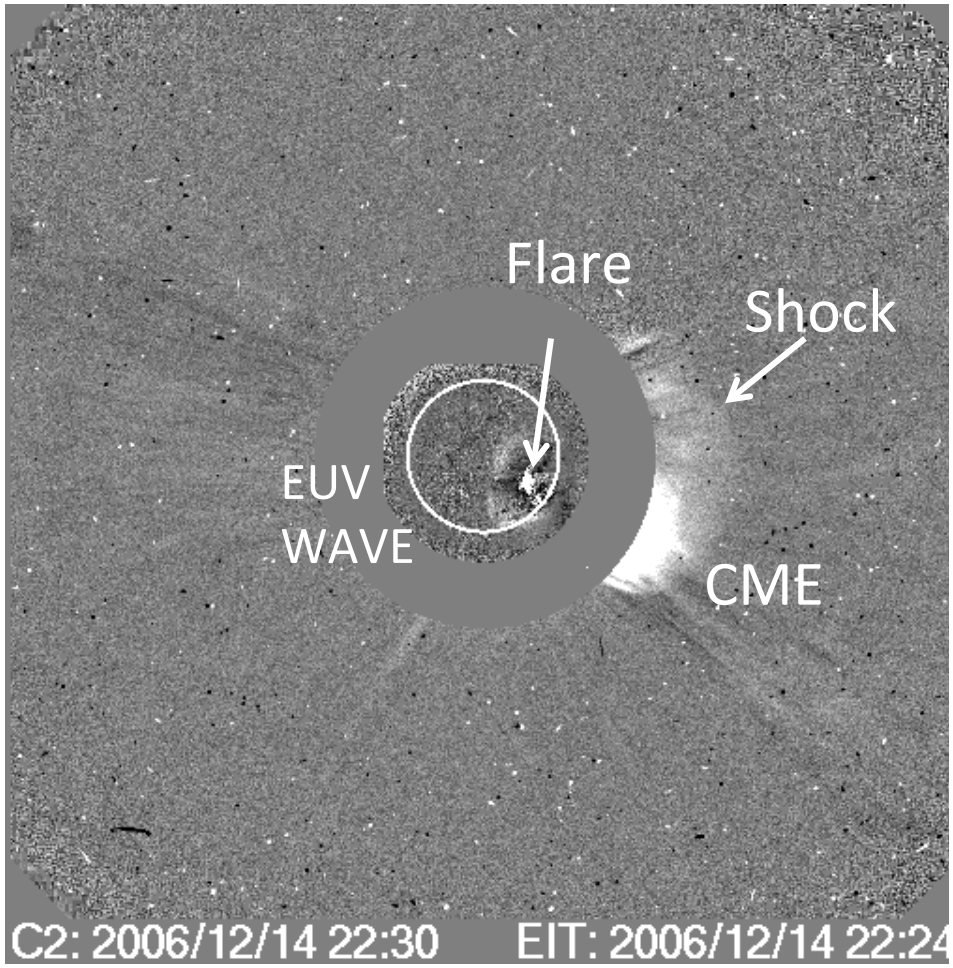


SOHO/LASCO & EIT Difference Images overlaid

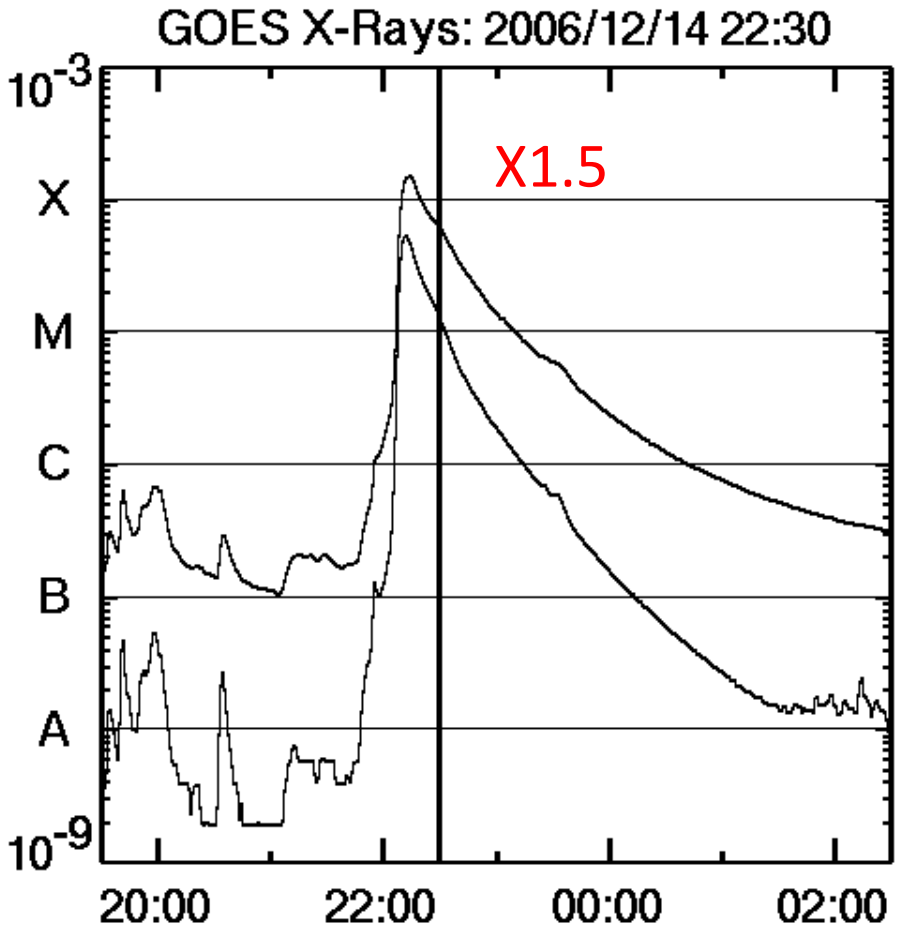

# Moon is a natural occulting disk

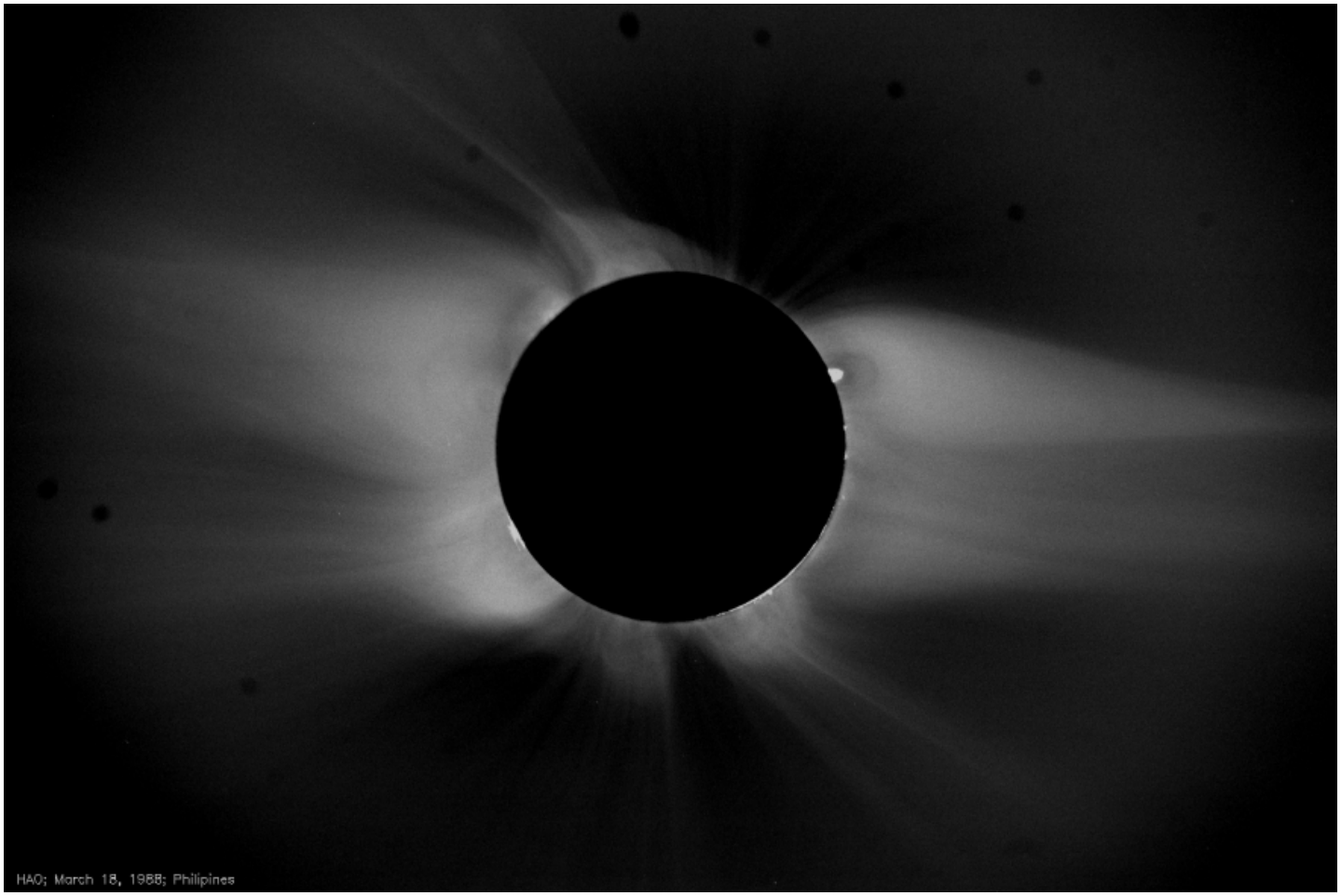


Courtesy: HAO

Prominence, coronal cavity and overlying streamer: Look like a CME before taking off!

# CME in Old Eclipse Pictures: 1860 July 18

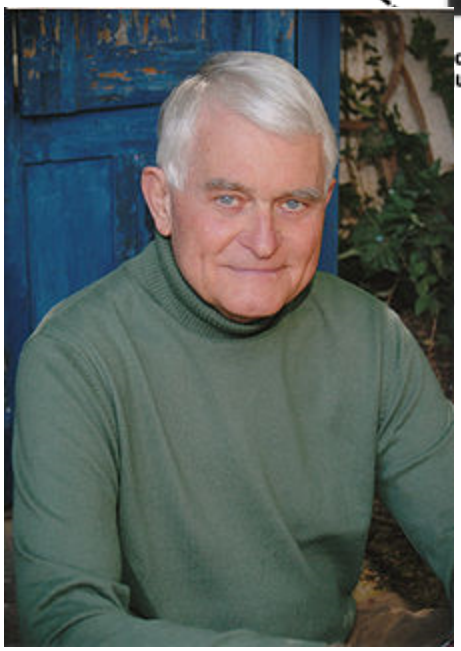

J. A. Eddy (1931 – 2009)




Fig. 4. Selected drawings of the corona (from Ranyard, 1879), made by different observers along the path of totality in Spain during the 1860 eclipse. Times are relative to mid-totality at Tempel's station at Torreblanca

Eddy, 1974 estimated the CME speed to be 200-500 km/s

# Coronagraphs

Bernard Lyot (1939)

INTERNALLY OCCULTED REFRACTING CORONAGRAPH (LYOT)

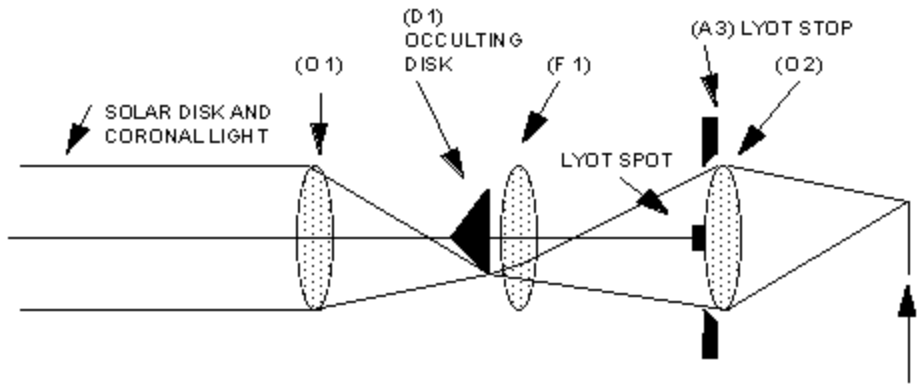


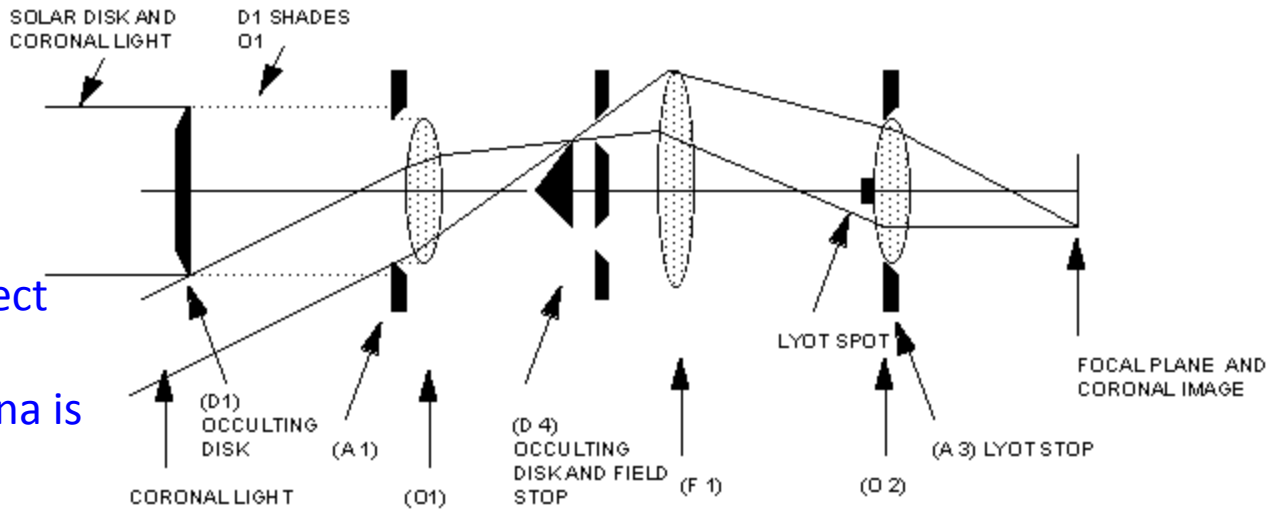


EXTERNALLY OCCULTED REFRACTING CORONAGRAPH (NEWKIRK)

The occulting disk prevents direct photospheric light from falling on the objective lens. The corona is about a million times dimmer than the photosphere

# Brief history

- Mass Ejections known for a long time from H-alpha prominence eruptions, type II radio bursts (e.g, Payne-Scott et al., 1947), and type IV radio bursts (Boischot, 1957)
- The concept of plasma ejection known to early solar terrestrial researchers (Lindeman, 1919; Chapman & Bartels, 1940; Morrison, 1954; Gold, 1955)
- CMEs as we know today were discovered in white light pictures obtained by OSO-7 spacecraft (Tousey, 1973)
- OSO-7, Skylab, P78-1, SMM, SOHO, and STEREO missions from space, and MLSO from ground have accumulated data on thousands of CMEs
- CME properties are measured in situ by many spacecraft since the 1962 detection of IP shocks (Sonett et al., 1964)

# The first white-light CME from OSO-7

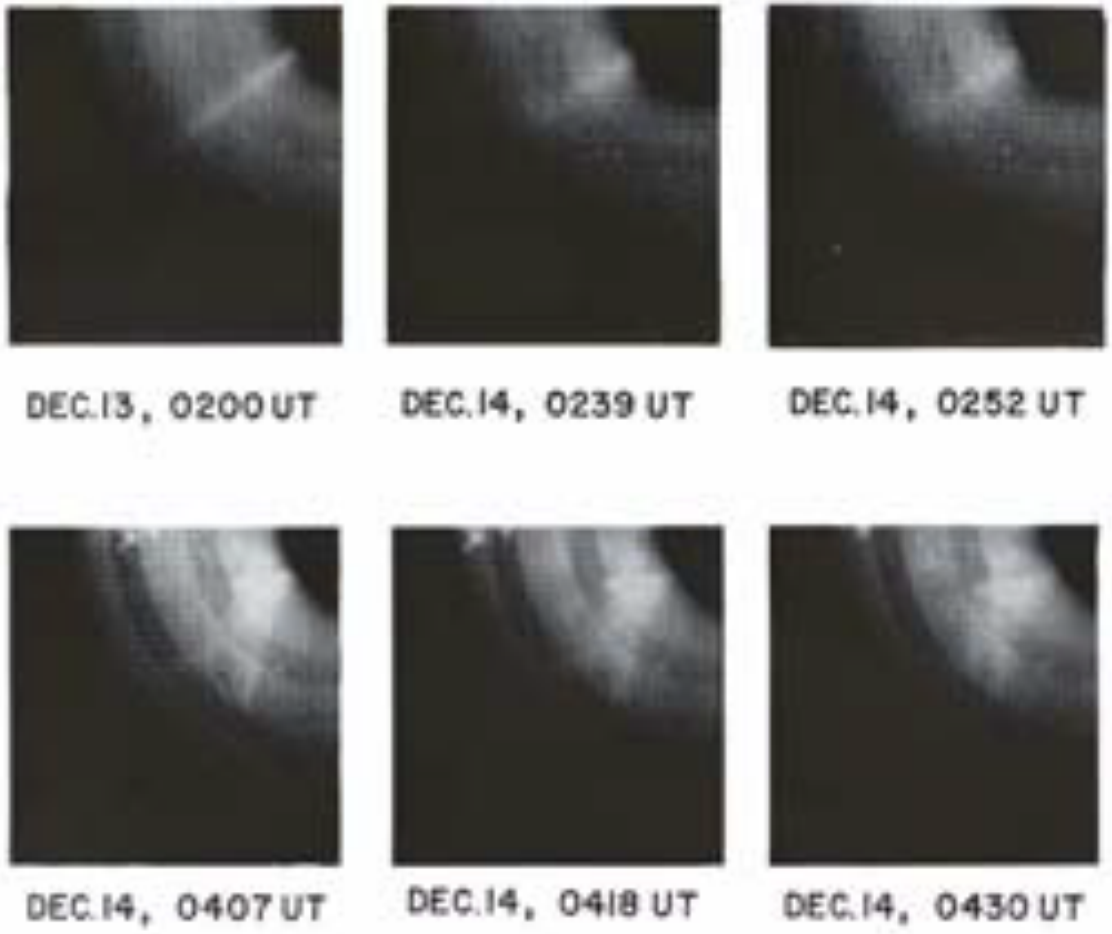


Tousey, 1973
reported on the 13-14 Dec 1971
coronal transient (1000 km/s)

Skylab
Solwind on P78-1
Coronagraph/Polarimeter on SMM
SOHO/LASCO ←
STEREO/SECCHI
MLSO Mark IV K -Coronameter

David Roberts, the electronics engineer noticed the change and thought his camera was failing…

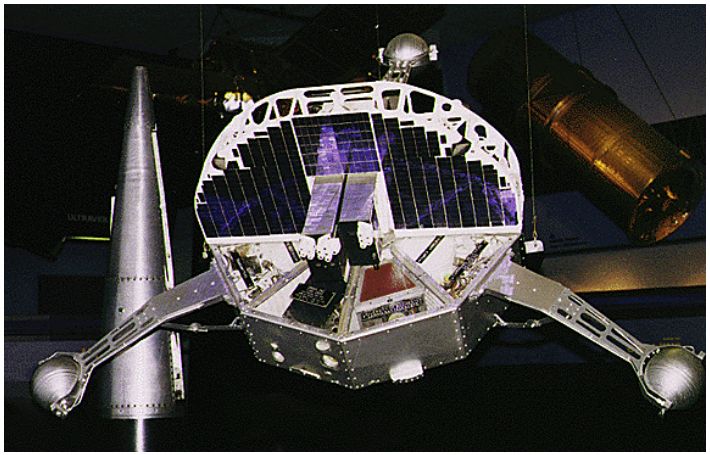

NASA's OSO-7

# Prominences Understood by the end of 19th Century

17 GHz Nobeyama radioheliograph

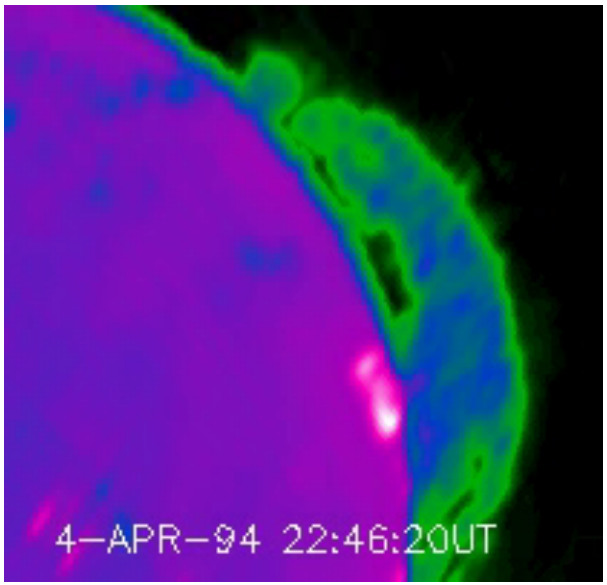


Gopalswamy & Hanaoka, 1998

Angelo Secchi

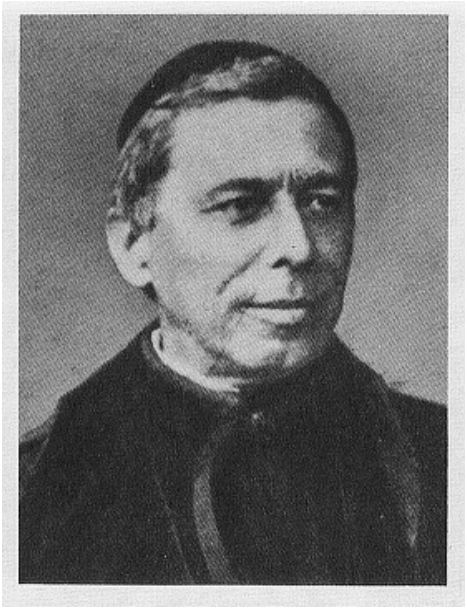

1868: Janssen & Lockyer demonstrated that prominences could be viewed outside of eclipses using spectroscope

1871: Secchi classified active and quiescent prominences
Prominence eruptions with speeds exceeding 100s of km/s became well known (Fenyi, 1892)

# Type II Radio Bursts are caused by electrons accelerated in the CME shock

Ruby Payne-Scott
1912 – 1981

The whole pattern drifts;
140 MHz in 6 min
df/dt = 0.4 MHz/s

Plasma density
5.0 x$10^8$ $cm^{-3}$

1.2 x$10^8$ $cm^{-3}$

0.4 x$10^8$ $cm^{-3}$

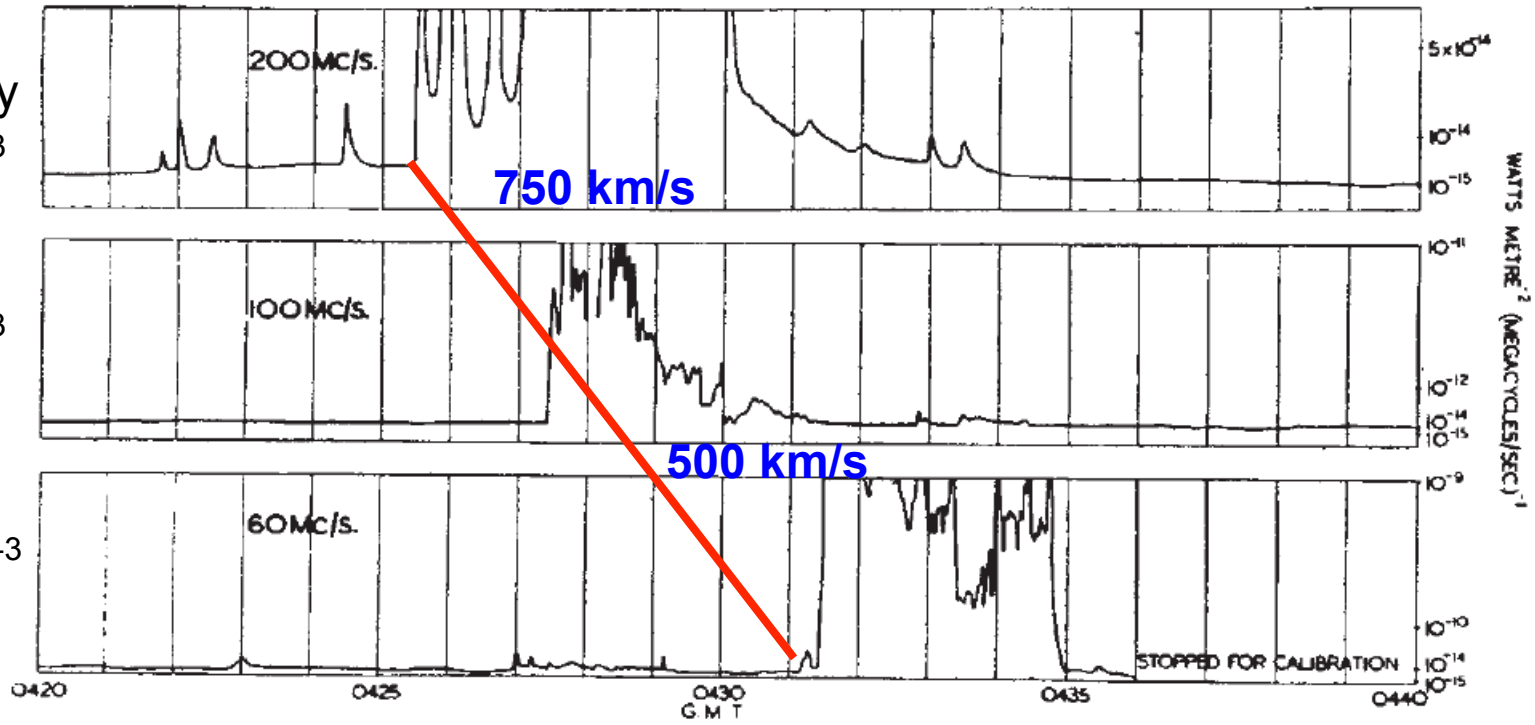


Nature 260, 256, 1947

LARGE OUTBURST OF MARCH 8, 1947

# Type III & Type II Radio Bursts

Type III (electron beams) v ~ 0.3 c

Type II (shocks) v ~ 600 km/s

$df/dt = df/dr.dr/dt = (V/2)\, f\, n^{-1}(dn/dr)$

$V = 2L(d\ln f/dt)$

$f \sim n^{1/2}$ (plasma frequency)

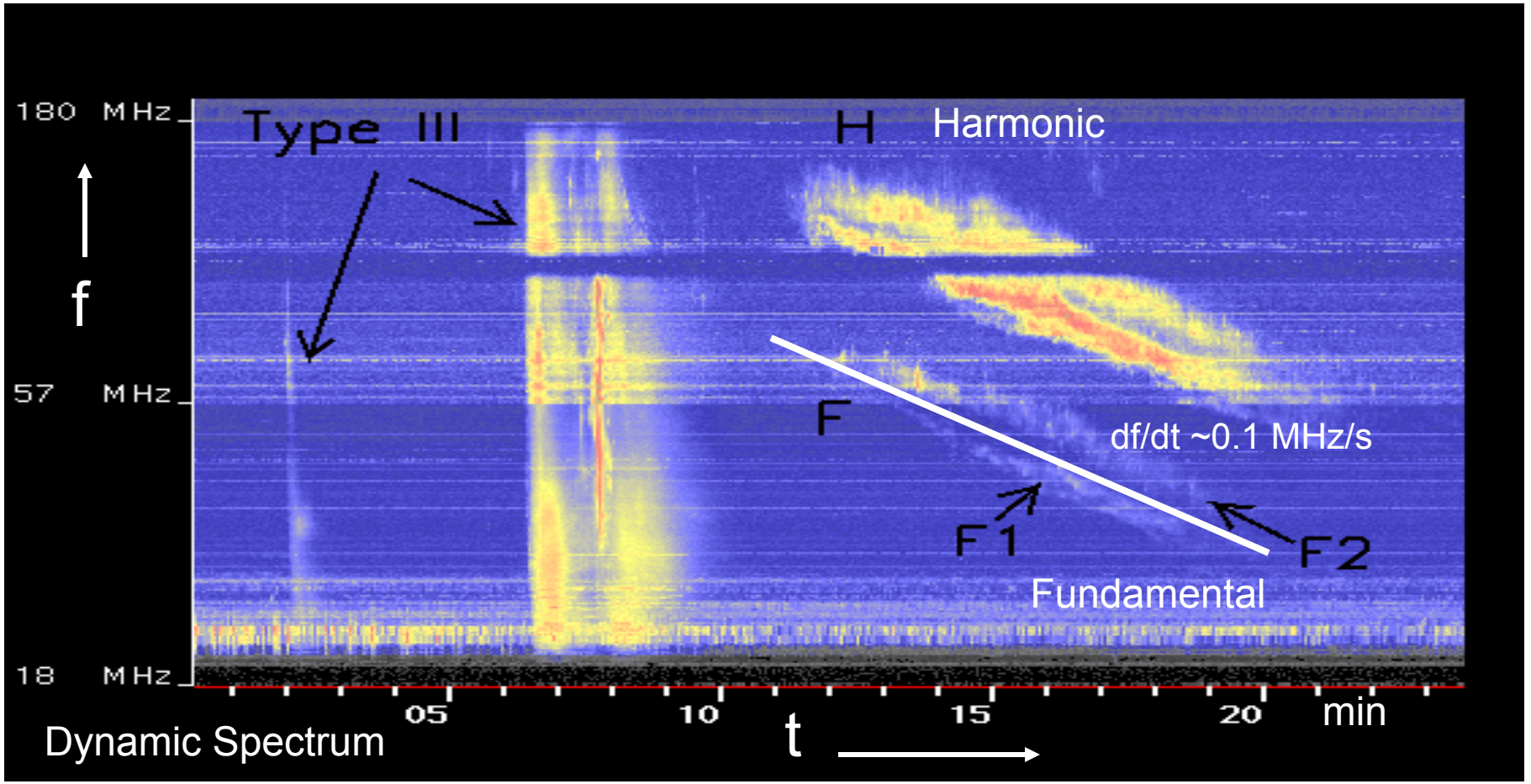

# Moving type IV burst (Boischot, 1957)

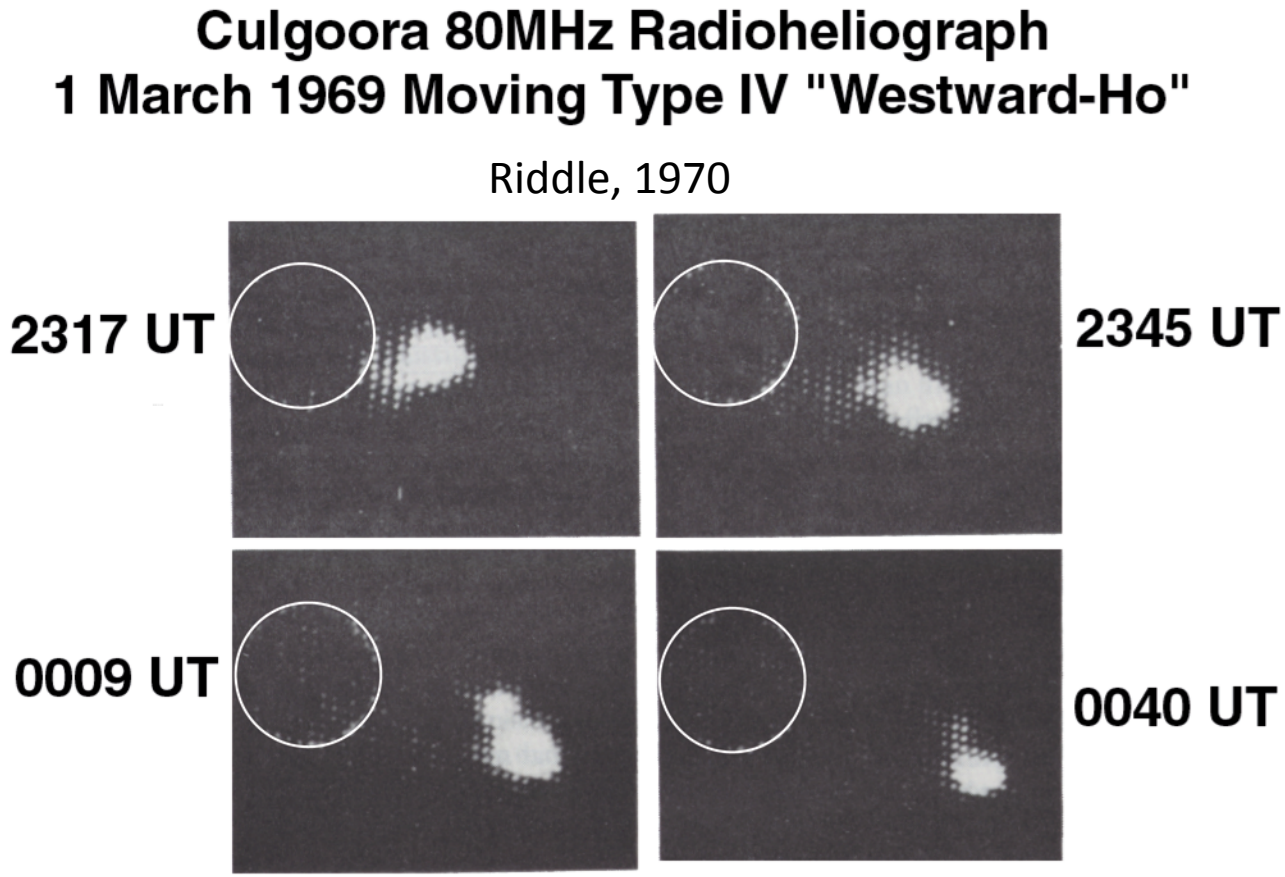


Accelerated electrons trapped in moving magnetic structures associated with the CME

# Shock in the IP medium

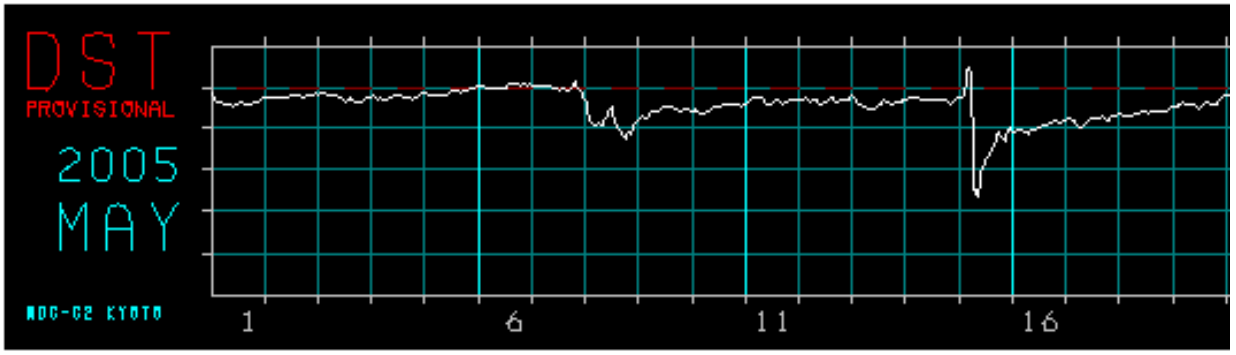


In 1953 T. Gold proposed IP shock to explain Sudden Commencement (Gas Dynamics of Cosmic Clouds, North Holland Publishing, 1955)

Energetic storm particle events were associated with shocks at 1 AU (Bryant, 1962)

Interpreted as shock accelerated by Rao et al. (1967)

T. Gold (1920 – 2004)

# Mariner 2 Detects IP shock

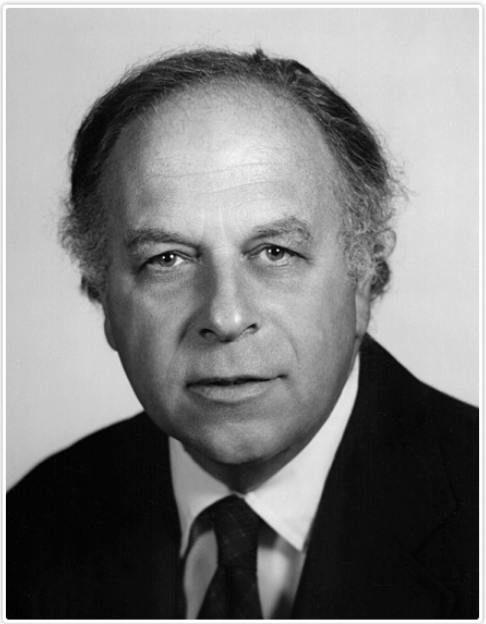

C P Sonett (1924 -2011)

IP shock followed by
Sudden commencement 4.7 h later

Confirming Gold's suggestion

Taylor (1969) statistical study of
IP shocks and SCs

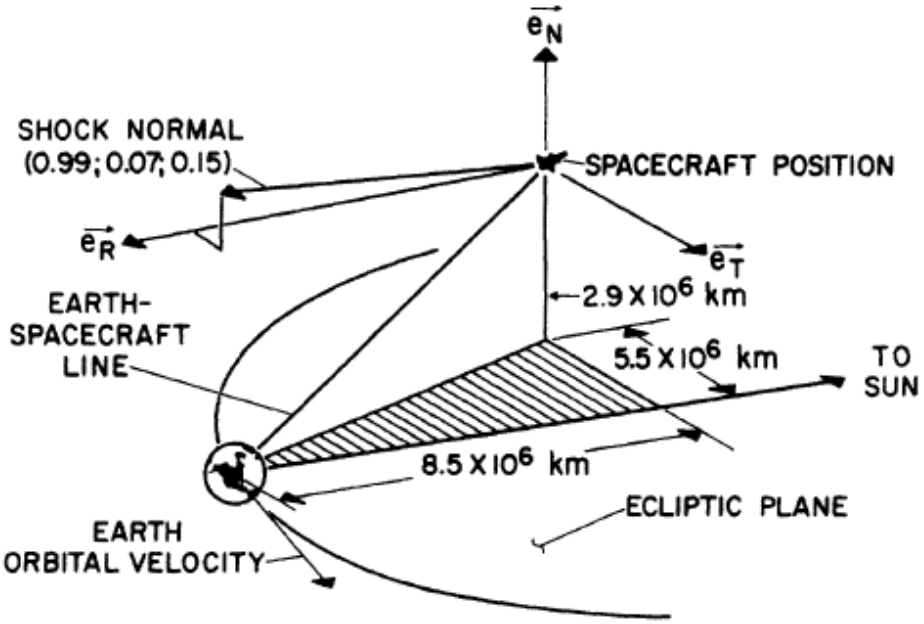


FIG. 1. Geometry of the Mariner II orbit on 7 October 1962. The shock normal direction computed from the change in the magnetic field is indicated. $\vec{e}_R, \vec{e}_N, \vec{e}_T$ are unit vectors defining a coordinate system along the radius vector from the sun, toward the ecliptic north pole, and along $\vec{e}_N \times \vec{e}_R$, respectively.

Sonett et al., 1964, Phys. Rev. Lett

# Flux rope: Old and new

Gold's picture of an IP CME is pretty much the same as what we have today.

Koomen et al. (1974) associated a white-light CME with the "Gold bottle"
Sheeley et al. 2000 white-light shock

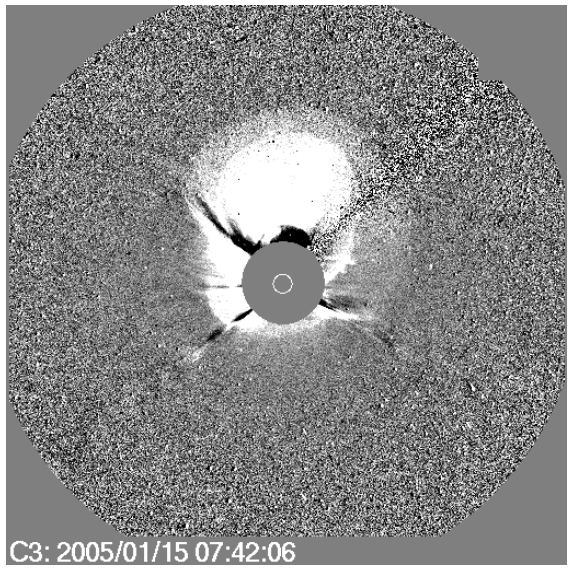


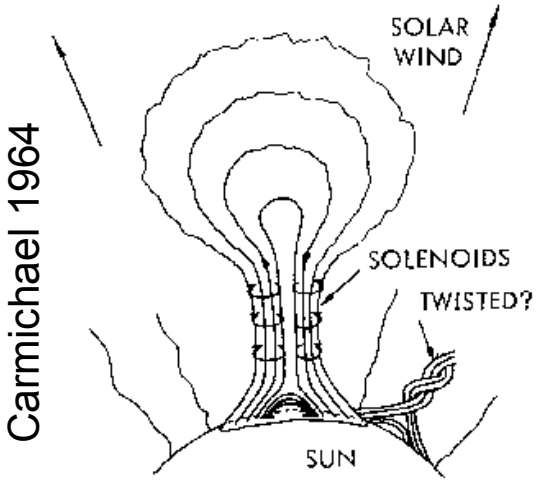


Carmichael 1964

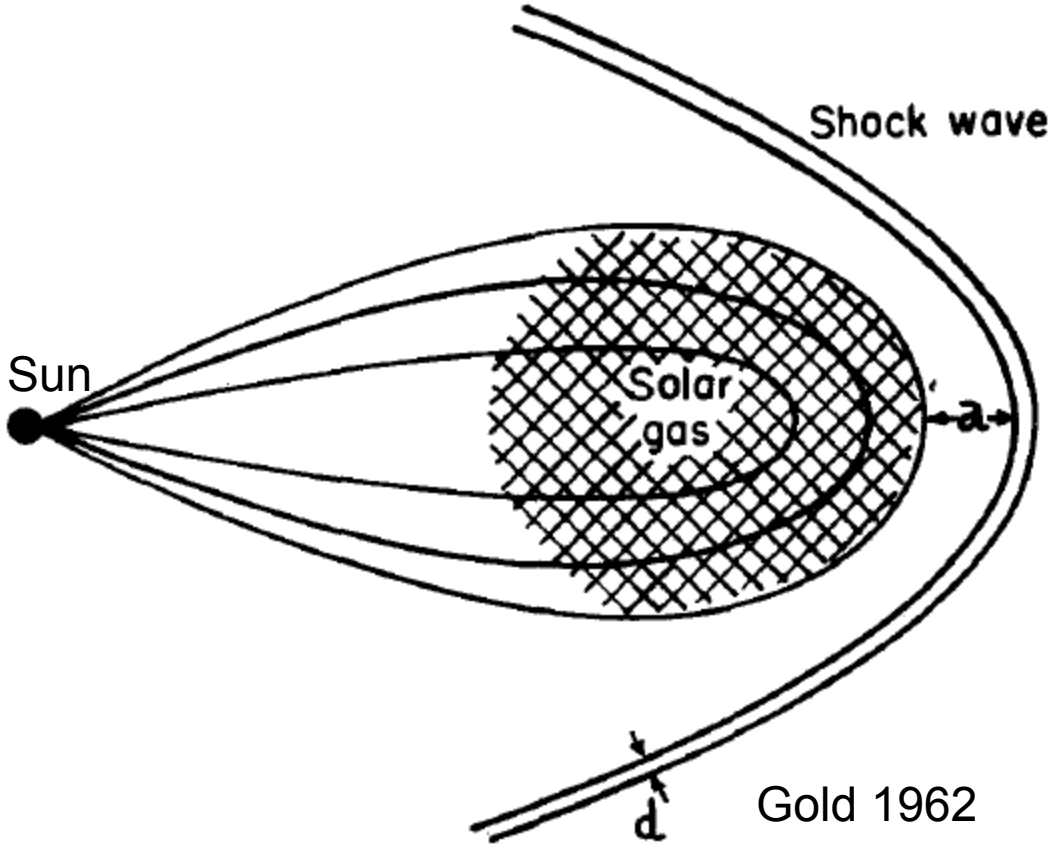


Gold 1962

"Idealized configuration in space, showing solar plasma cloud, the drawn-out field and the shock wave ahead" (Gold 1962)

# High Energy Plasmas & Particles

Solar Wind

Plasma Ejected from the Sun
(Coronal Mass Ejections – CMEs)

Energetic Particles

SOHO coronagraph movie showing two CMEs

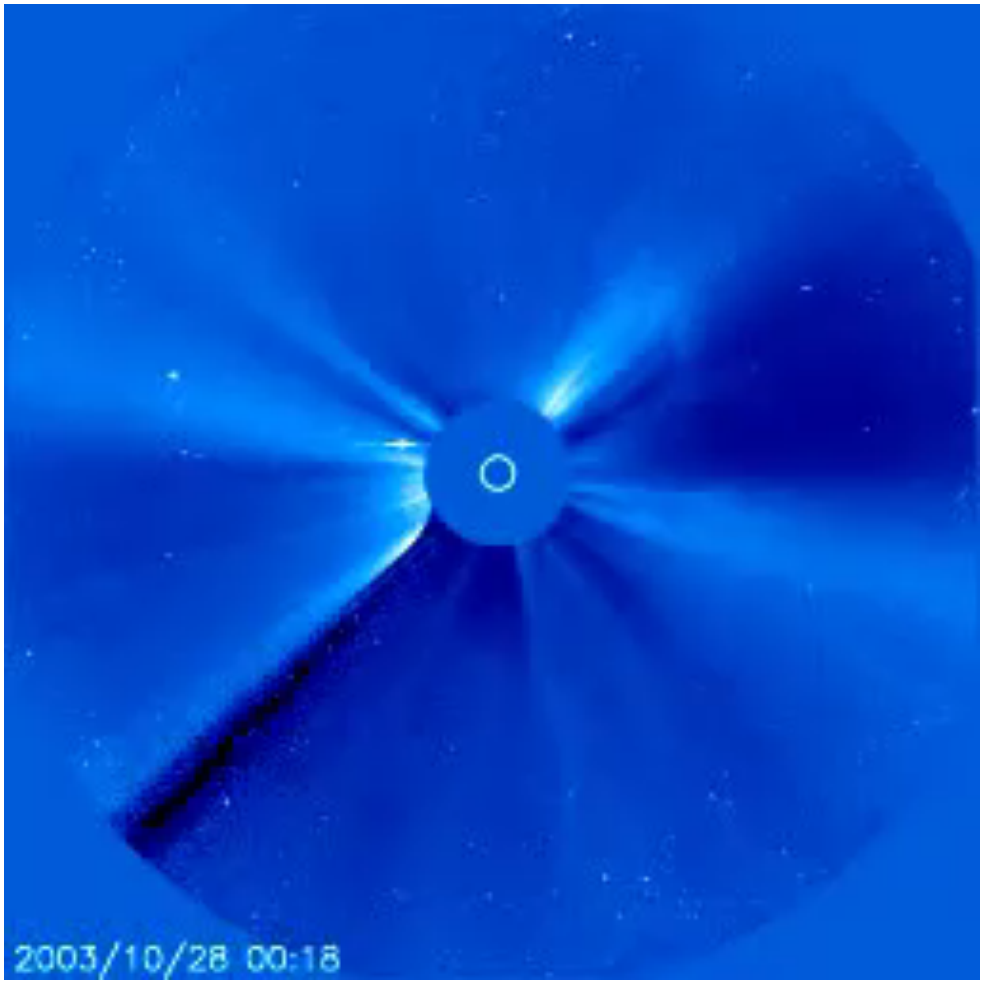

# Animation of Halloween 2003 CMEs

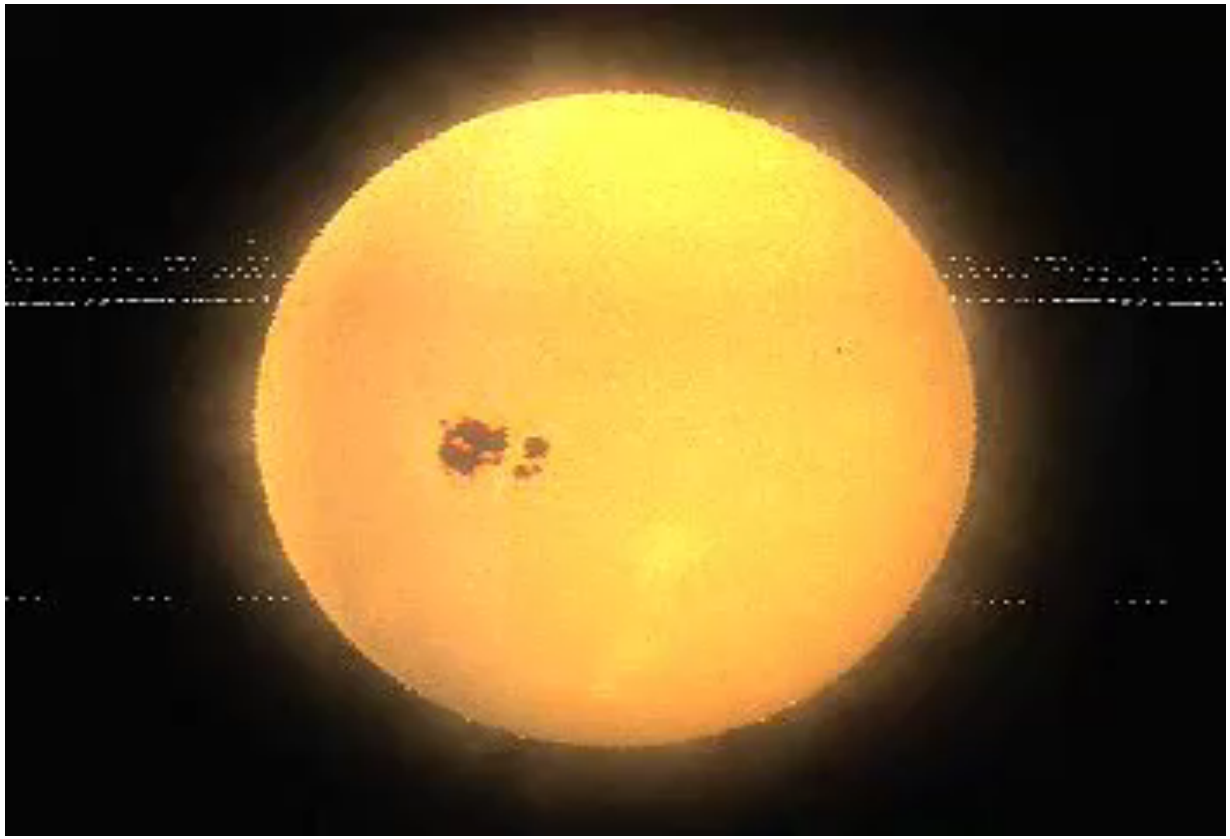

Consequences of the CMEs were observed at Earth, Jupiter, Saturn and even at the edge of the solar system where the Voyagers were located. The CMEs took 6 months to reach the termination shock.

CMEs represent the most energetic phenomenon in the heliosphere

# Solar Disturbances can affect the entire solar system!

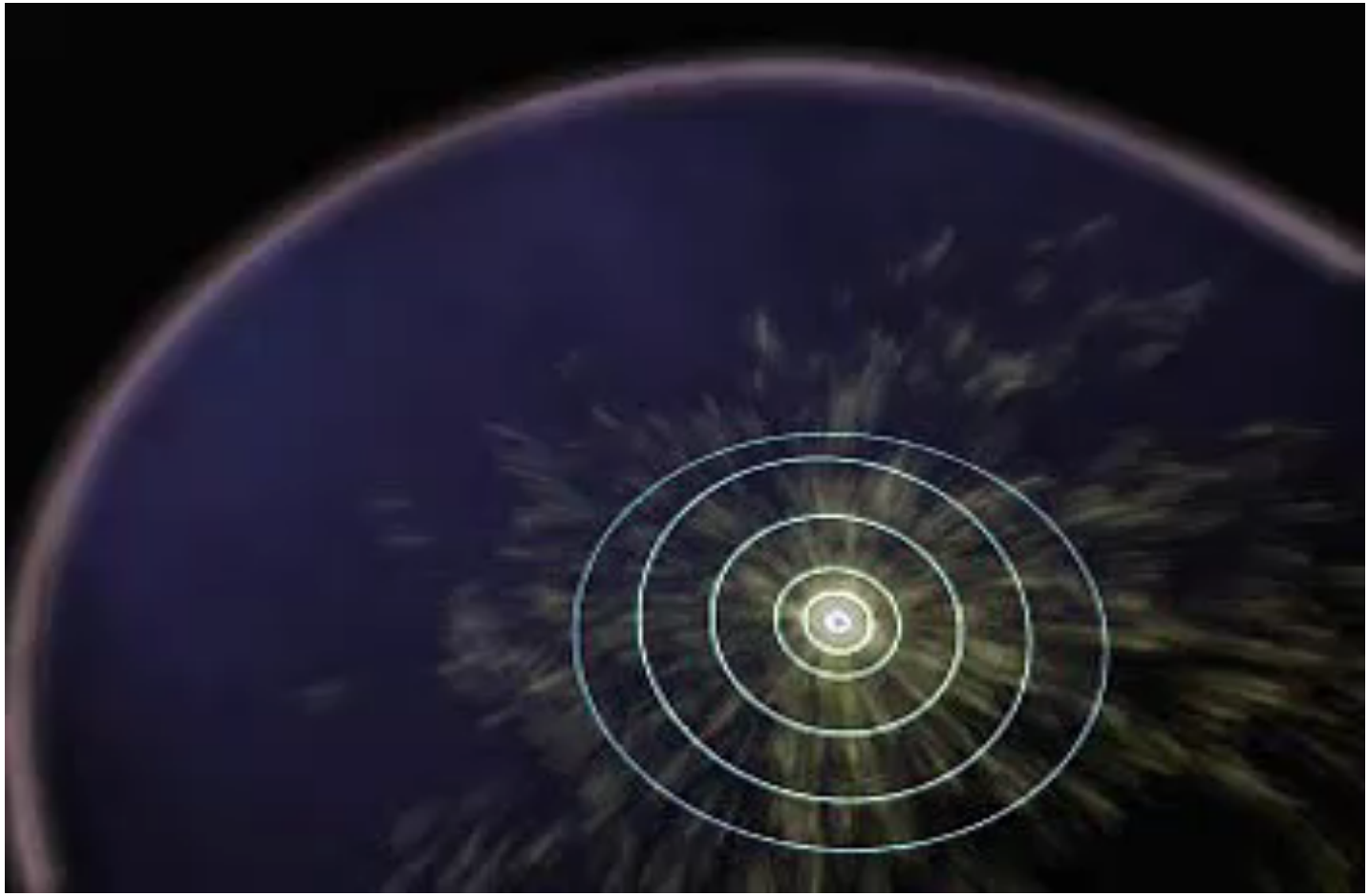

Animation showing the 2003 October November solar eruptions (based on Voyager 1 and 2 observations). Demonstrates the impact of solar events throughout the heliosphere

# What is a CME?

CME can be defined as the outward moving material in the solar corona which is distinct from the solar wind

This image shows three main CMEs from The solar and Heliospheric Observatory (SOHO) mission's Large Angle and Spectrometric Coronagraph (LASCO)

SOHO Coronagraph movie

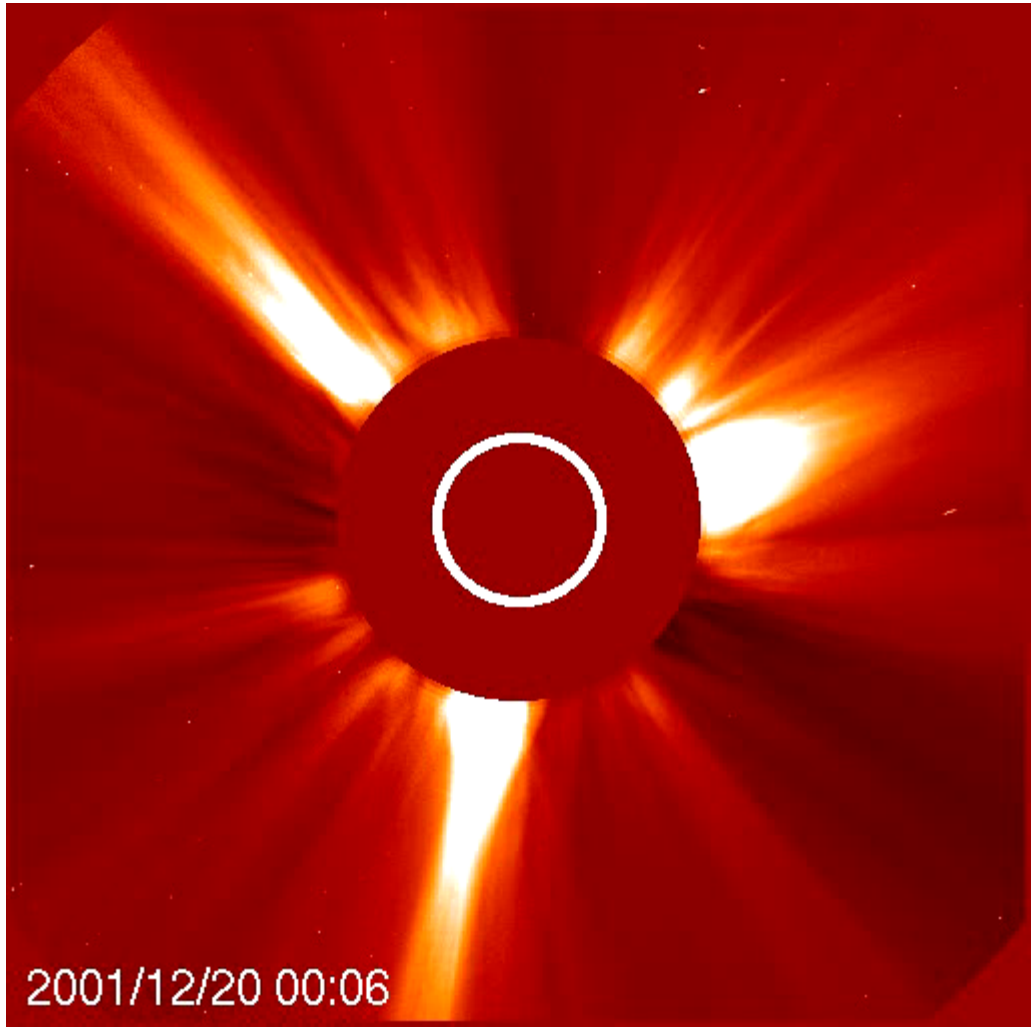

# Hindode Jets

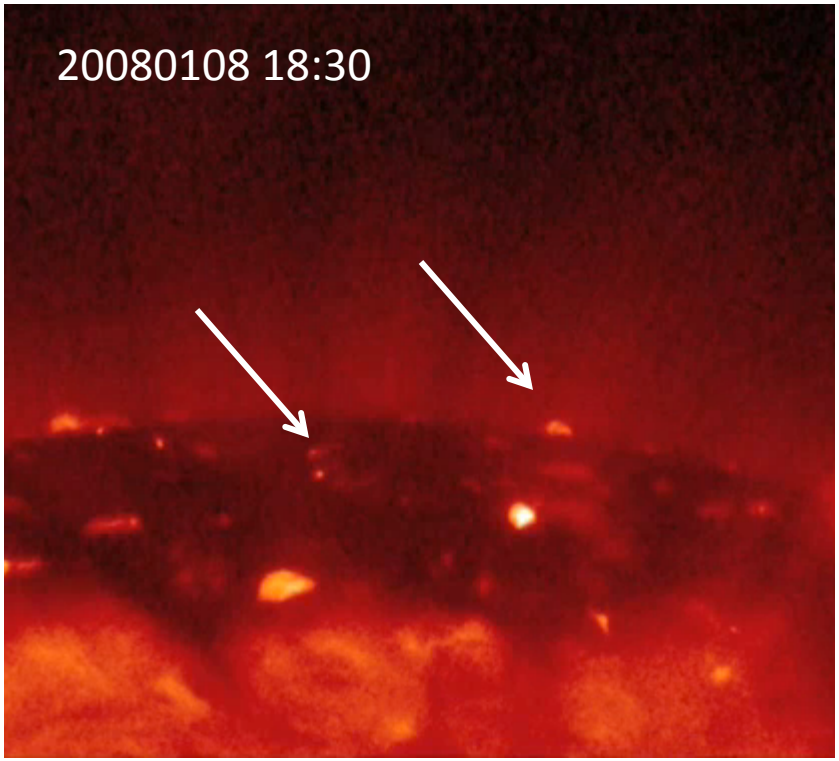


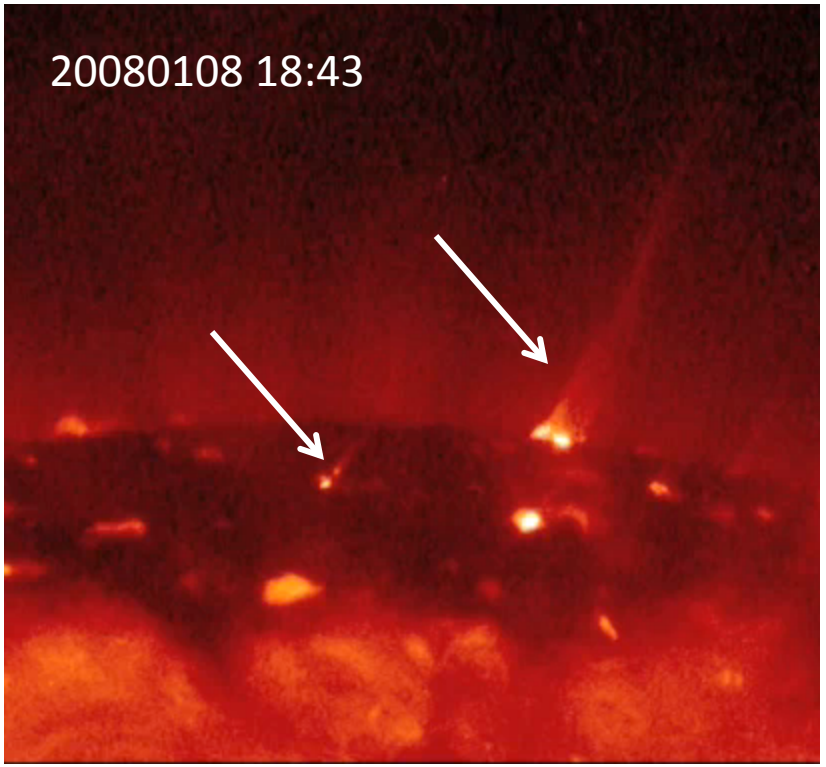

# Morphological Properties

CMEs have spatial structure:
bright front, dark void, & prominence core

When the CMEs are fast, they drive fast mode MHD shock

The shock can accelerate particles and produce sudden commencement when arriving at Earth

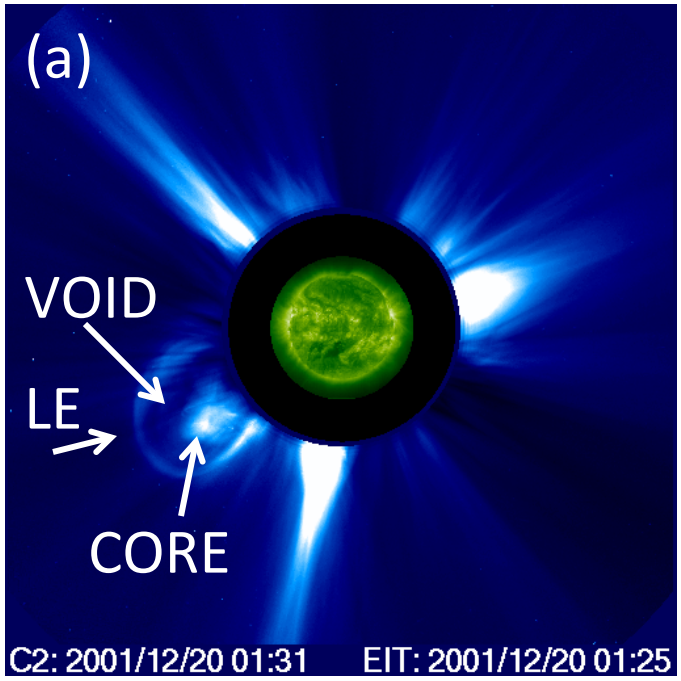


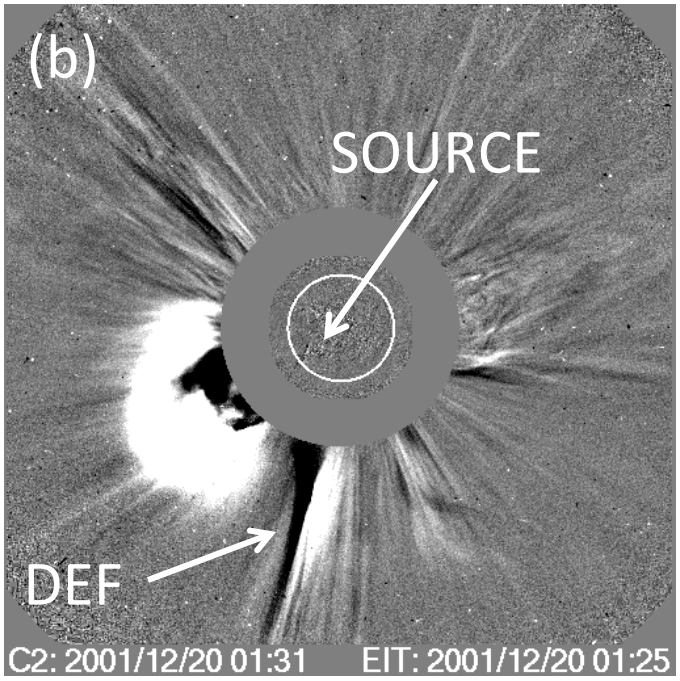


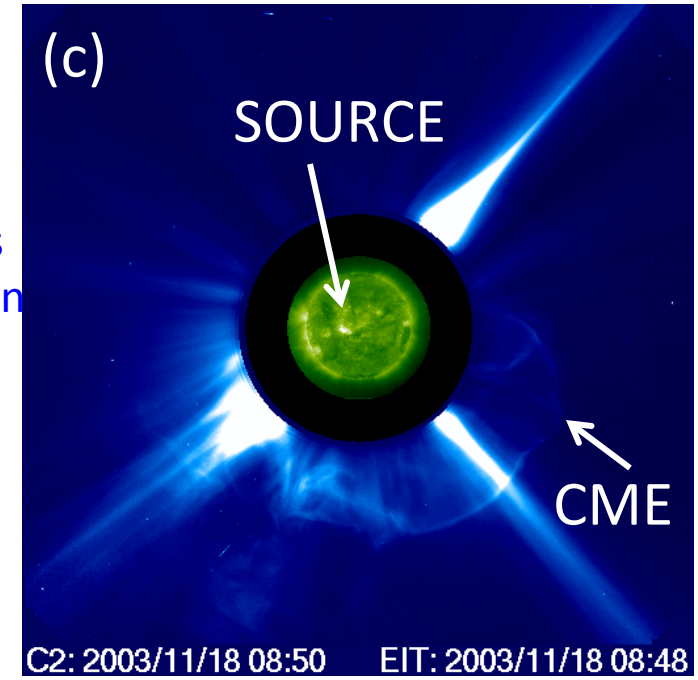


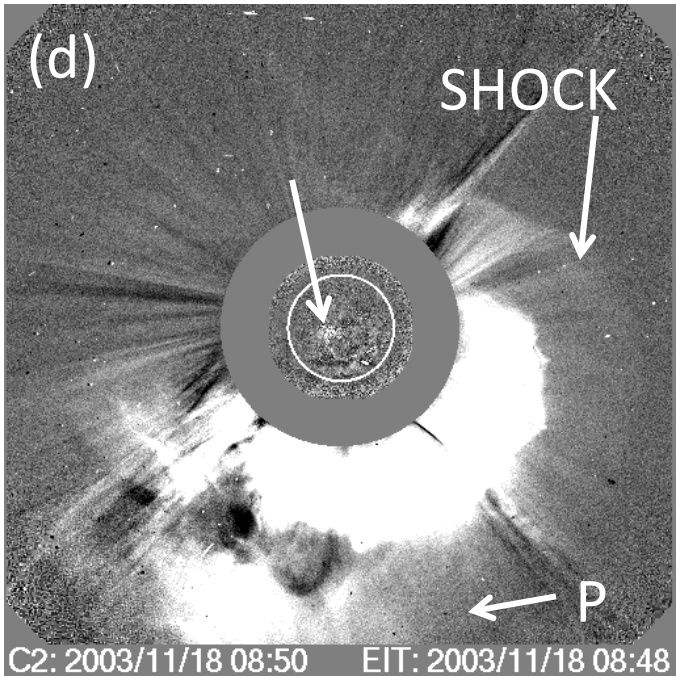

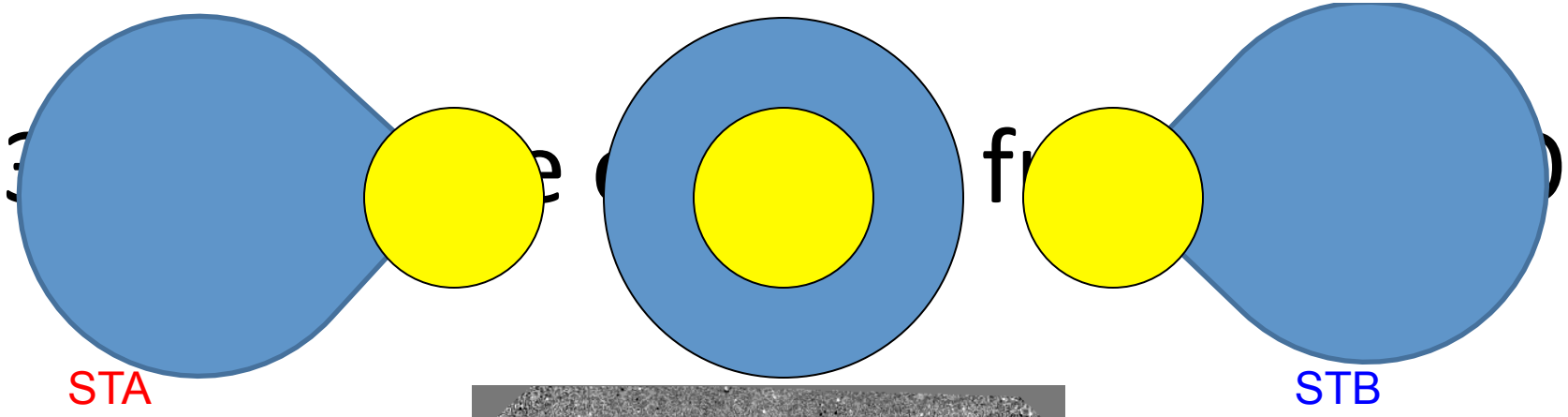


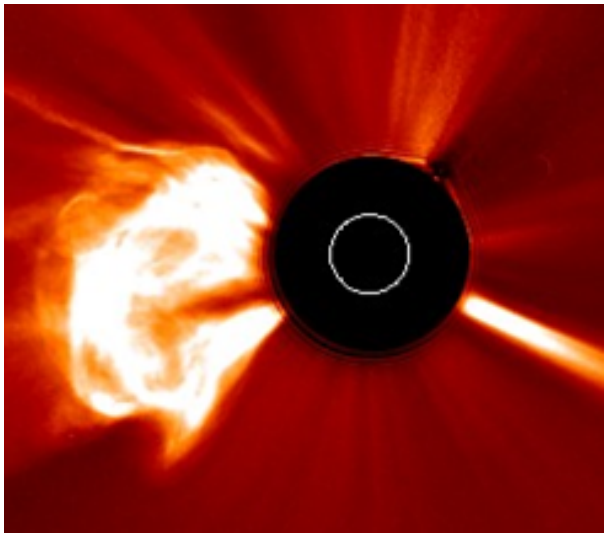

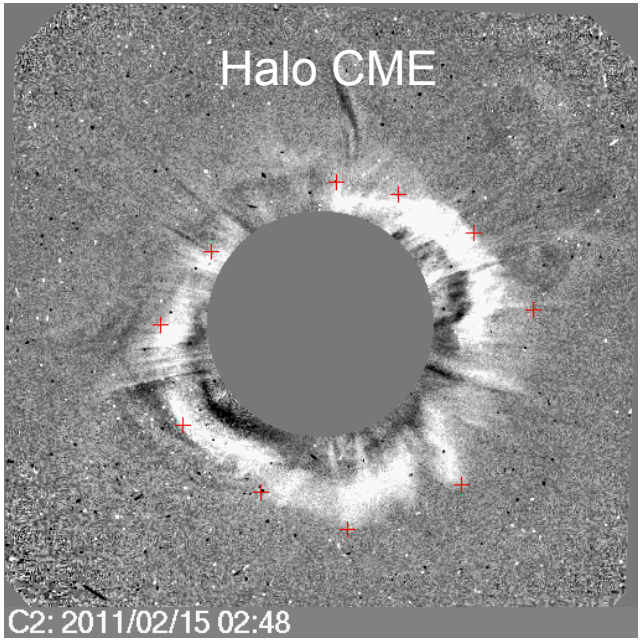


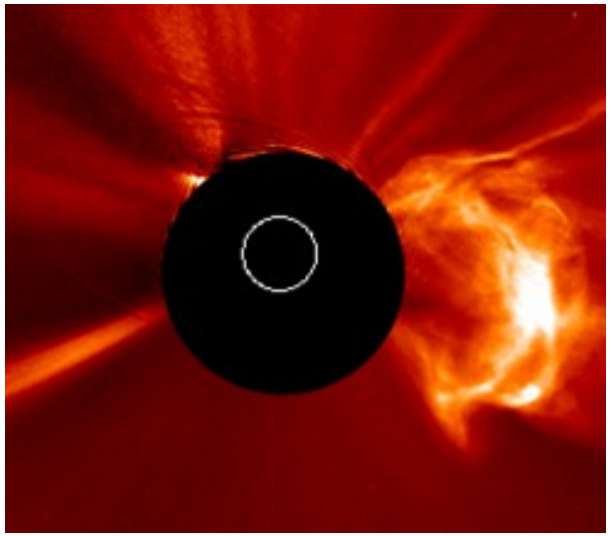

Limb CME

Limb CME

3-D Structure of CMEs: look like a balloon as is clear from three views

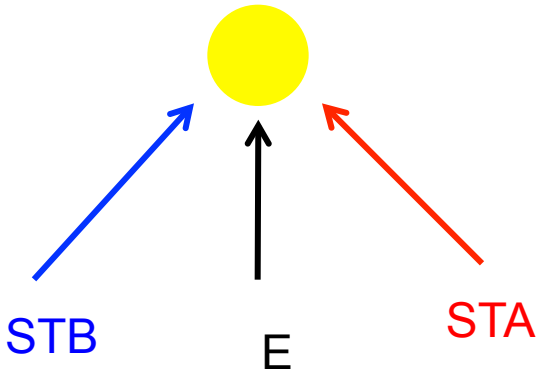


STEREO-A & B and SOHO coronagraphs

# Physical Properties

Three-part structure
Illing & Hundhausen, 1986

Four-part structure when shock driving

The bright front is thought to be material compressed by the flux ropes (dark void). Both are at coronal temperature but they have different densities

temperature and densities of various structures are shown

Coronagraph image + EUV image combined

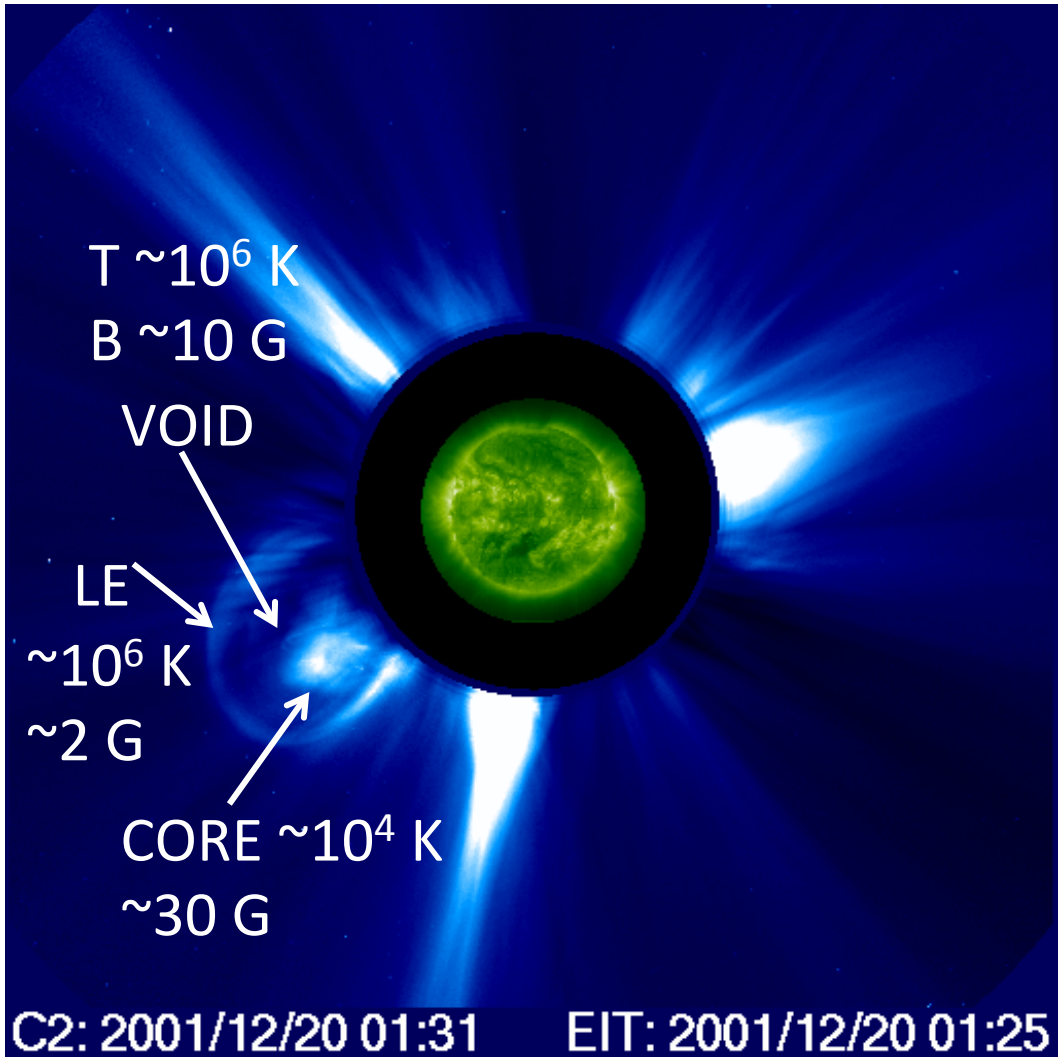

# Kinematic Properties

- Based on height-time measurements of CMEs at the leading edge.
- The measurements refer to the sky plane, so they may be subject to projection effects
- Linear fit to the height-time data points gives average speed within the coronagraphic field of view
- Quadratic fits give acceleration

# Basic Attributes of a CME:

## Speed, Width & CPA

Base Difference: $F_n - F_o$
Running Difference: $F_n - F_{n-1}$
$F_n$, $F_{n-1}$, $F_o$ are images at times $t_n$ , $t_{n-1}$ and $t_o$

CPA = Angle made by CME apex with Solar North

Width = PA2 – PA1

Speed = dh/dt
Acceleration = $d^2h/dt^2$

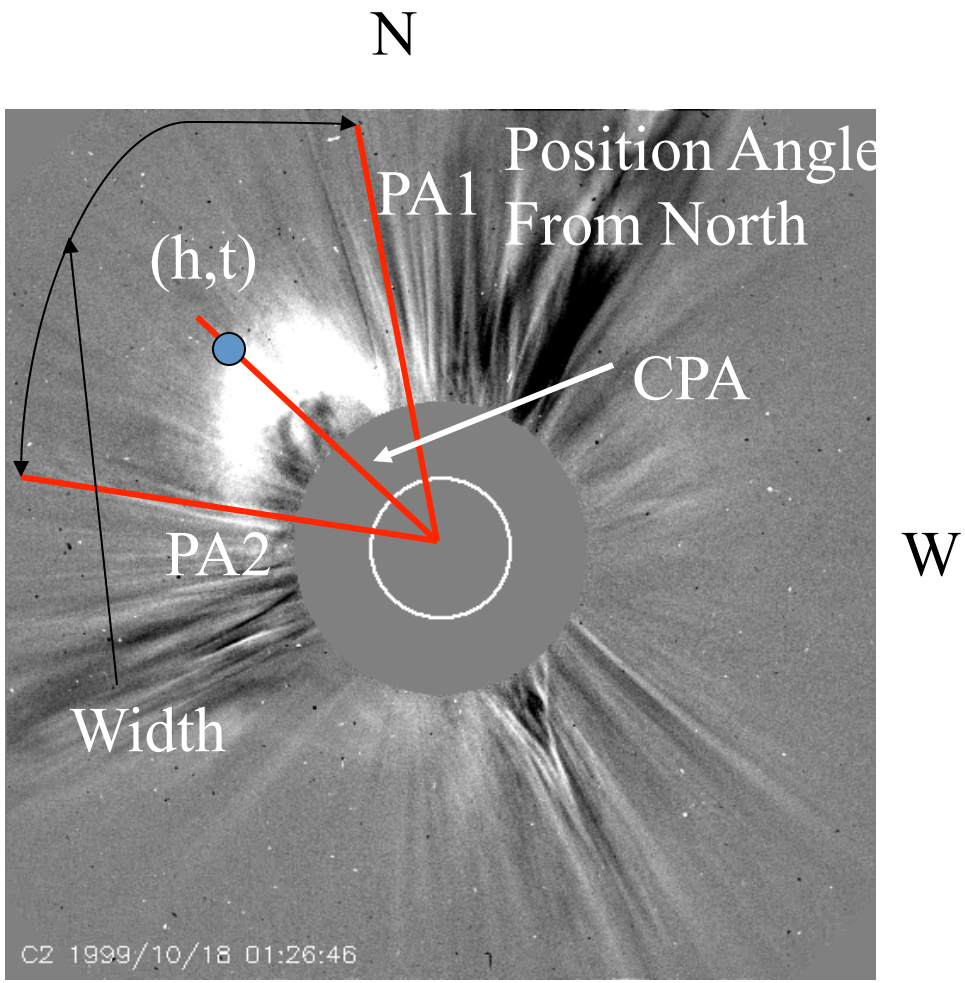


In the exercise session you will measure the speed and width of two CMEs

# Kinematic Properties: Speed & Width

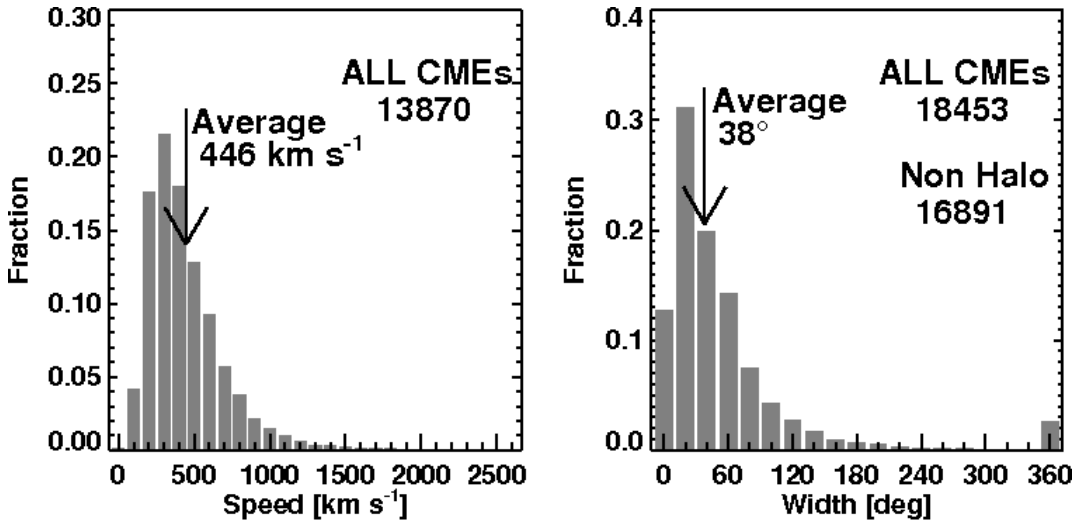

# Acceleration in LASCO C2/C3 FOV

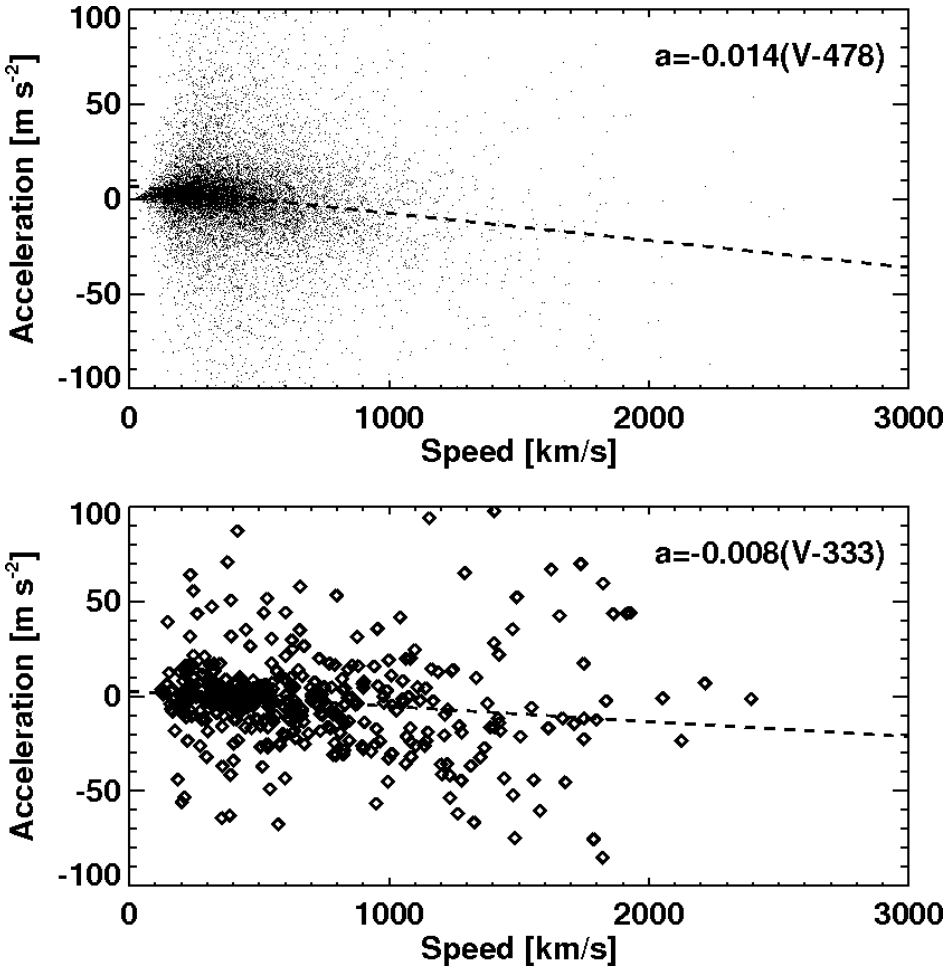


The measured acceleration is a combination of accelerations due to the propelling force, gravity, and aerodynamic drag.

$a = a_p - a_g - a_d$

In the SOHO coronagraph, the measurements are made beyond 2.5 solar radii

By this distance $a_p$ and $a_g$ are weakened significantly

So, the measured acceleration is therefore mostly due to aerodynamic drag:
$a = - a_d$
and is referred to as residual acceleration

$a_p$ can be 2-3 orders of magnitude higher than the residual acceleration.

# Acceleration from LASCO C1, EIT

Gopalswamy & Thompson 2000

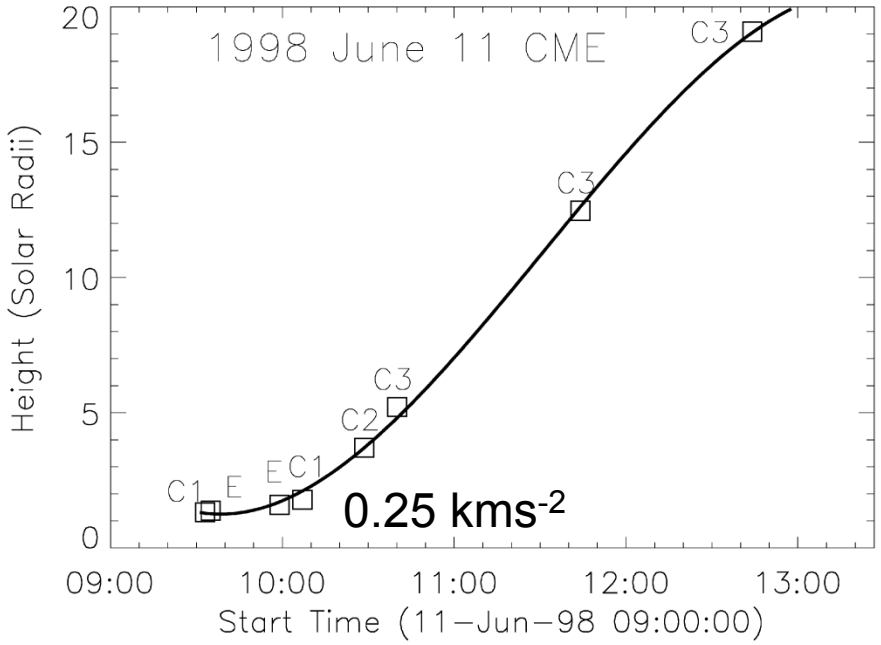


$$h = 3.1 - 0.1t + 1.5\times10^{-3}t^2 - 3.4\times10^{-6}t^3$$

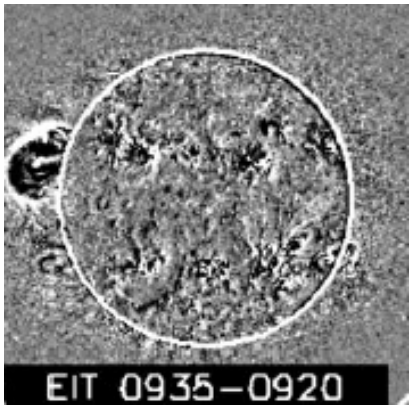


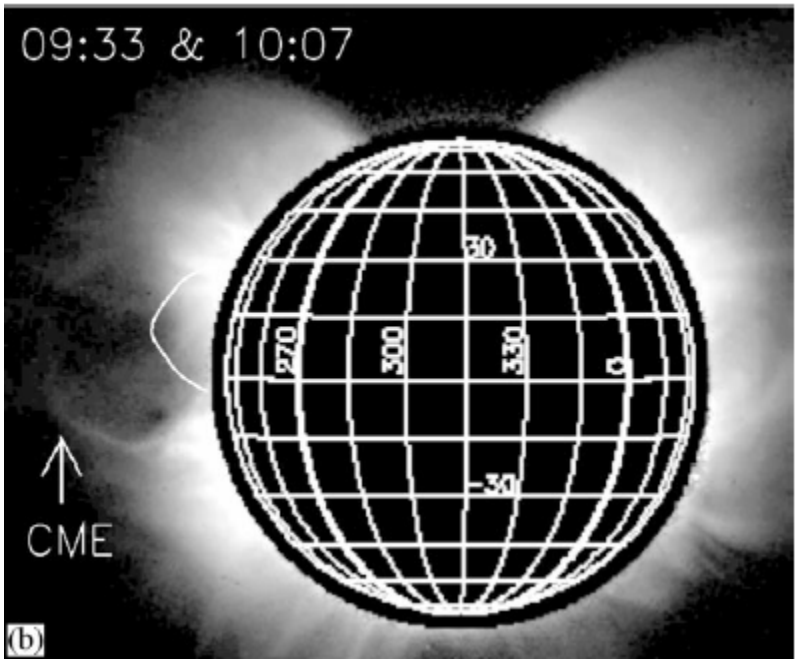


Before June 1998, SOHO had inner coronagraph that measured CMEs close to the surface. The height-time measurement can be fit to a 3rd order polynomial indicating early acceleration and later deceleration ($a_p$ = 0.25 kms$^{-2}$ and residual acceleration = -36 ms$^{-2}$ )

# Initial Acceleration of CMEs

Bein et al., 2011

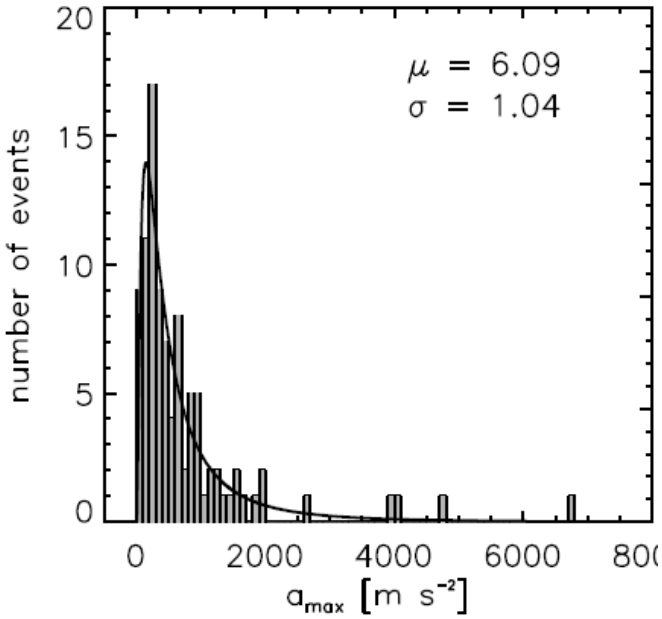


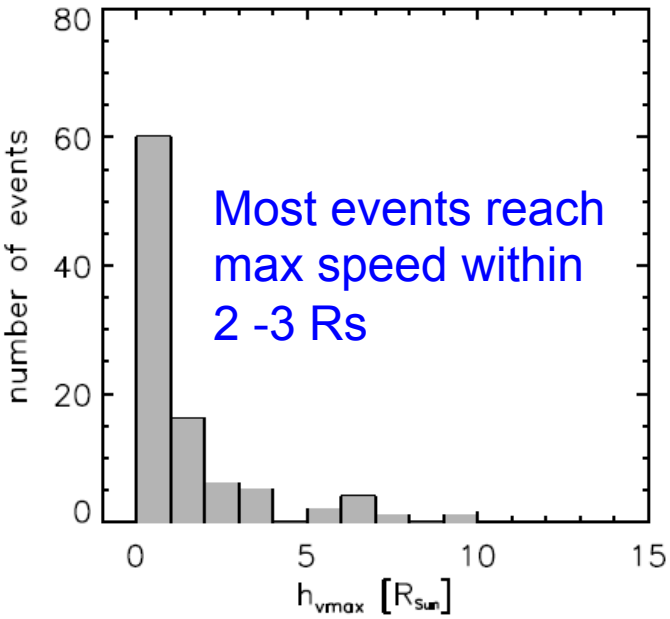


Gopalswamy et al. 2011

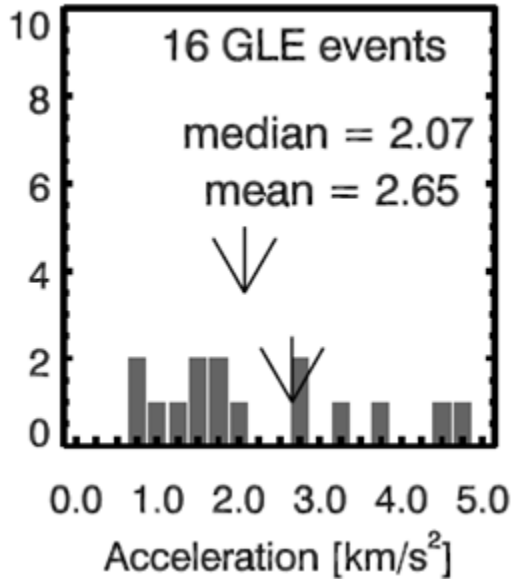


- STEREO/EUVI COR1
- 95 CMEs
- $a_{max}$: 0.02 to 6.8 kms$^{-2}$
- Height at Vmax: 1.17 to 11 Rs

- Ultrafast CMEs
- CME acceleration = Flare acceleration
- $a$: 0.5 to 7.5 kms$^{-2}$

# Mass & Kinetic Energy

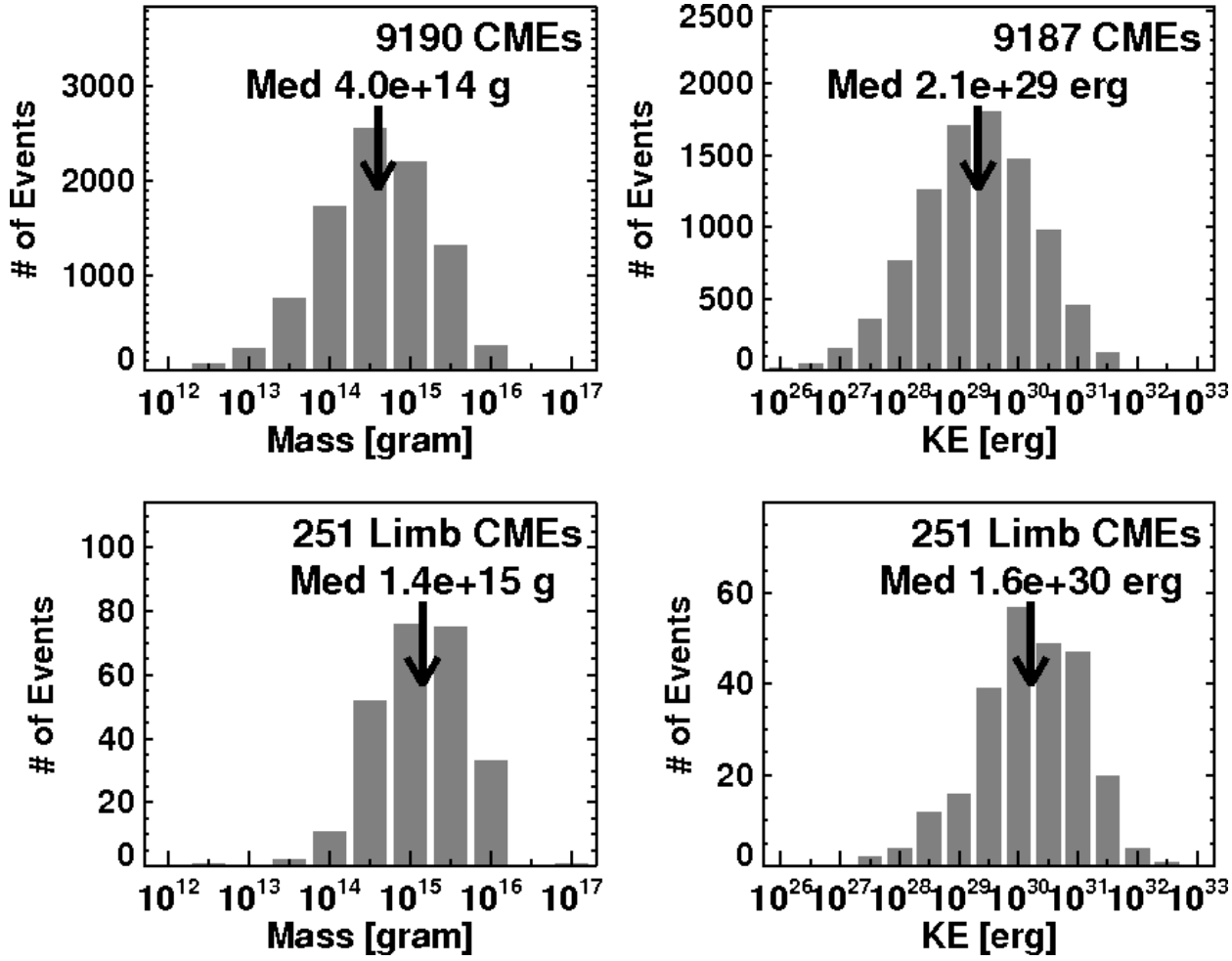


The CME mass can be determined from the excess brightness due to the CME and how many electrons are needed to produce this brightness. Once the mass and speed are known, the CME kinetic energy can be determined. Limb CMEs give the true distribution because they are not subject to projection effects

# Solar Cycle Variation

- CMEs come from closed field regions on the Sun (e.g. Sunspot regions).
- CME speed and rate in phase with sunspot number (CME rate SSN are well correlated)
- There are exceptions especially during solar maximum phase
- Cycle 23 and 24 (when good CME observations are available) give details of this correlation

# CME Rate & Speed (Rotation Averaged)

#CMEs per year
~$10^3$

Mass per CME
~$4 \times 10^{14}$ g

Mass loss due to CMEs
~$4 \times 10^{14}$ kg.yr$^{-1}$
= $2 \times 10^{-16}$ Ms. yr$^{-1}$

Solar wind mass loss:
~$2 \times 10^{-14}$ Ms. yr$^{-1}$

During solar maximum, CME mass loss up to 10% of solar wind flux

Daily Rate

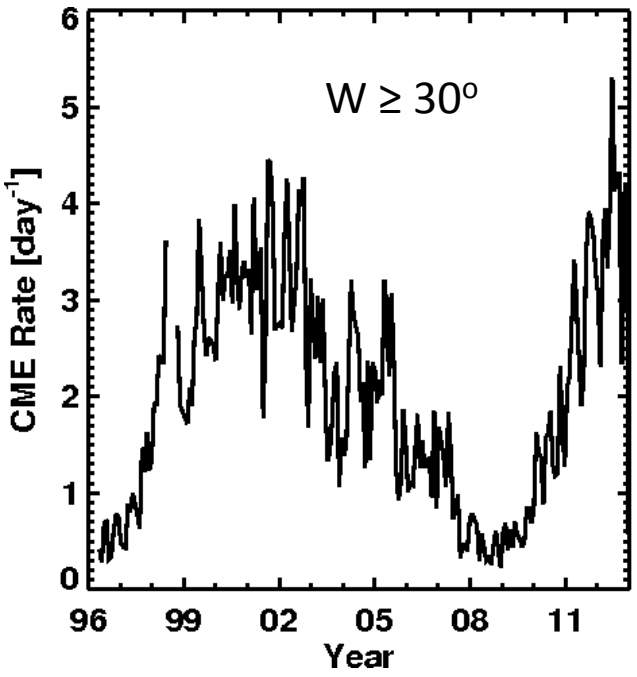


Average CME speed

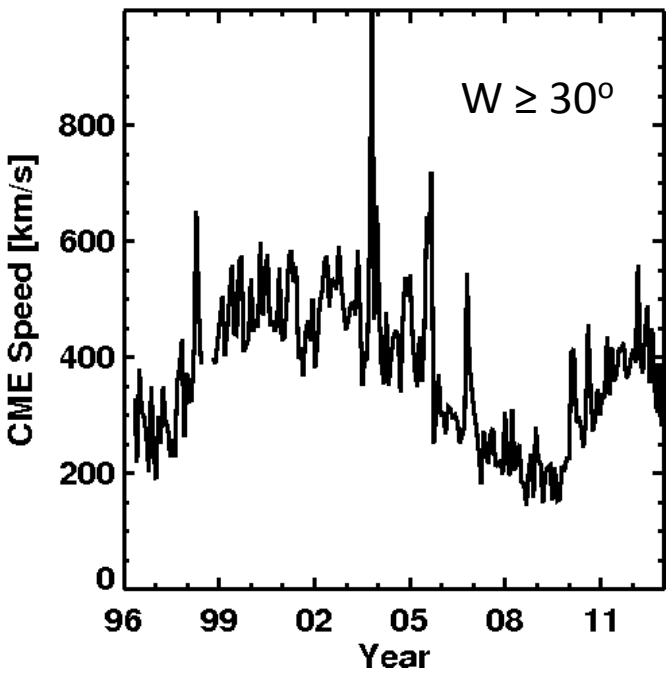


The rate is ~0.5 per day during the solar minimum and exceed ~4 per day during solar maximum

The CME speed also varies with solar cycle: CMEs are generally faster during solar maxima

# CME Rate Compared with Sunspot Number (SSN)

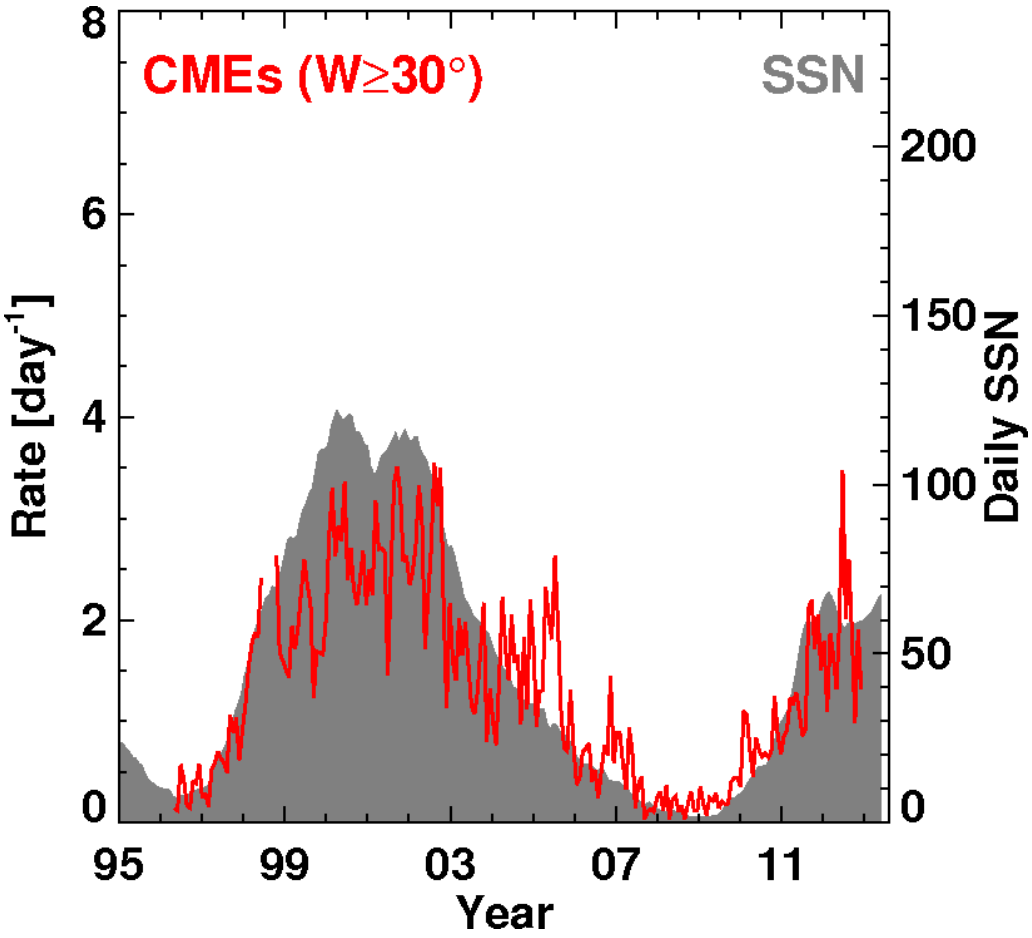


Over all similarity between CME rate and sunspot number

Many deviations

CME rates are similar between cycles 23 and 24

The sunspot number is smaller:

The Sun is in a strange state

# CME Rate well correlated with SSN

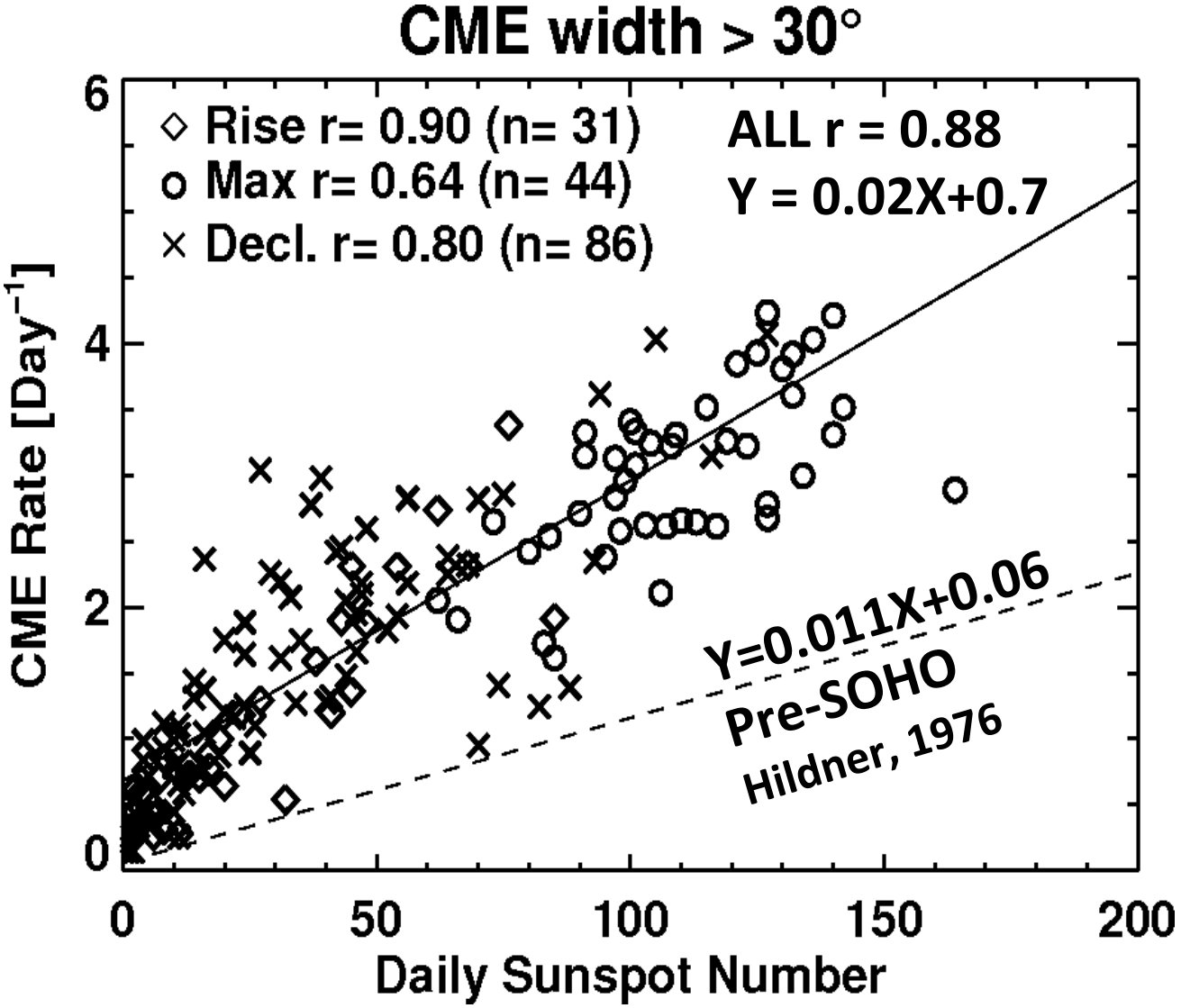


Weaker correlation during maximum phase: CMEs from outside sunspots – Polar crown filaments

The pre-SOHO (SMM, Solwind) data indicate a smaller slope because of the lower sensitivity and smaller field of view compared to the LASCO coronagraphs.

# Prominence Eruption Sites

Prominence eruptions can be used to track the rush to the poles & max phase

Low level of activity during cycle 23/24 minimum

Severe north-south asymmetry

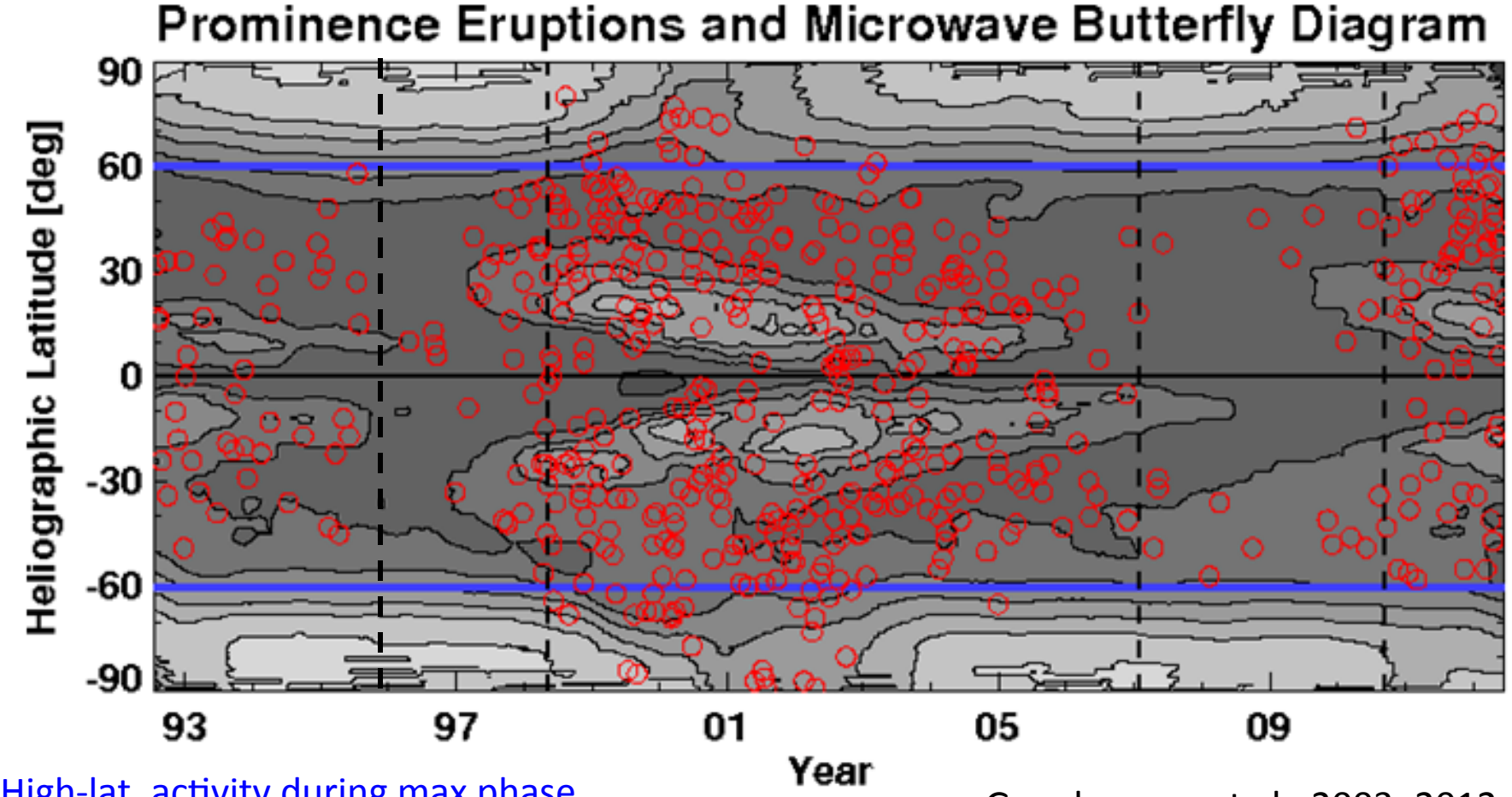


High-lat. activity during max phase

Gopalswamy et al., 2003; 2012

# Halo CMEs

- CMEs that appear to surround the occulting disk in sky-plane projection
- No different from other CMEs, except that they must be faster and wider on the average to be visible outside the occulting disk
- Halos affect a large volume of the corona
- Most of the halos may be shock-driving
- Halos can be heading away or toward Earth. Those heading toward Earth are important for space weather

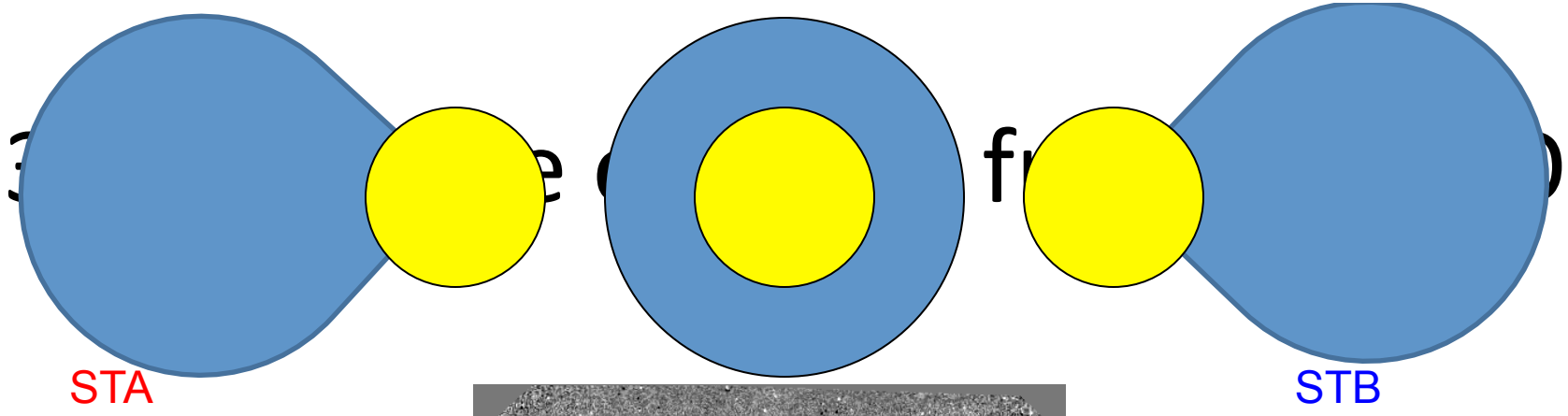


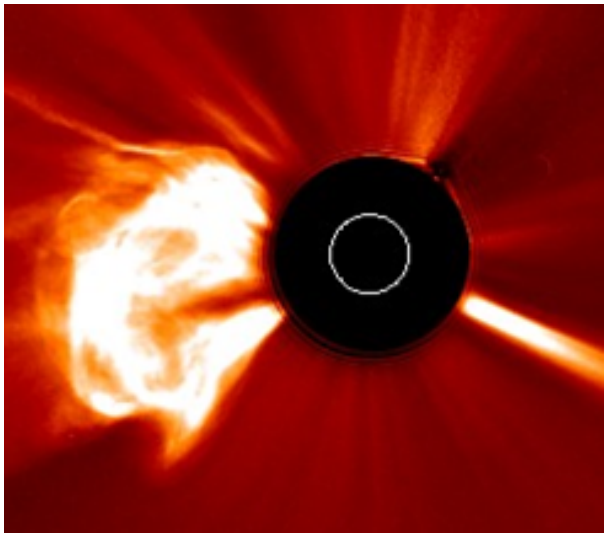

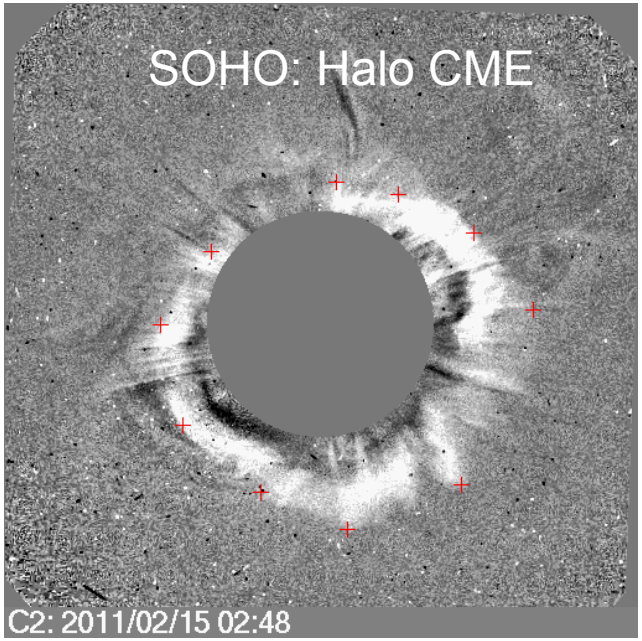


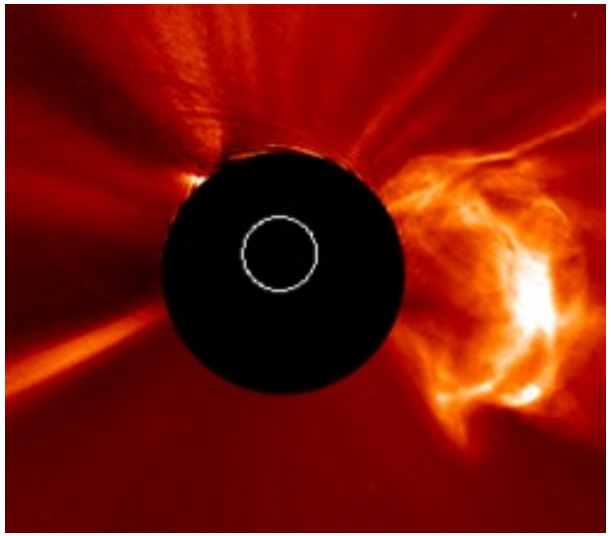

Limb CME

Limb CME

3-D Structure of CMEs

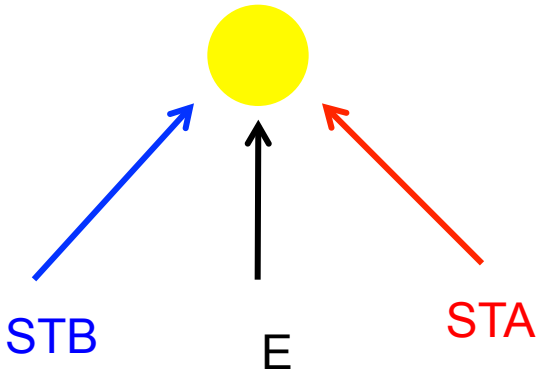


Simultaneous STEREO and SOHO observations demonstration that halo CMEs are normal CMEs

# Halo CMEs

Halo CMEs, discovered in Solwind data (Howard et al. 1982), have been recognized in the SOHO era as an important subset relevant for space weather (Gopalswamy et al., 2010)

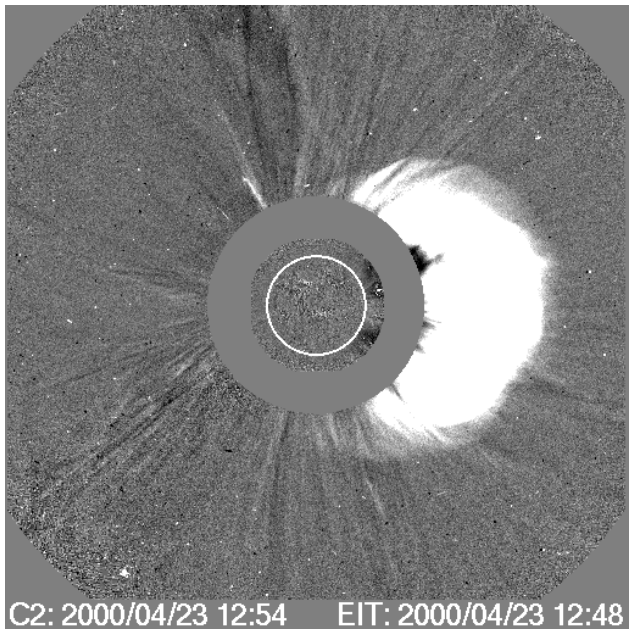


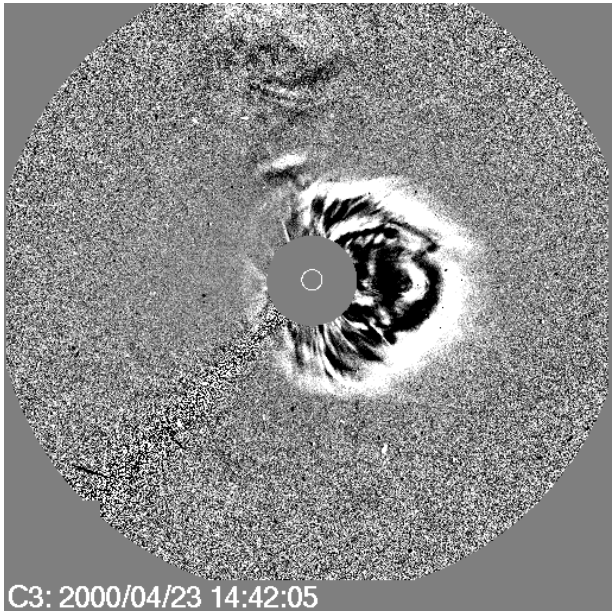


Partial halo becomes asymmetric halo

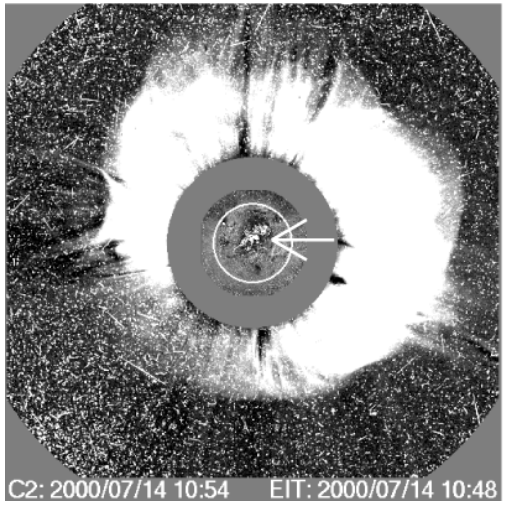


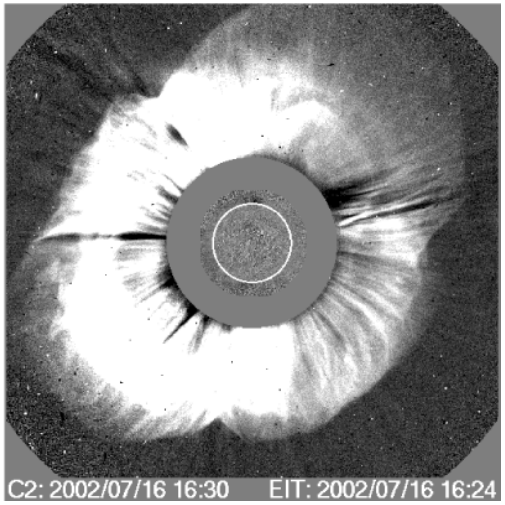


Front-side halo back-side halo

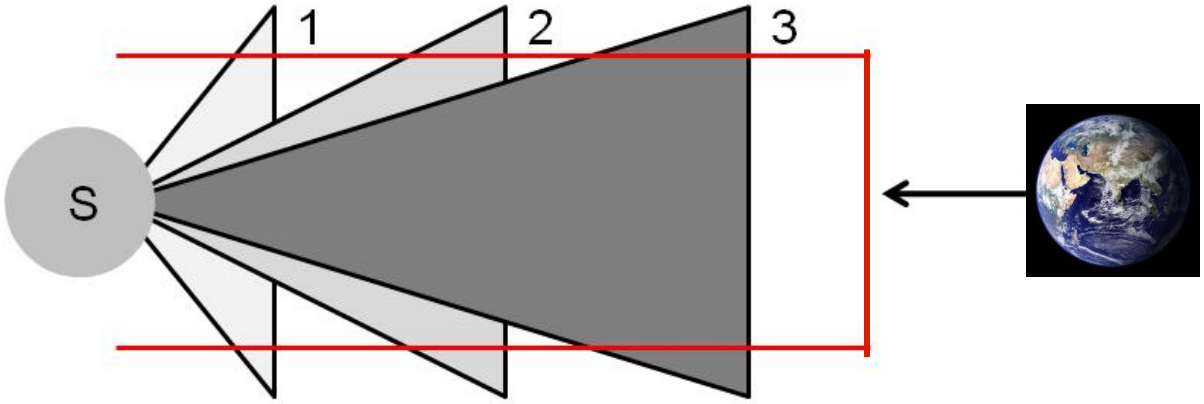

# Halo CMEs are generally wide

The three cones 1, 2, 3 represent 3 CMEs

Frontside halos (earth-directed)

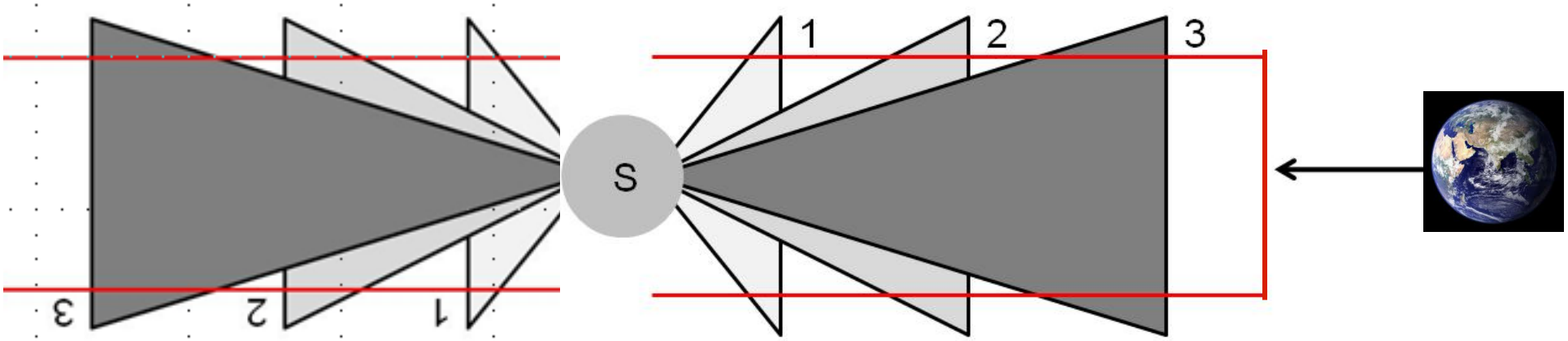


backside halos
(anti-earthward)

Portions outside the red lines appear as halos
1, 2, 3 represent three CMEs with decreasing widths. 1 will appear as halo immediately. 3 has to travel a long distance before appearing as halo. Some may never become a halo or fade out before becoming a halo.

# Halo CME Properties

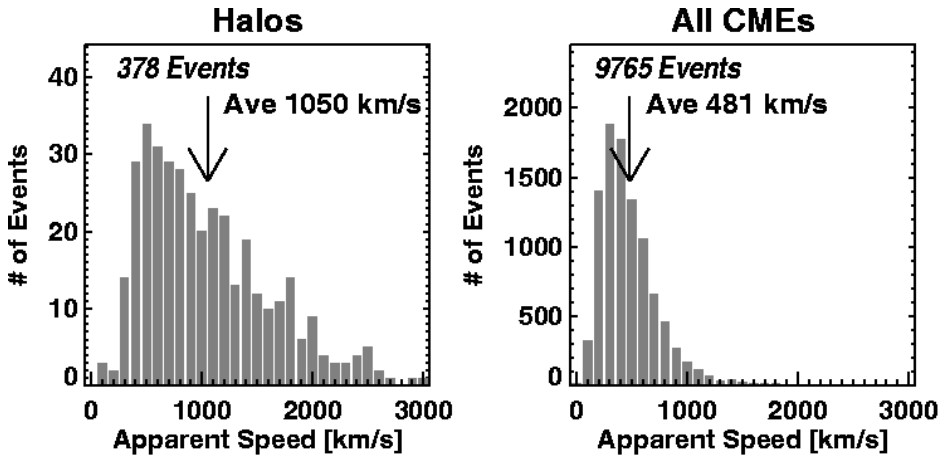


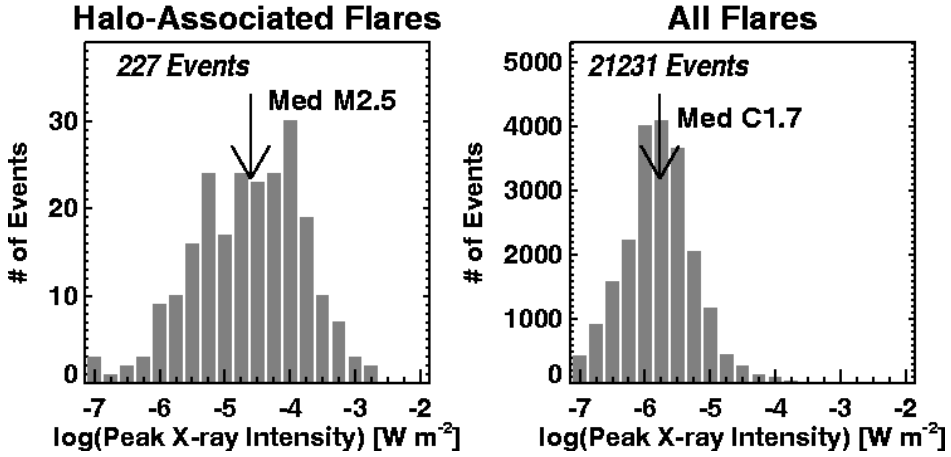


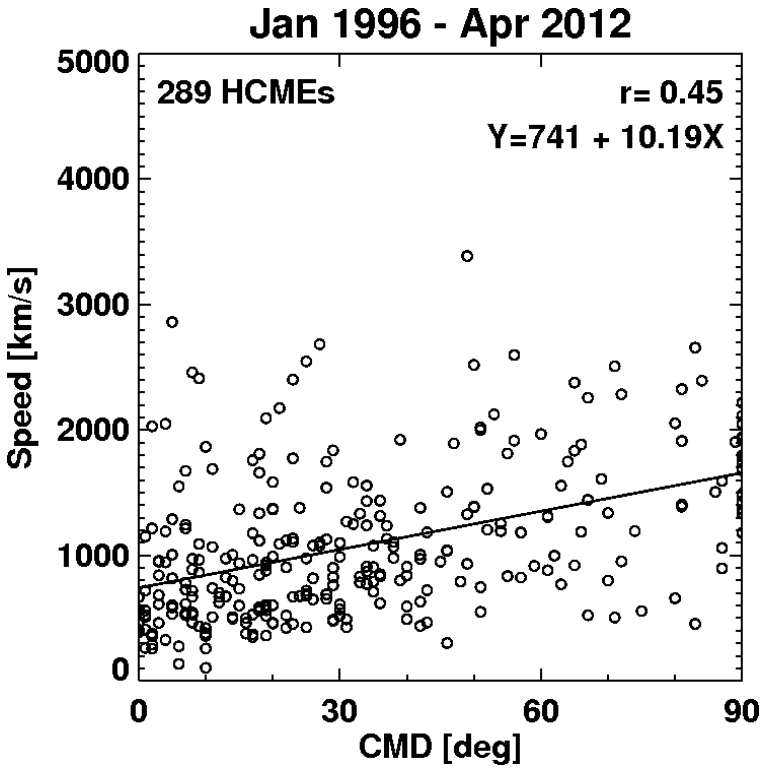


Only ~3.5% of all CMEs are halos

Halos are ~ 2 times faster than the average CME (halo CMEs are subject to large projection effects)

Flares associated with halo CMEs are larger

Higher kinetic energy: travel far into the interplanetary medium and impact Earth

# Faster and Wider CMEs are More Energetic

Wider CMEs are faster

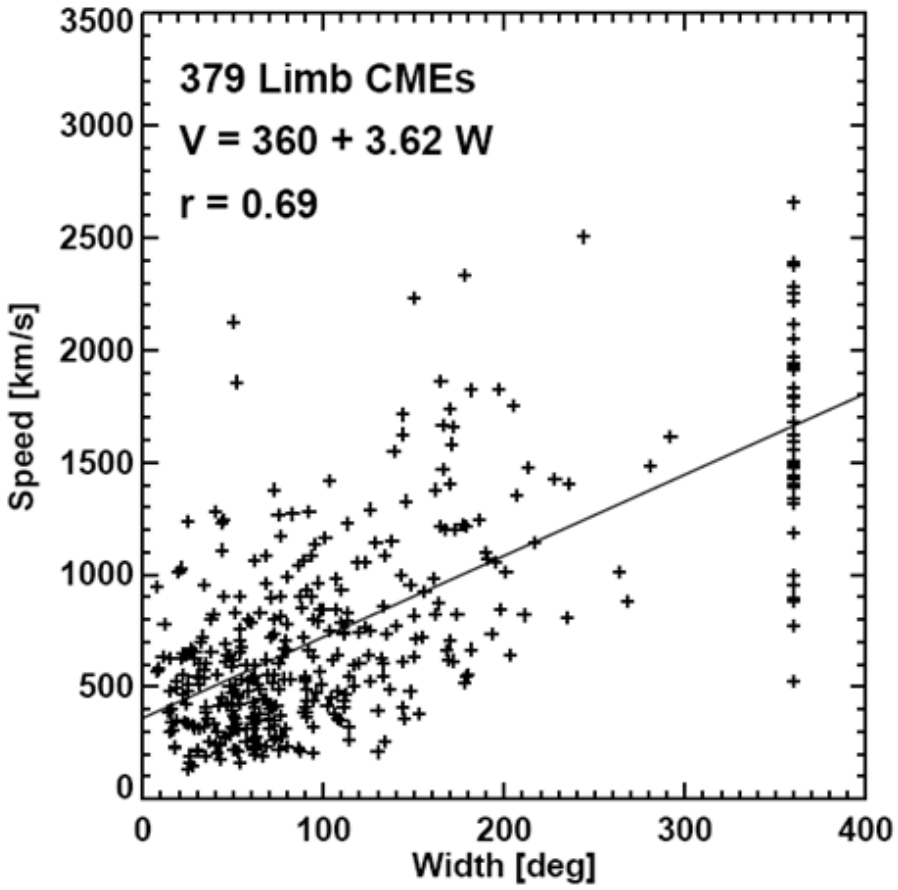


Wider CMEs are more massive

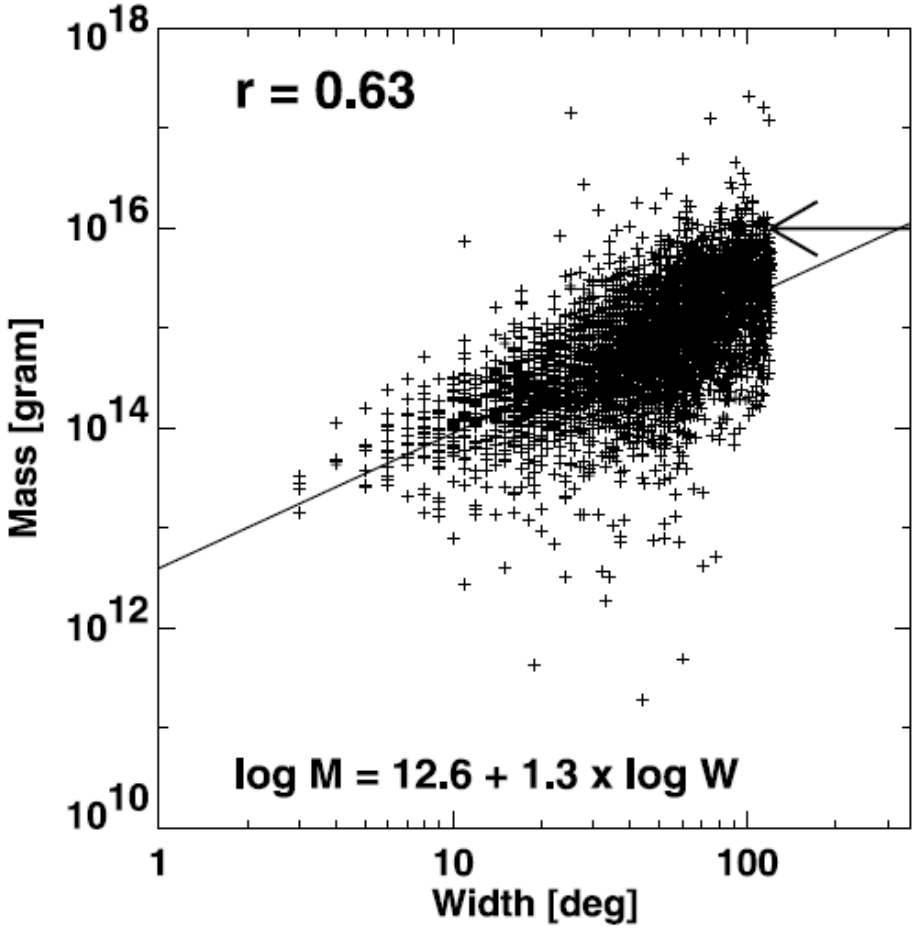


Halo CMEs are more energetic

Fraction of halos is a measure of the energy of a CME population

# Halo Fraction of Some CME Populations

**Table 1** Speed and width of the special populations of CMEs

| | Halos | MCs | Non-MCs | Type IIs | Shocks | Storms | SEPs |
|---|---|---|---|---|---|---|---|
| Speed (km $s^{-1}$) | 1,089 | 782 | 955 | 1,194 | 966 | 1,007 | 1,557 |
| % Halos | 100 | 59 | 60 | 59 | 54 | 67 | 69 |
| % Partial halos | – | 88 | 90 | 81 | 90 | 91 | 88 |
| Non-halo width (°) | – | 55 | 84 | 83 | 90 | 89 | 48 |

Gopalswamy et al. 2010

# Solar Source Regions

- CMEs originate from closed magnetic field regions (bipolar or multipolar configurations)
- Active regions
- Filament regions
- Loops connecting two active regions
- CME source regions are easily identified from the associated flare (close connection between CMEs and flares)

# An Eruption Region

Photospheric Magnetogram

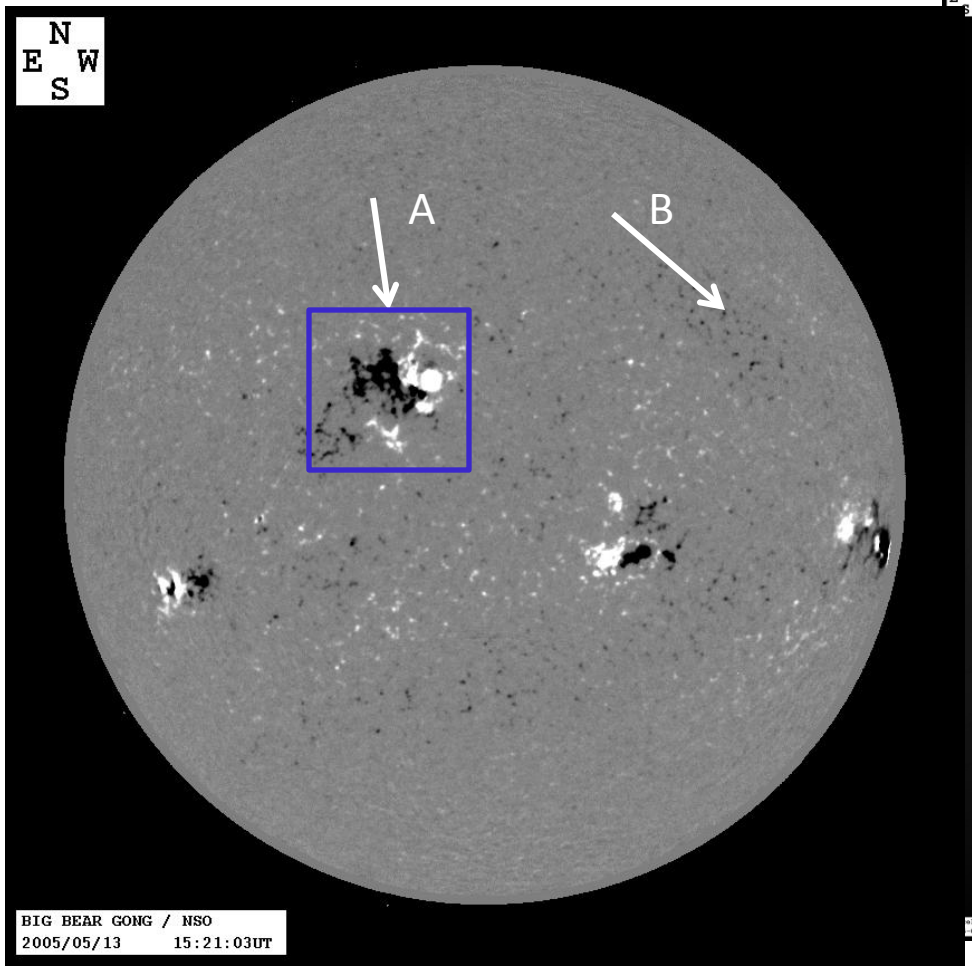


Chromosphere (H-alpha)

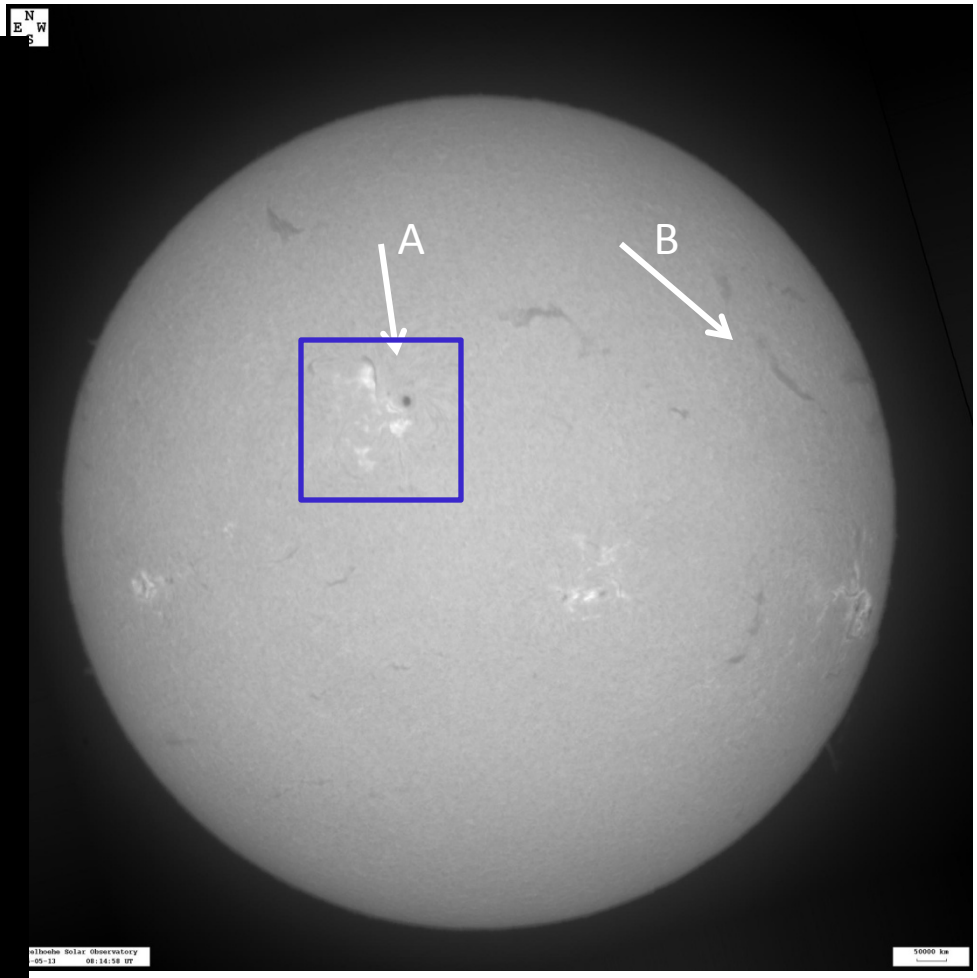


A: active region

B: Filament region (also bipolar, but no sunspots)

Both regions have filaments along the polarity inversion line

# The Sunspot Region “A” Erupts

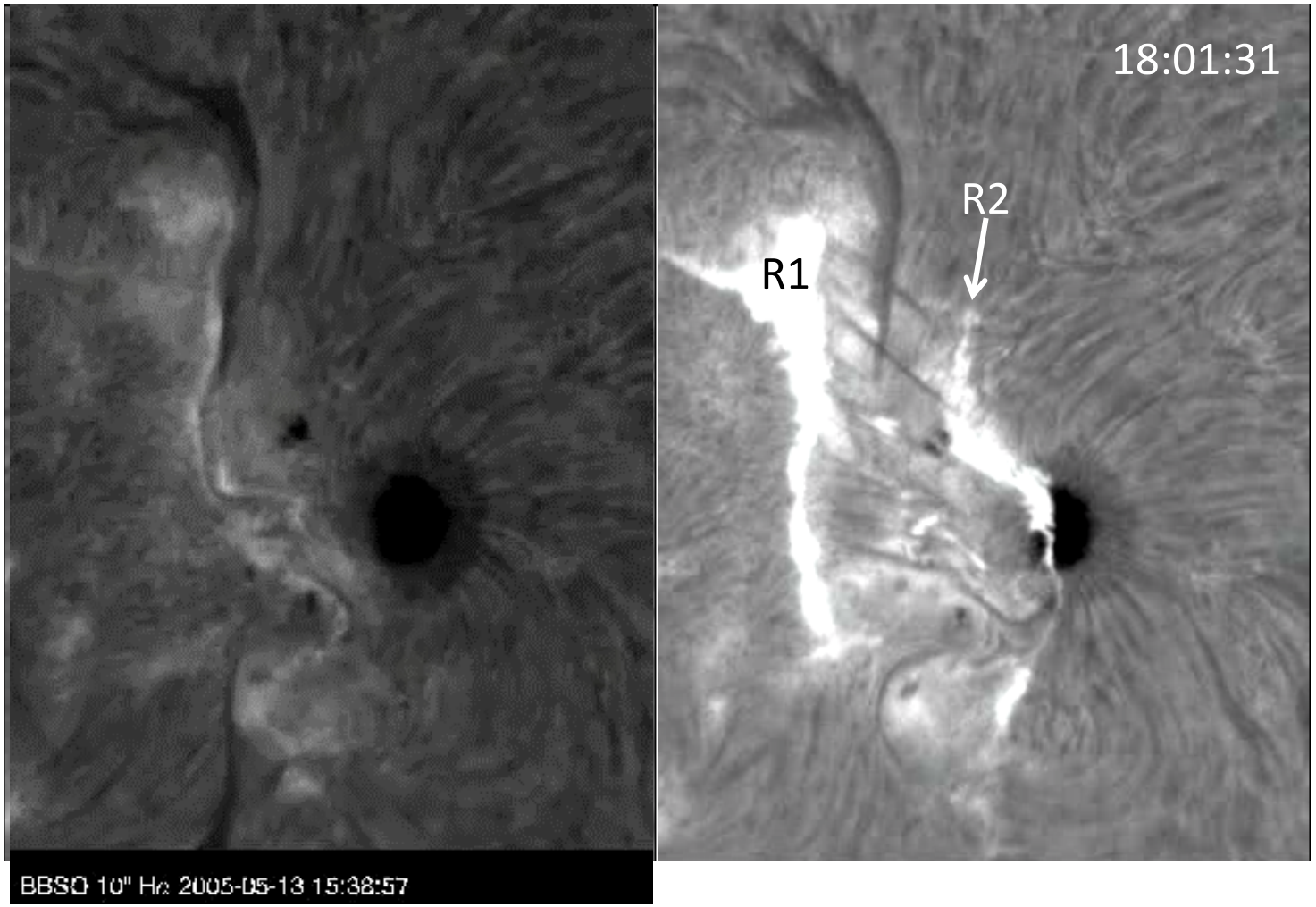


There is also wave going away from the eruption region. Part of the filament disappears

Flare arcade

# Filament eruption

Difference image (SOHO/EIT)

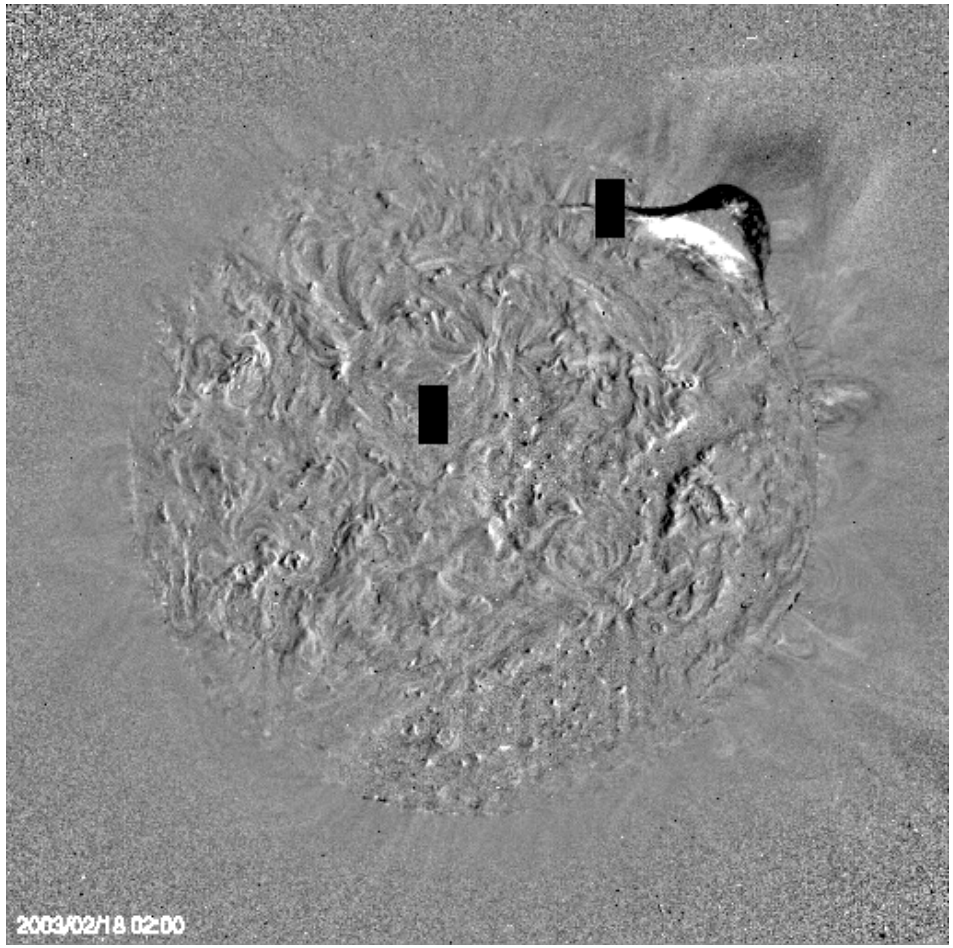


Flare from a non-sunspot region

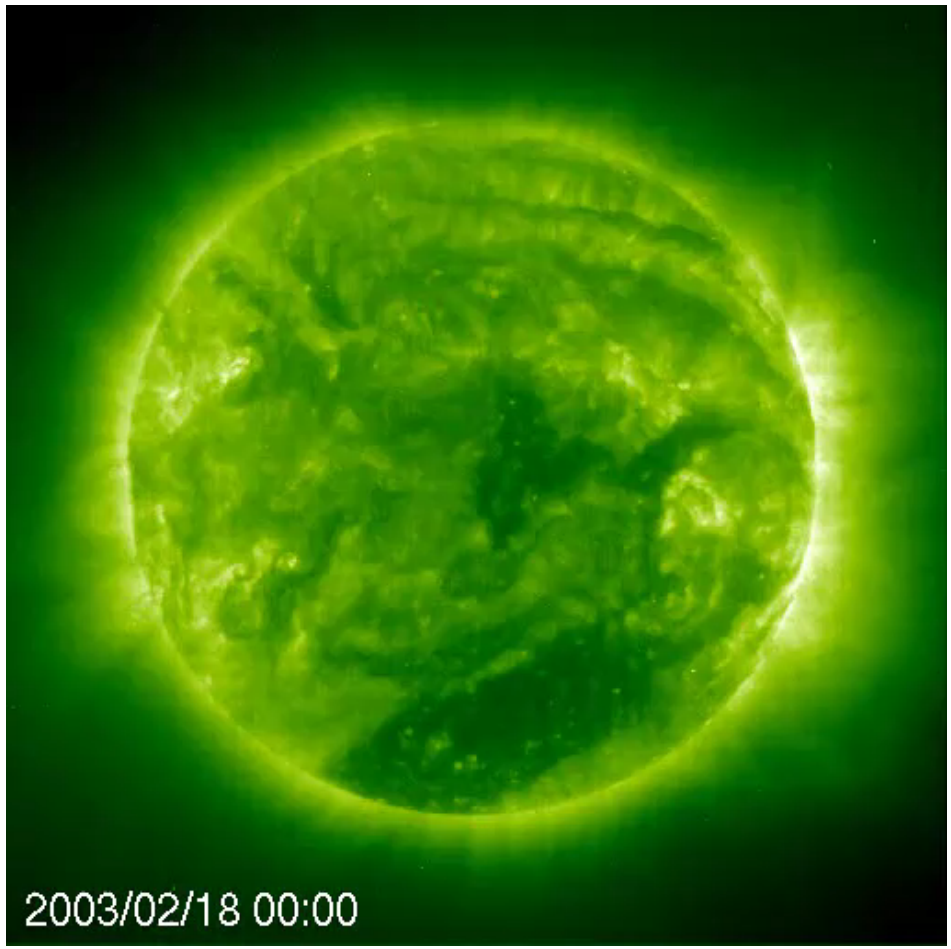


Note the CME overlying the filament in EUV

# Filament Eruption in EUV

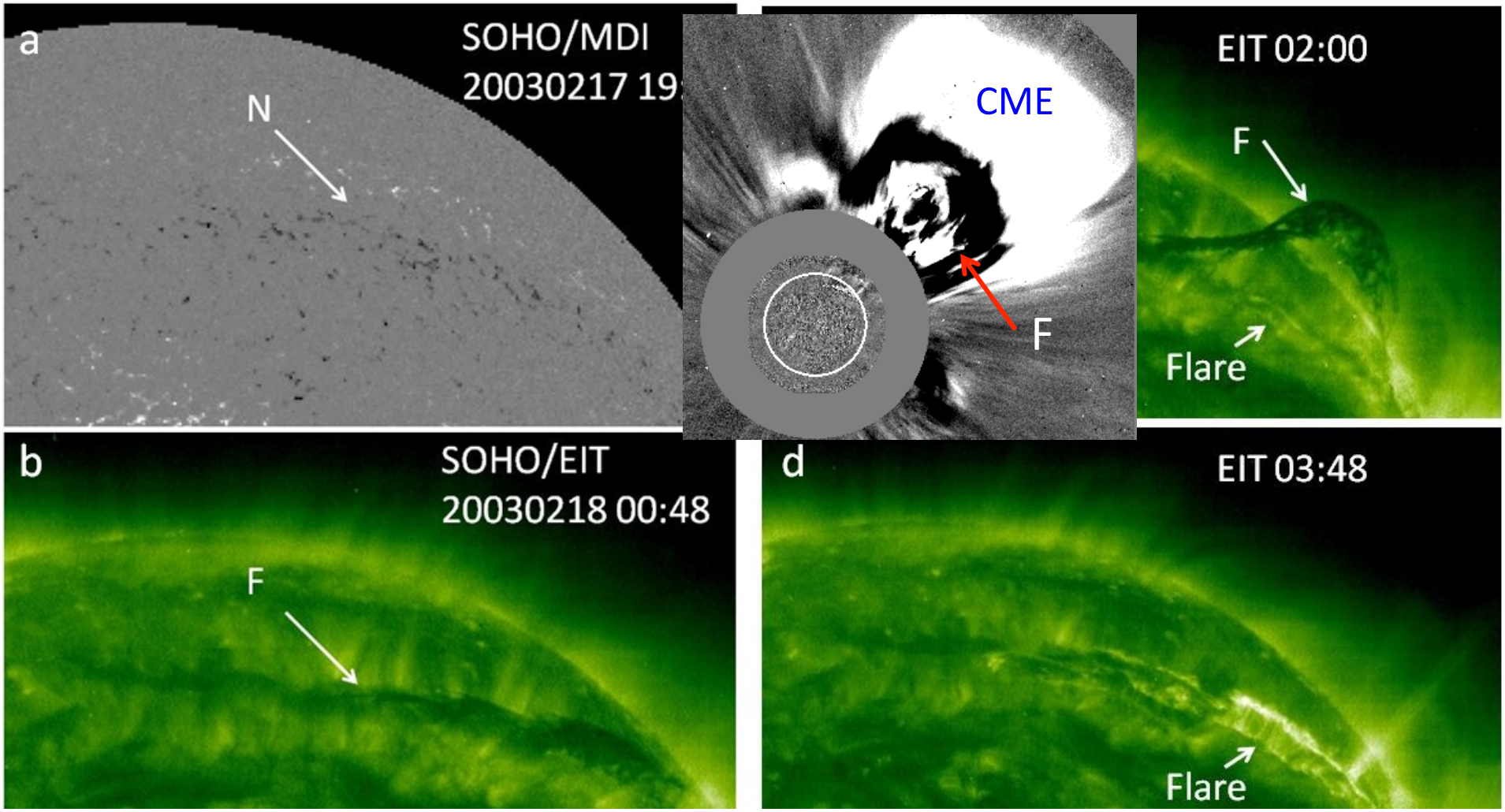


Filament (F) along neutral line (N). Flare loops under F; F becomes substructure of CMEs

# Coronal Dimming and Eruption Geometry

PIL – polarity inversion line (between + and -)
D1, D2 – dimming regions in which the flux rope (FR) is rooted
PEL – post eruption loops
R1, R2 – flare ribbons with hard X-ray (HXR) and microwave (μ) source locations.

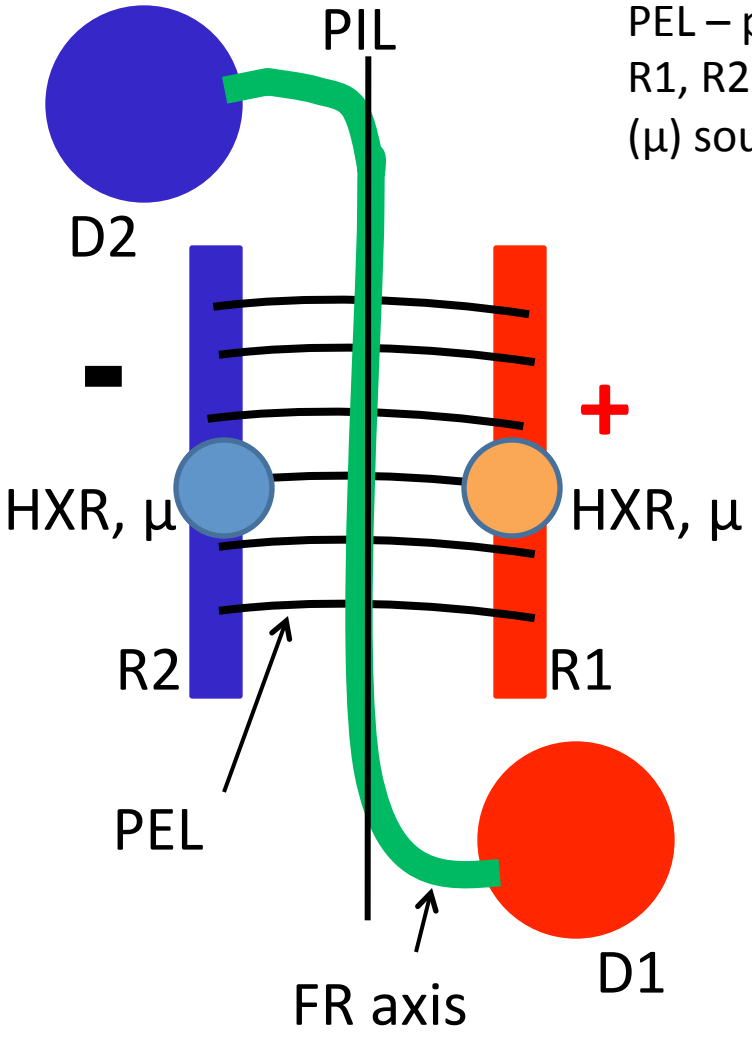


FR

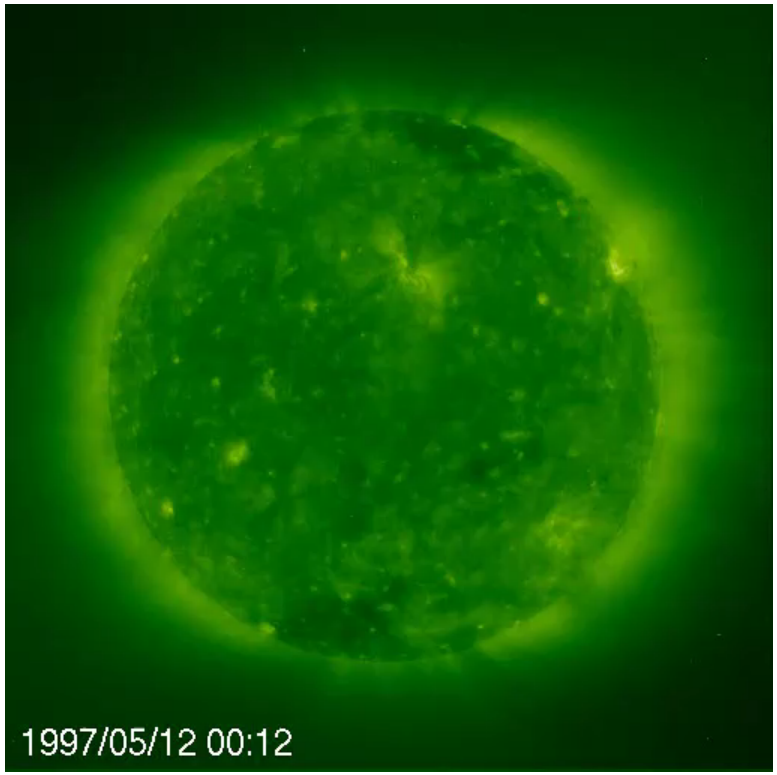


Dimming: Sites of flux rope legs?

# Where does the energy come from?

Extrapolated field lines on TRACE coronal images

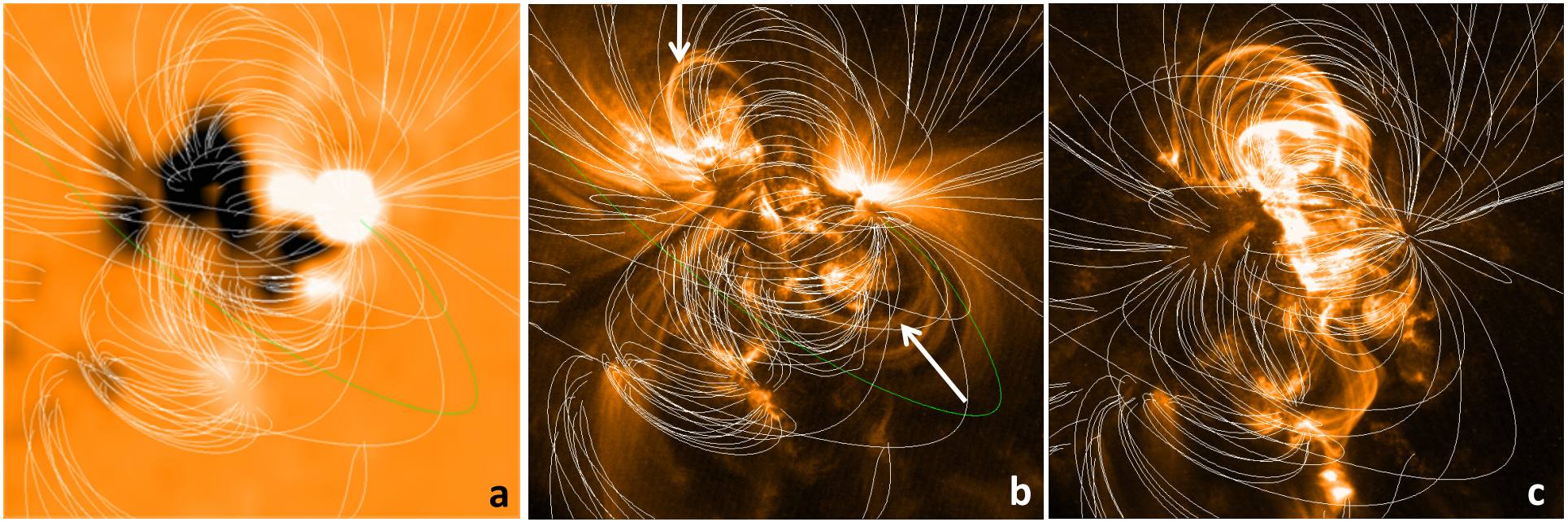


2005/05/13 14:56:00

Photospheric magnetogram with potential field extrapolation

2005/05/13 15:25:56

Actual coronal structure is "distorted" from potential field → free energy (FE)
Distortion due to current J.
Lorentz force JxB propels the CME

2005/05/13 21:26:36

Free energy went into the CME kinetic energy
Arcade is now potential (no more current J)

De Rosa & Schrijver

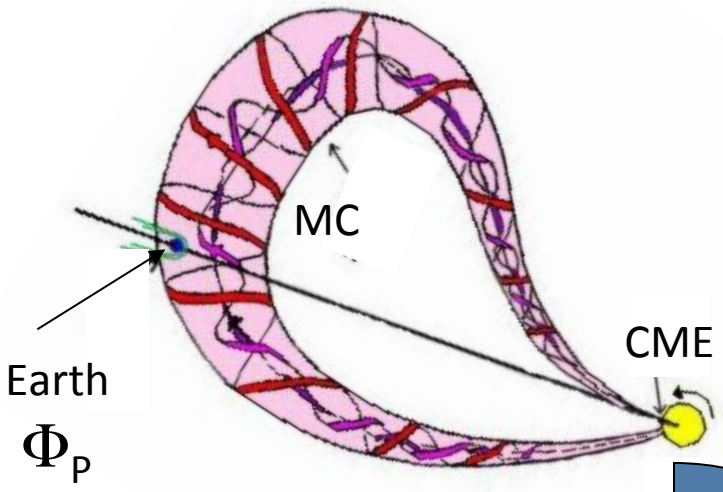


Marubashi 1997

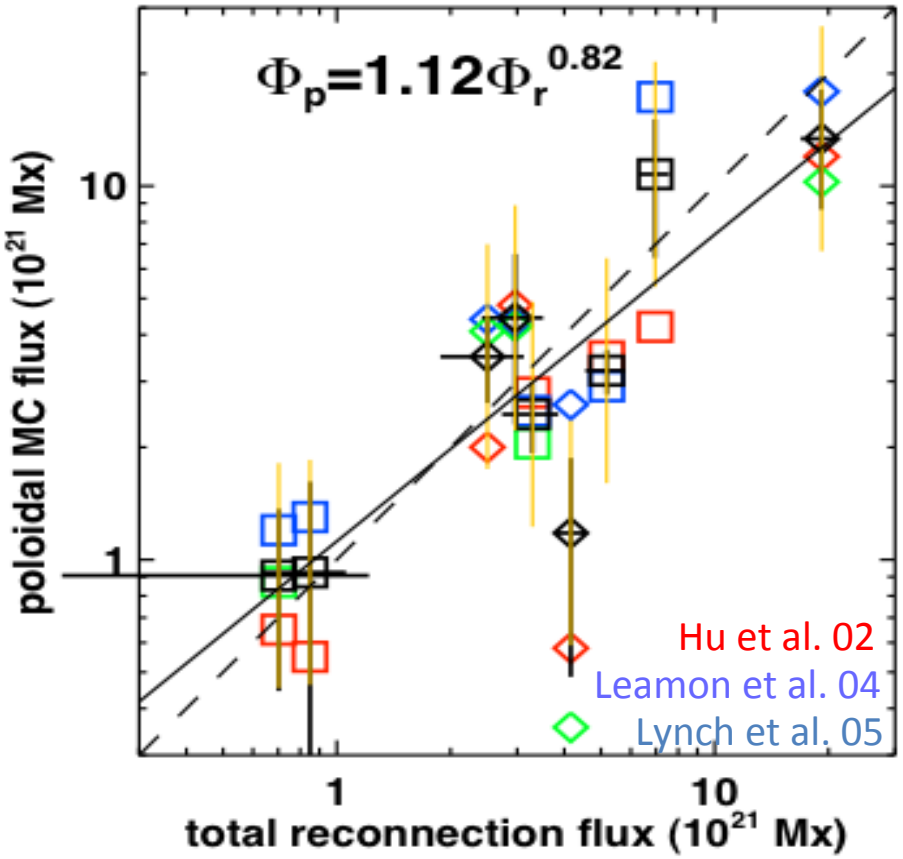


Qiu et al. 2007

Longcope & Beveridge 2007

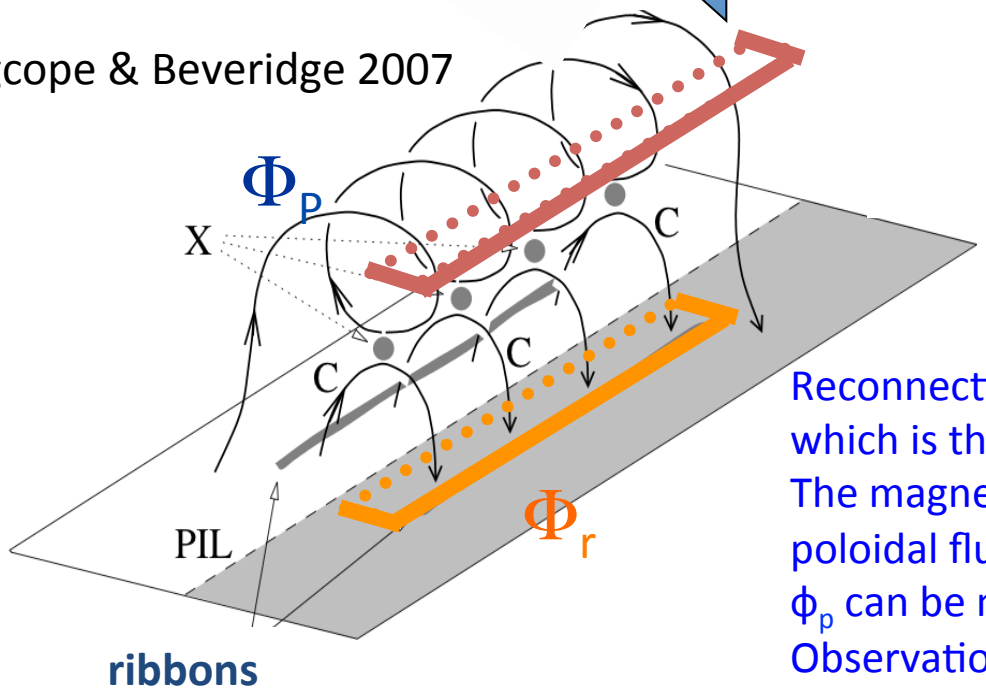


Reconnection forms the flare arcade and the flux rope, which is the fundamental magnetic structure of a CME. The magnetic flux in the flare ribbons ($\phi_r$) and the poloidal flux of the flux rope ($\phi_p$) must be the same. $\phi_p$ can be measured when the flux rope reaches earth. Observations support this flare CME connection

# CMEs & Space Weather

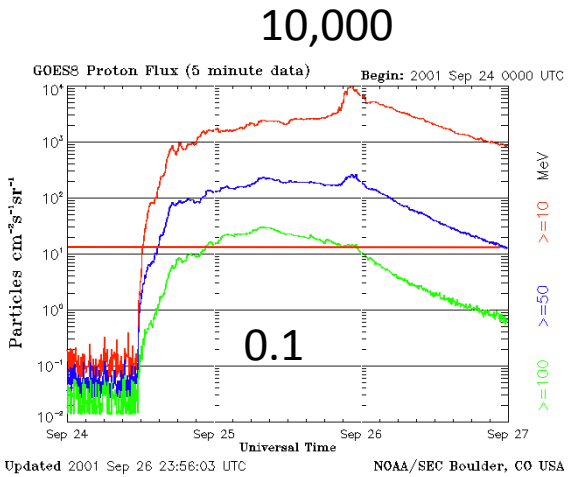


CMEs

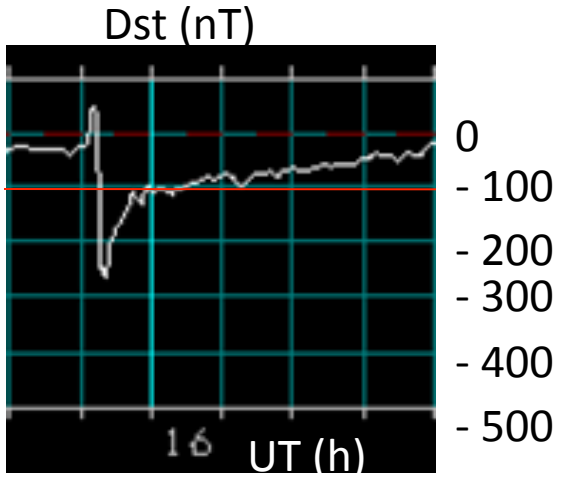


On the way and upon arrival

SEPs

Shock-driving Capability is Crucial

$V_{CME} - V_{SW} > V_{MS}$

Space systems
Airplanes
atmosphere

Magnetic storms

Upon arrival at Earth

Space systems
Magnetosphere
Ionosphere
Atmosphere
Ground

CME's Magnetic Structure Is Crucial (Bz <0)

# CMEs and SEPs

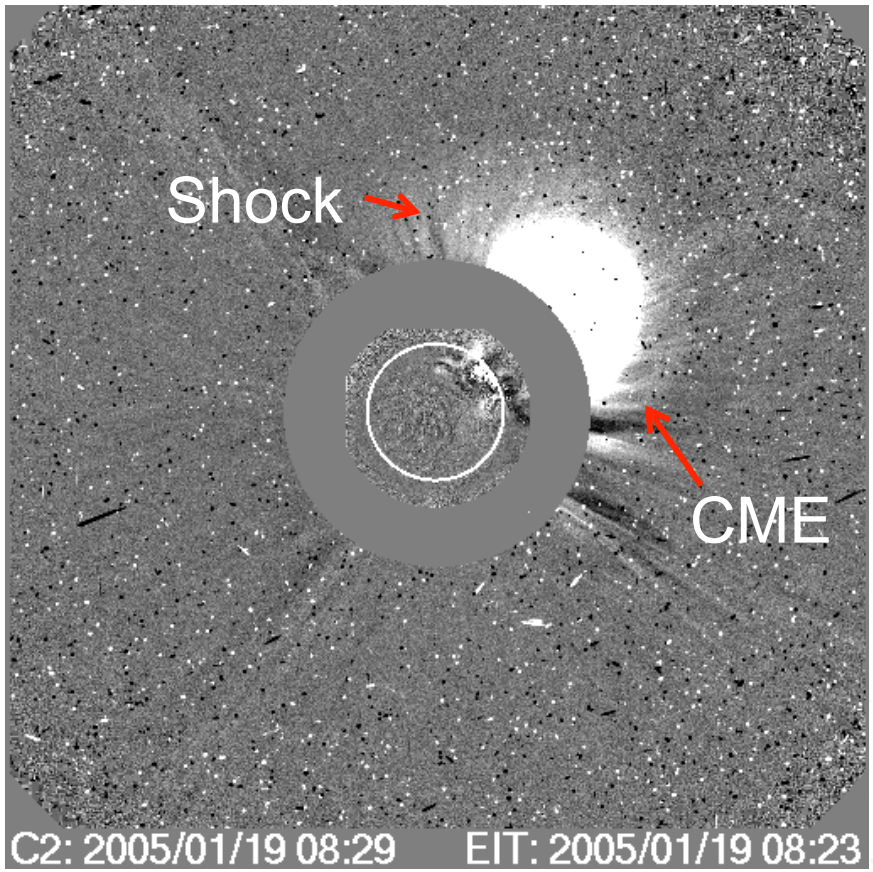


A fast CME driving a shock
(cdaw.gsfc.nasa.gov)

Solar Energetic Particles (SEPs) propagate along magnetic field lines in helical paths

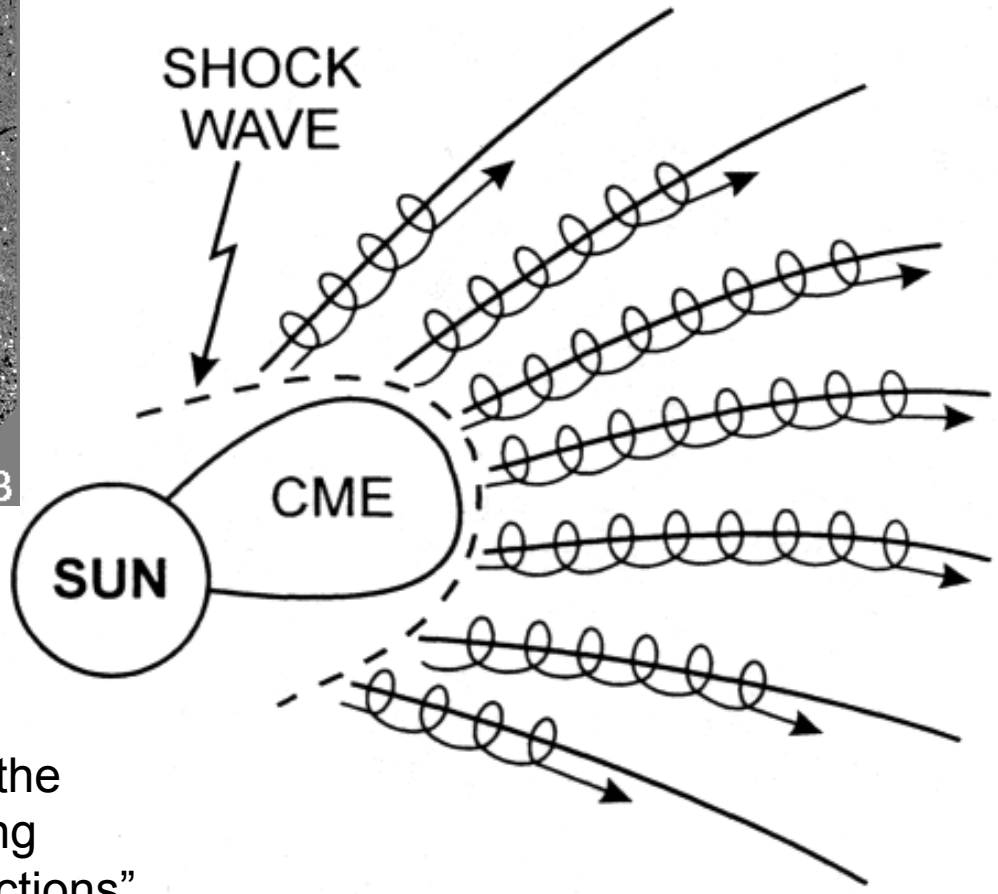


"energetic protons are accelerated in the shock front just ahead of the expanding loop structures observed as mass ejections"
***Kahler, Hildner, & Van Hollebeke (1978)***

# The Nozomi Killer?

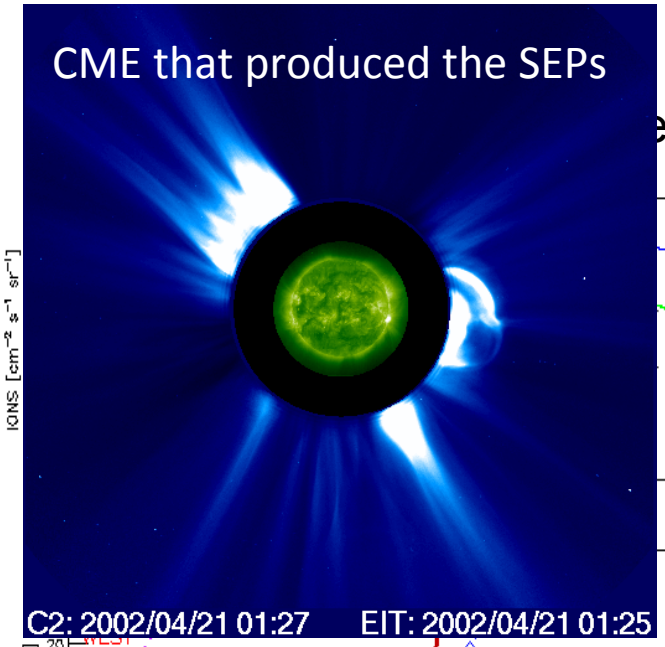


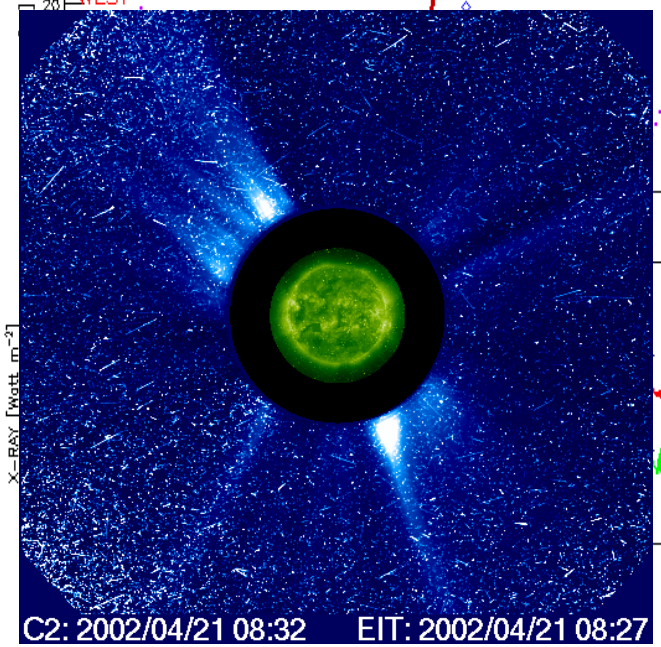


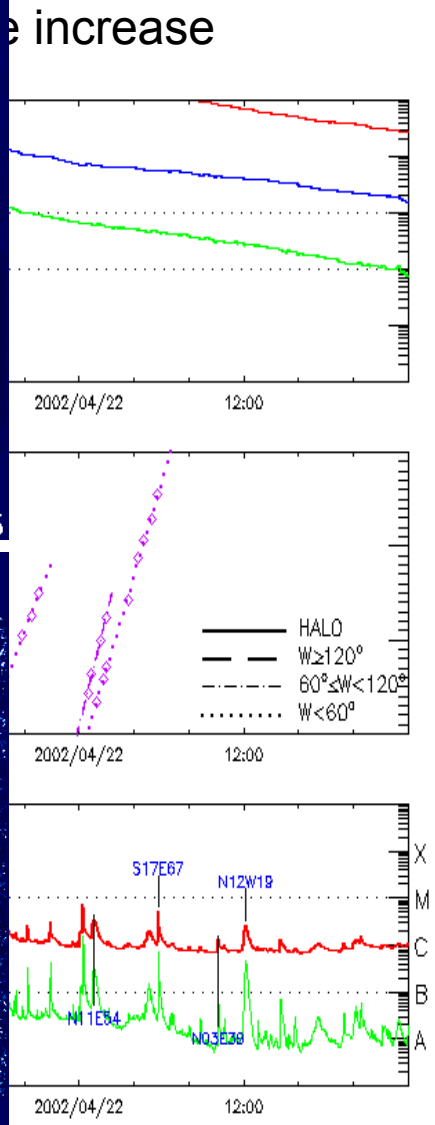


Japan's Mars mission, Nozomi ended six months before insertion into Mars orbit due to the April 21 2002 particle storm

Onboard communications and power systems were damaged

Nozomi = Hope

# Violent Particle Radiation in 2003 from sunspot regions numbered 484 & 486 along with SOHO CMEs

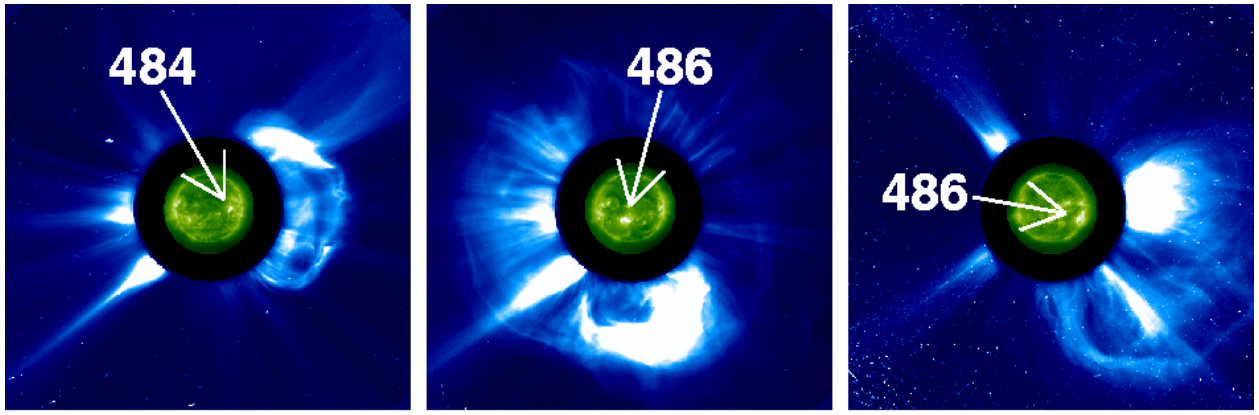


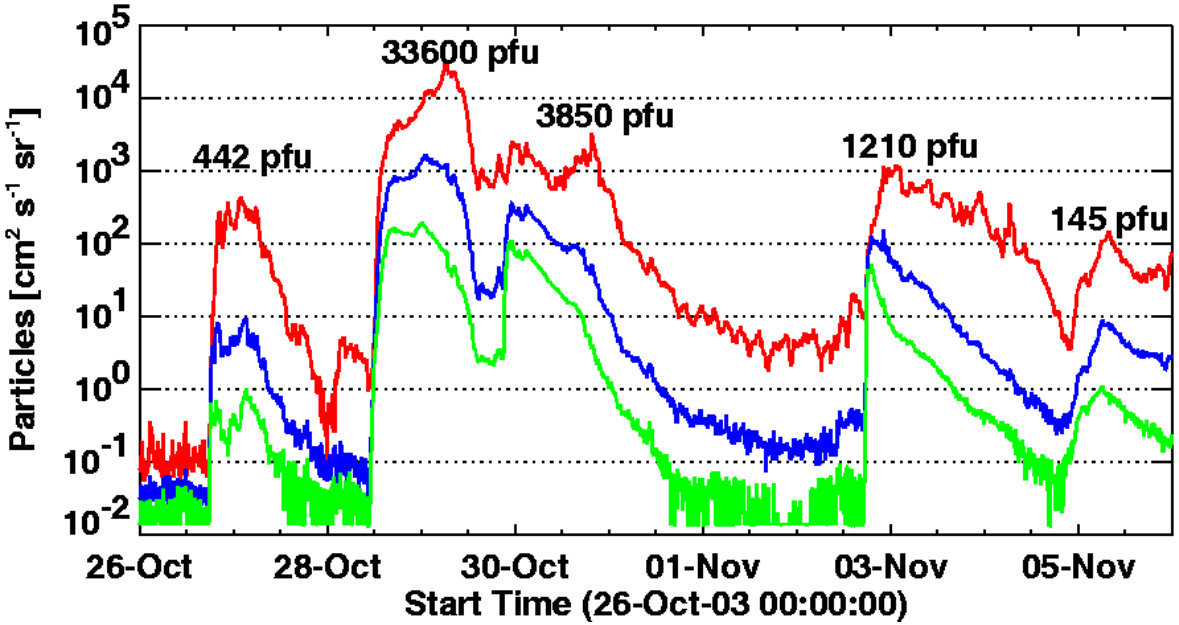


Earth immersed in particle radiation for nearly 2 weeks

# MARIE: The Martian Radiation Environment Experiment

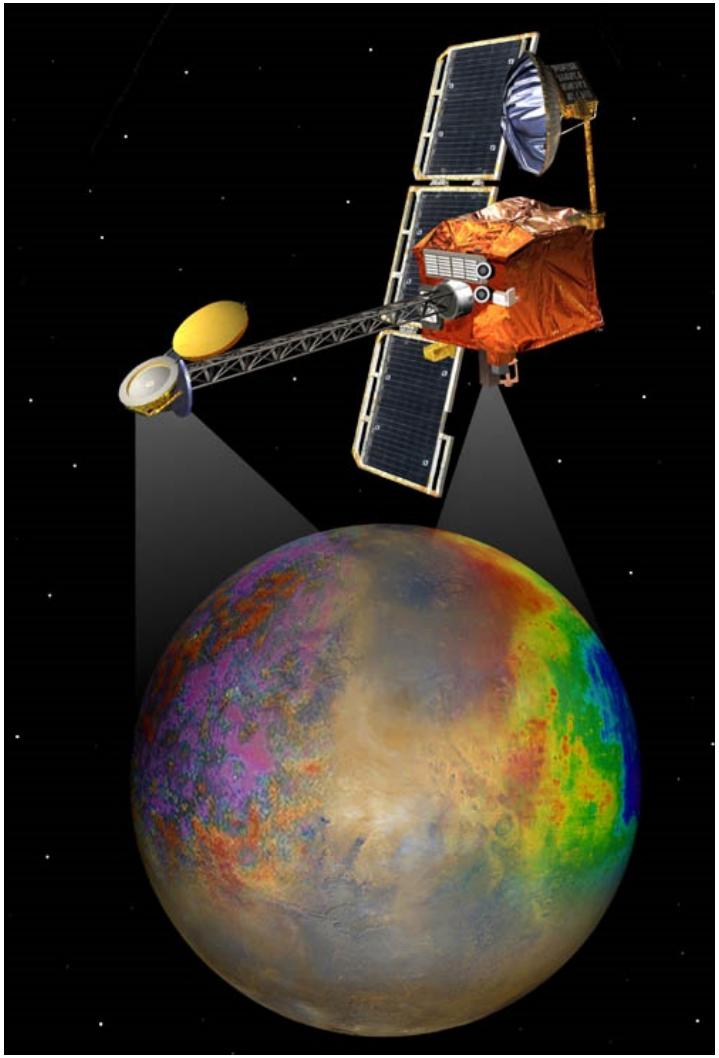

Mars Odyssey

The MARIE instrument on the Mars Odyssey gave us a first look at the radiation levels faced by a possible future astronaut crew.

The experiment took data on the way to Mars and in orbit, so that future mission designers will know better how to outfit human explorers for their journey to Mars.

Another SEP event in October 2003 rendered MARIE inoperative. It is ironic, as MARIE was designed to measure the radiation environment at Mars.

# SEP Producing CMEs

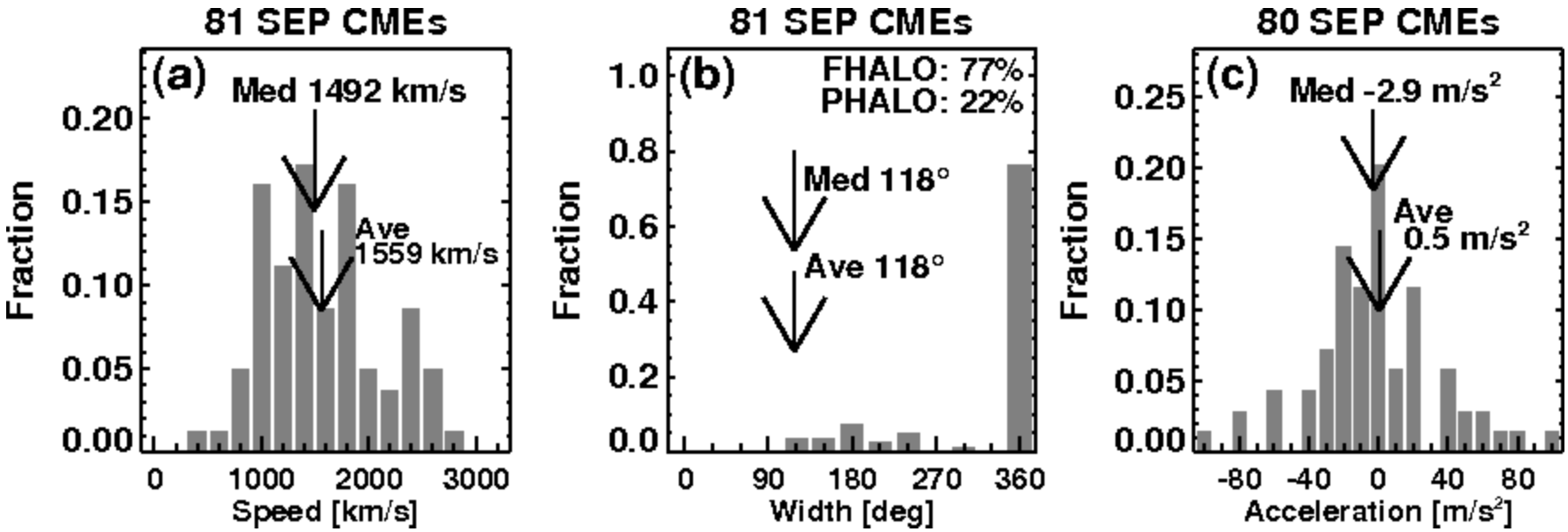


The CMEs are very fast

Almost all CMEs are halos or partial halos

Halo CMEs are generally wide

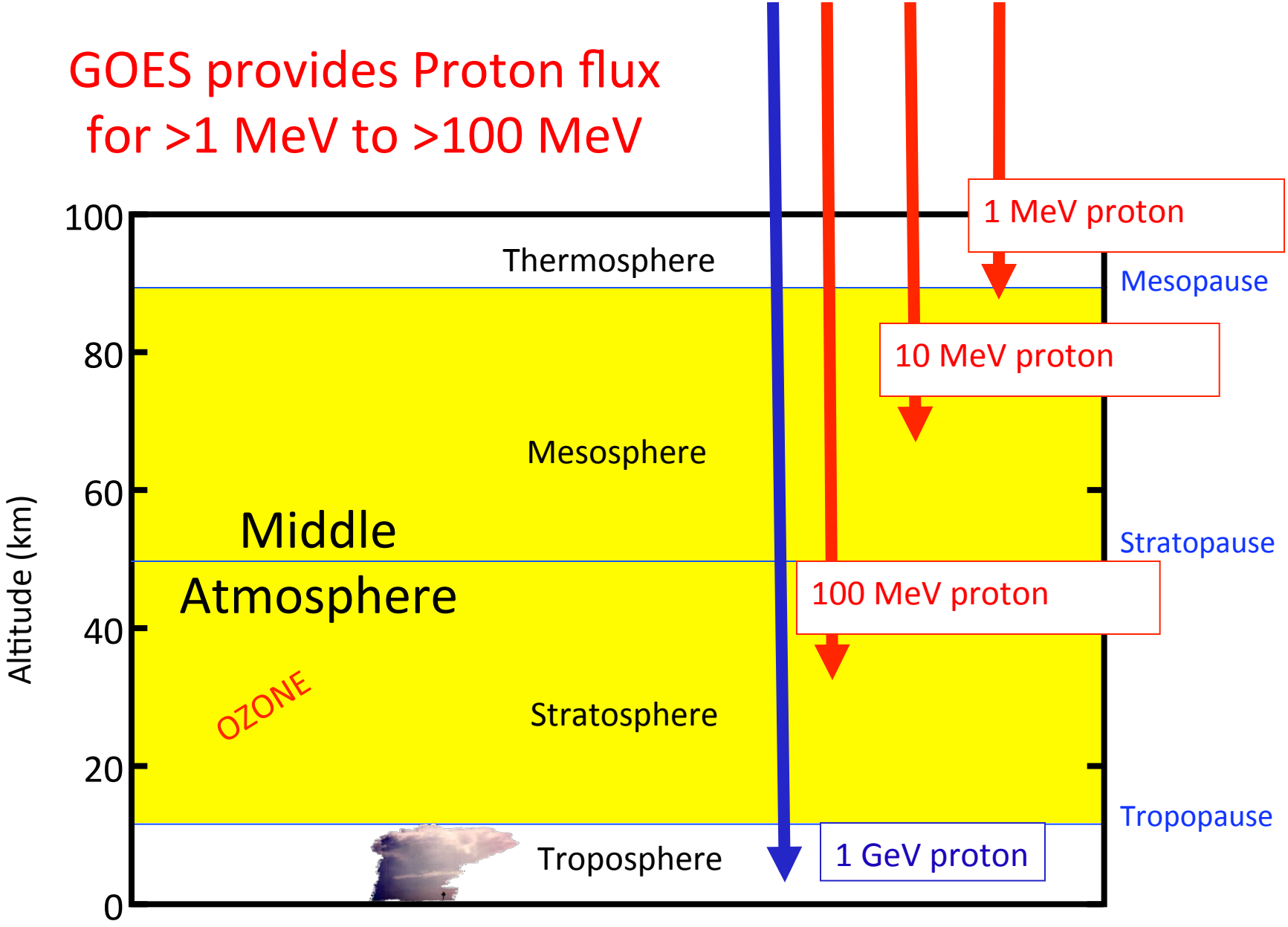


**Particle radiation from the Sun can destroy ozone**

courtesy: C. Jackman

# CMEs and Geomagnetic Storms

- Direct impact of CME plasma on Earth's magnetosphere
- Causes ring current enhancement
- Acceleration of electrons inside the magnetosphere
- Sudden commencement and exposure of geosynchronous satellites to the interplanetary space

# Satellites Exposed to Interplanetary Space during Geomagnetic Storms

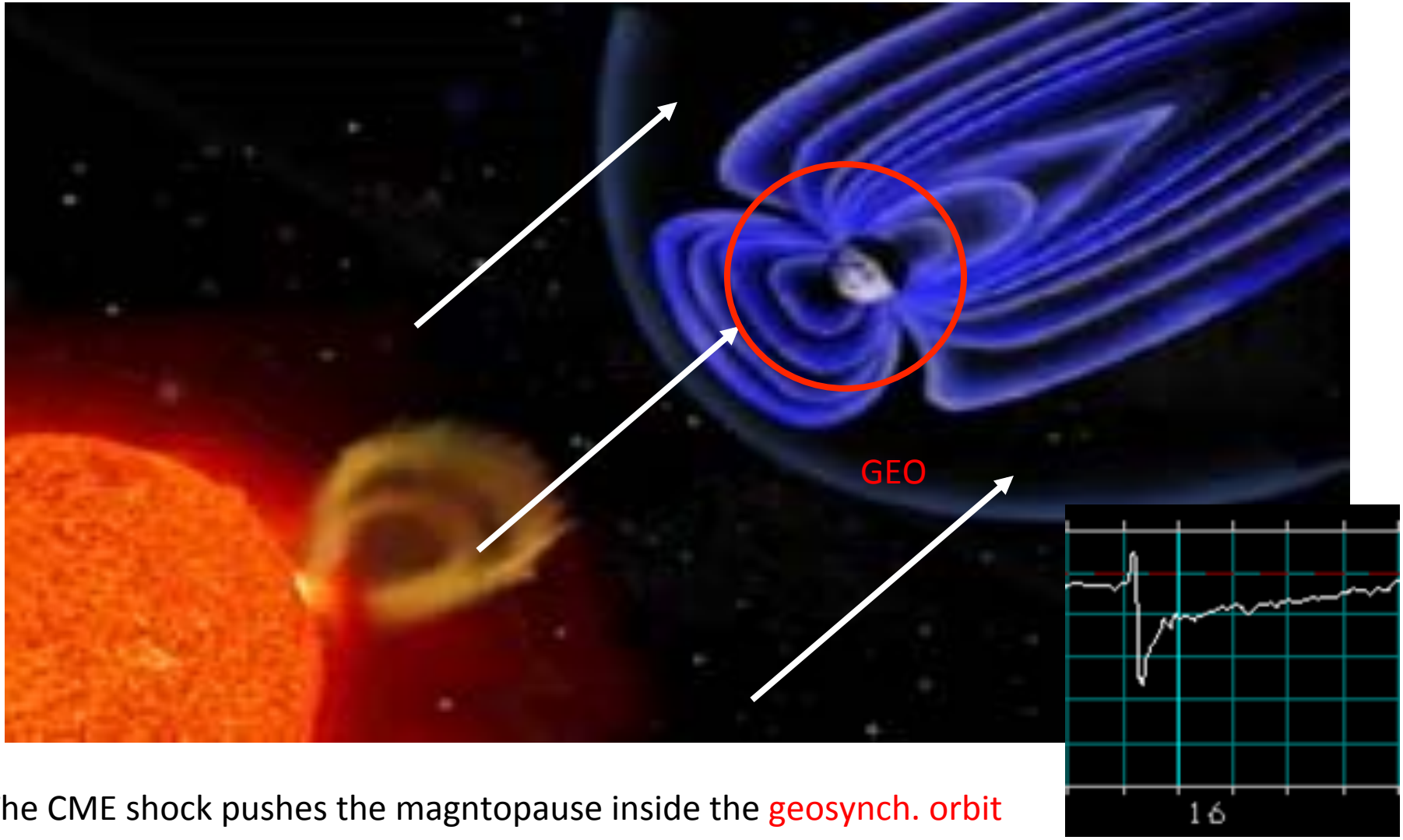


The CME shock pushes the magntopause inside the geosynch. orbit

CME Near Earth

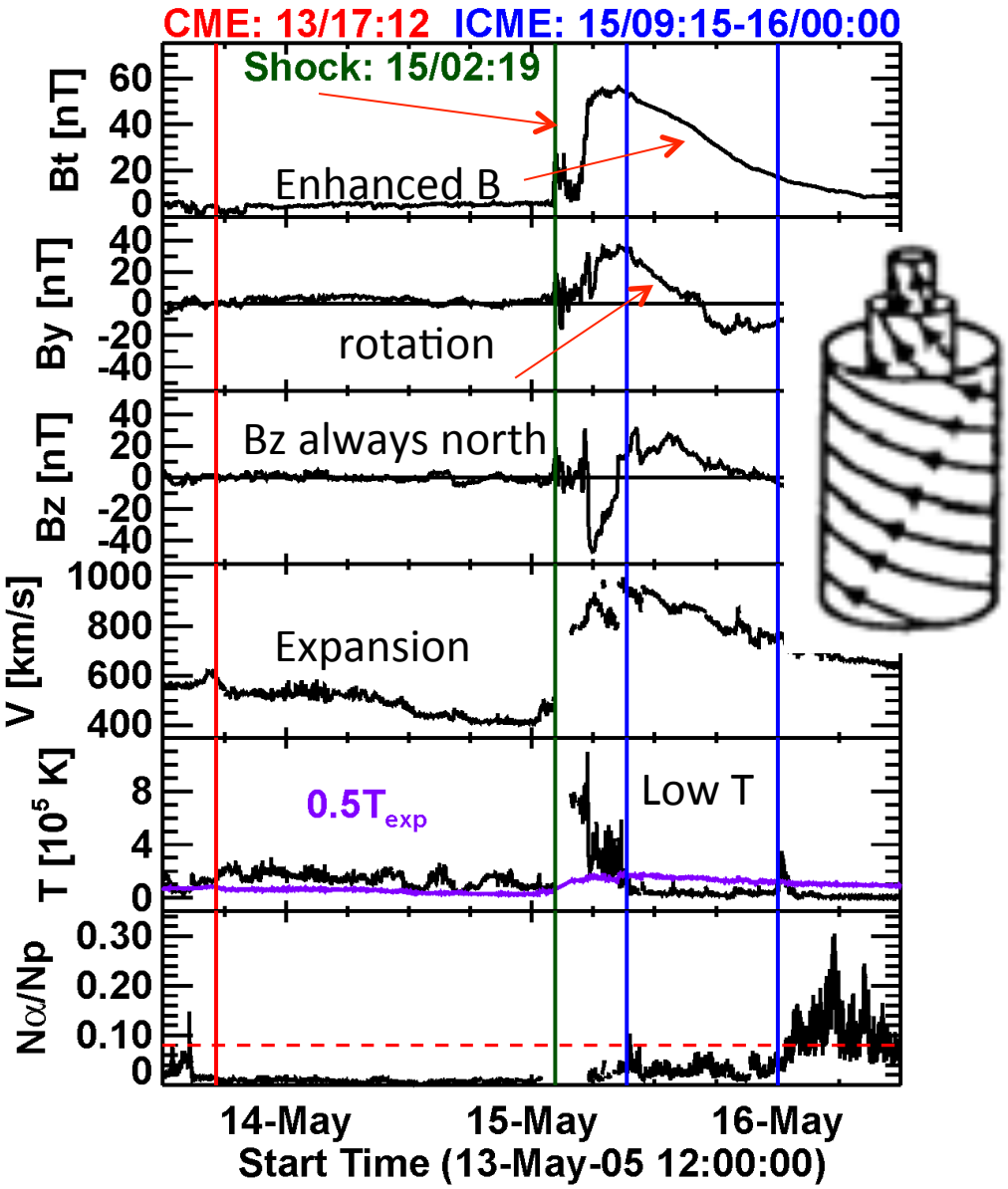


# SOHO CME

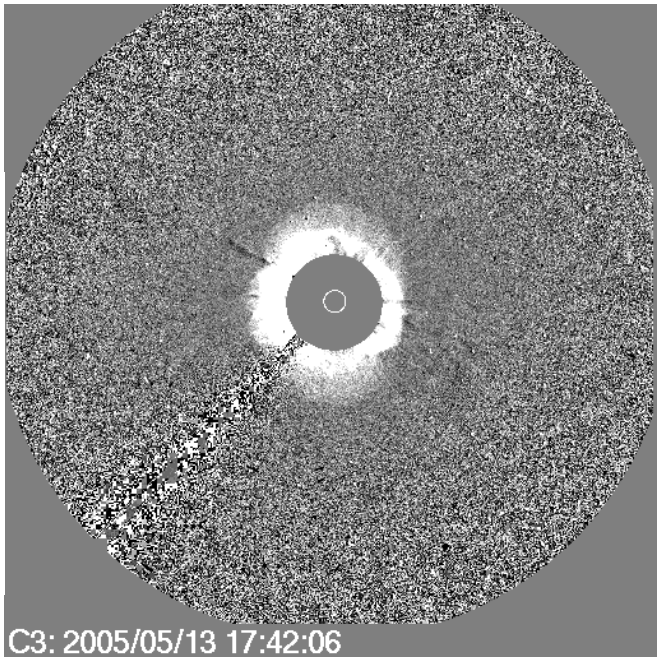


Clear magnetic field signature
Temperature signature is also clear
Alpha to proton ratio not clear
Solar wind speed clear

Shock – Sheath - Ejecta

Flux rope in white light: Chen et al. 1997

# Out of the Ecliptic B from CMEs

- Normal Parker-spiral field does not have a Bz component
- CMEs with flux rope structure (magnetic clouds) naturally produce the Bz component
- Magnetic field draping in the shock sheath can also cause Bz (Gosling & McComas, 1987; Tsurutani & Gonzalez, 1988)
- Corotating interaction regions and fast wind have Alfven waves that represent Bz, but the magnitude is relatively small

# Out of the ecliptic B component due to the CME and draping

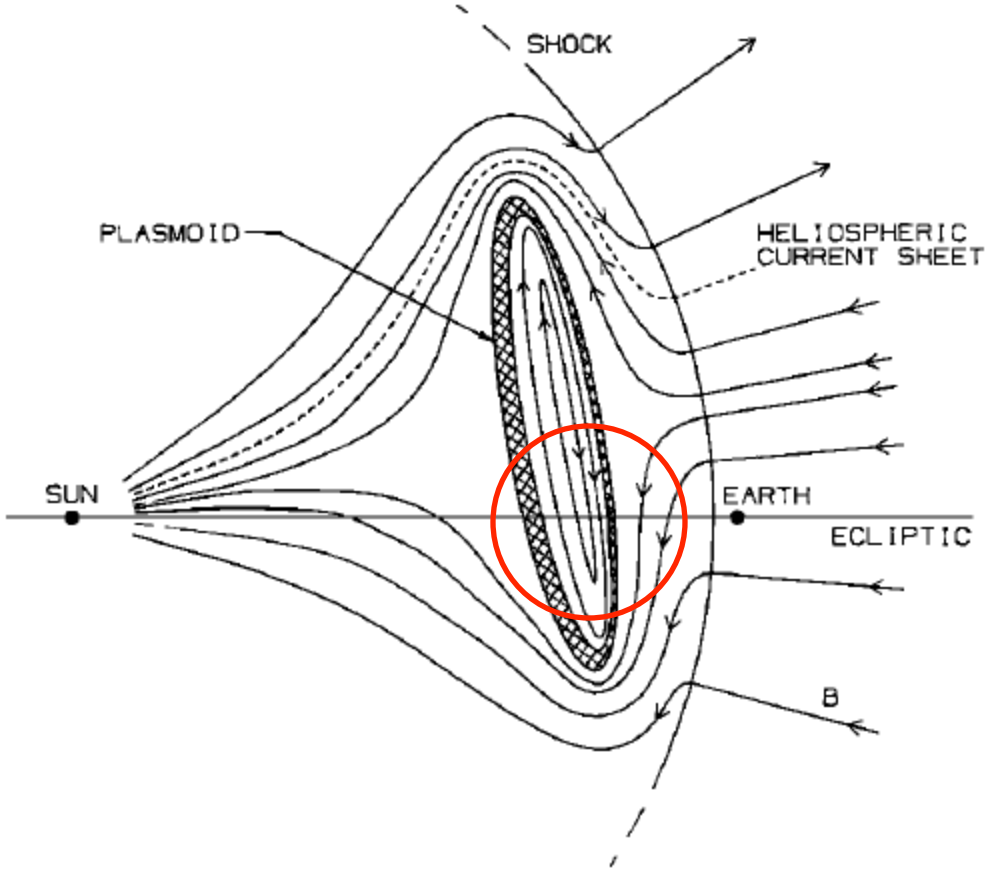


Gosling and McComas, 1987 GRL

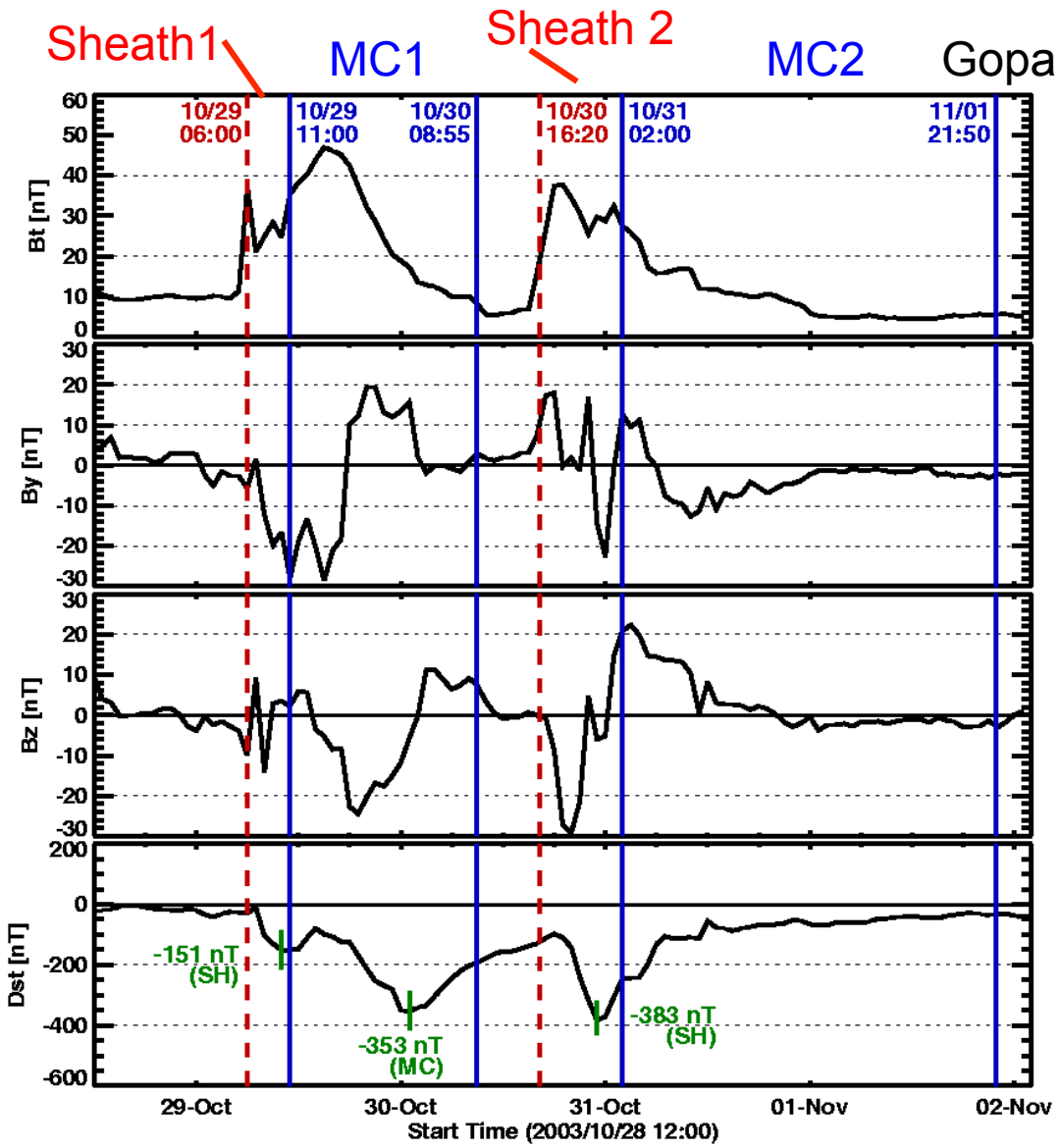


Gopalswamy et al., 2008

# Sheath Superstorm

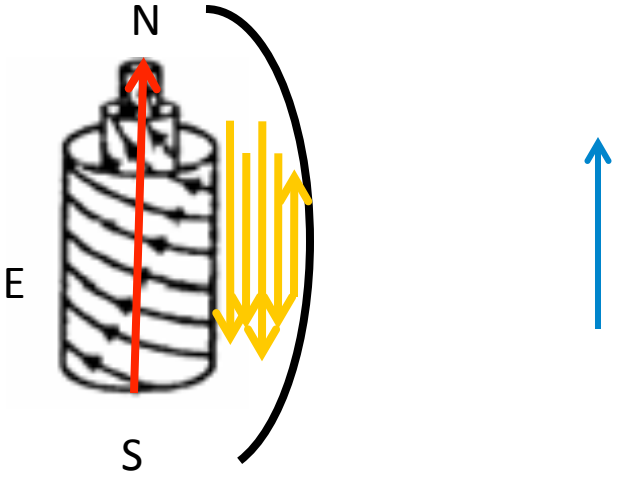


ENW (FN)

When MCs have high inclination the rotation is in the Y direction. In the Z-direction, the field will be always to the north or south. In this example, Bz is always north pointing so no storm. But there was a big storm due to the sheath consisting of intense south pointing Bz

Gosling and McComas1987; Tsurutani et al 1988

# Summary of MC Structure

Shock Sheath Cloud

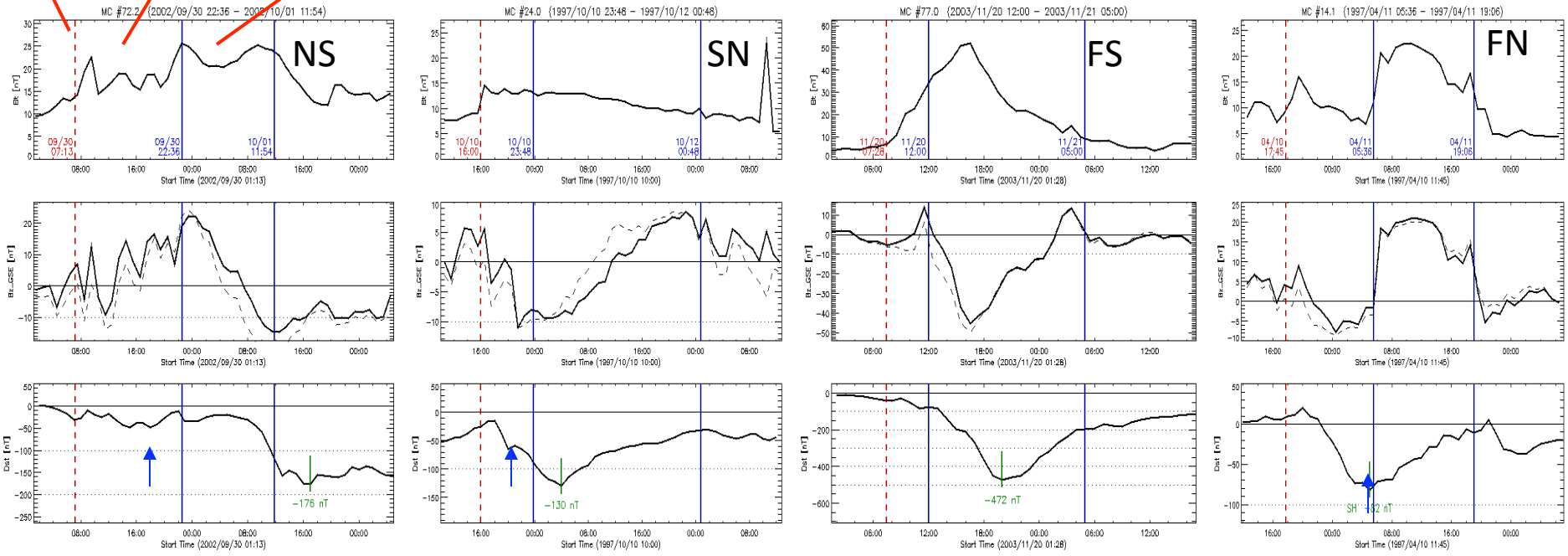

# Cloud & Sheath Storms

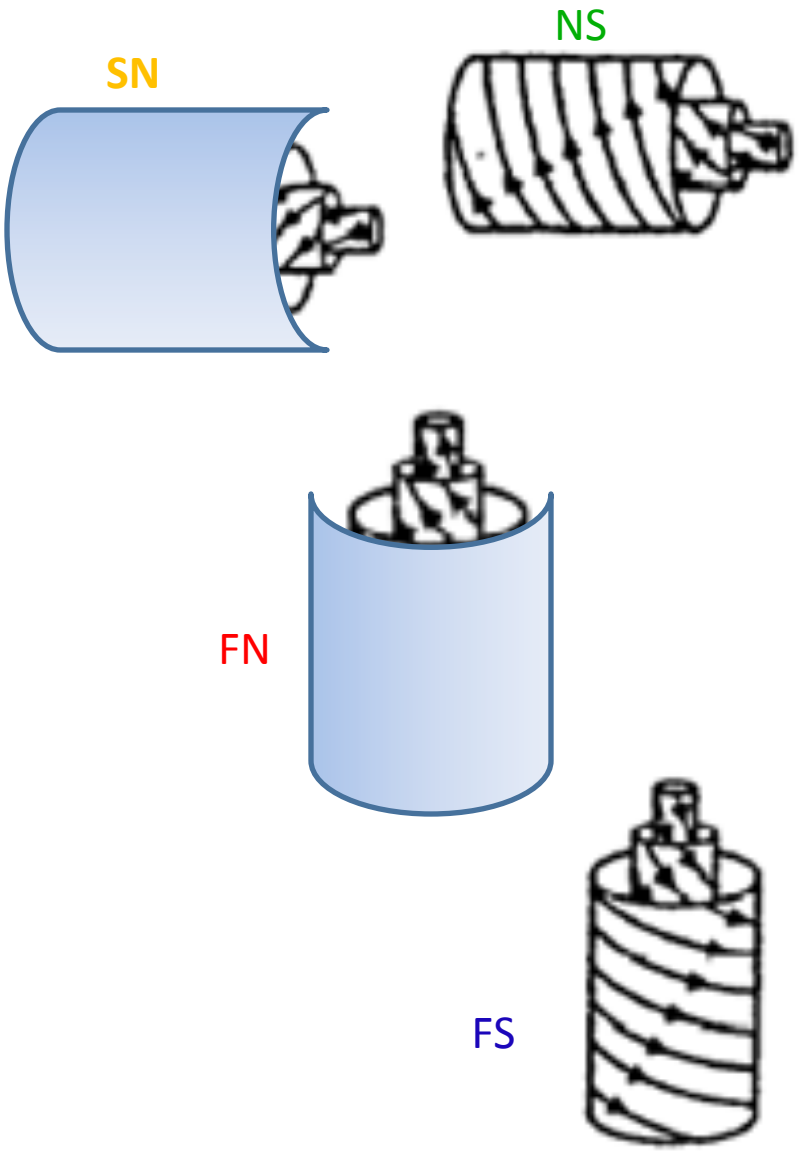


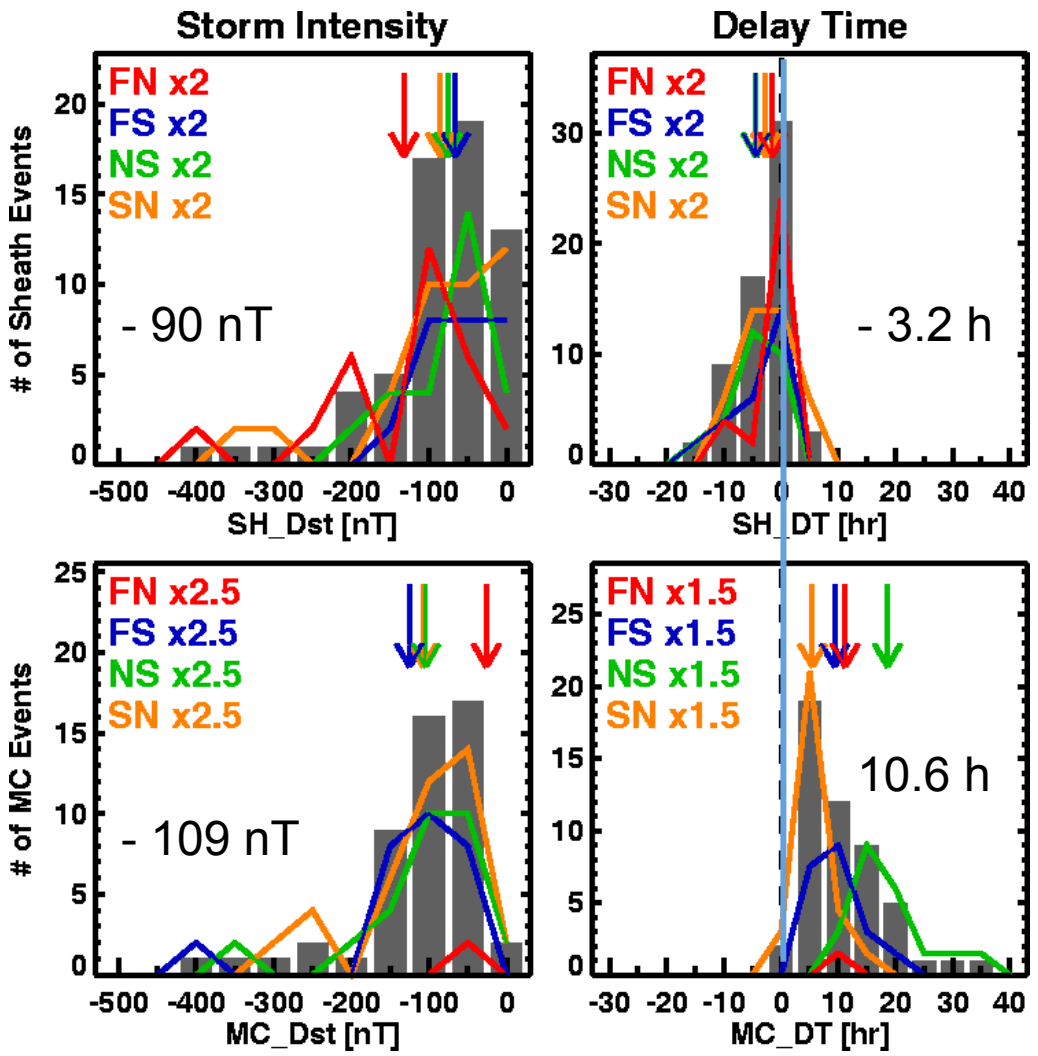

# CMEs Producing Geomagnetic Storms

Large Dst (≤ -100 nT) events from cycle 23 and the associated LASCO CMEs considered

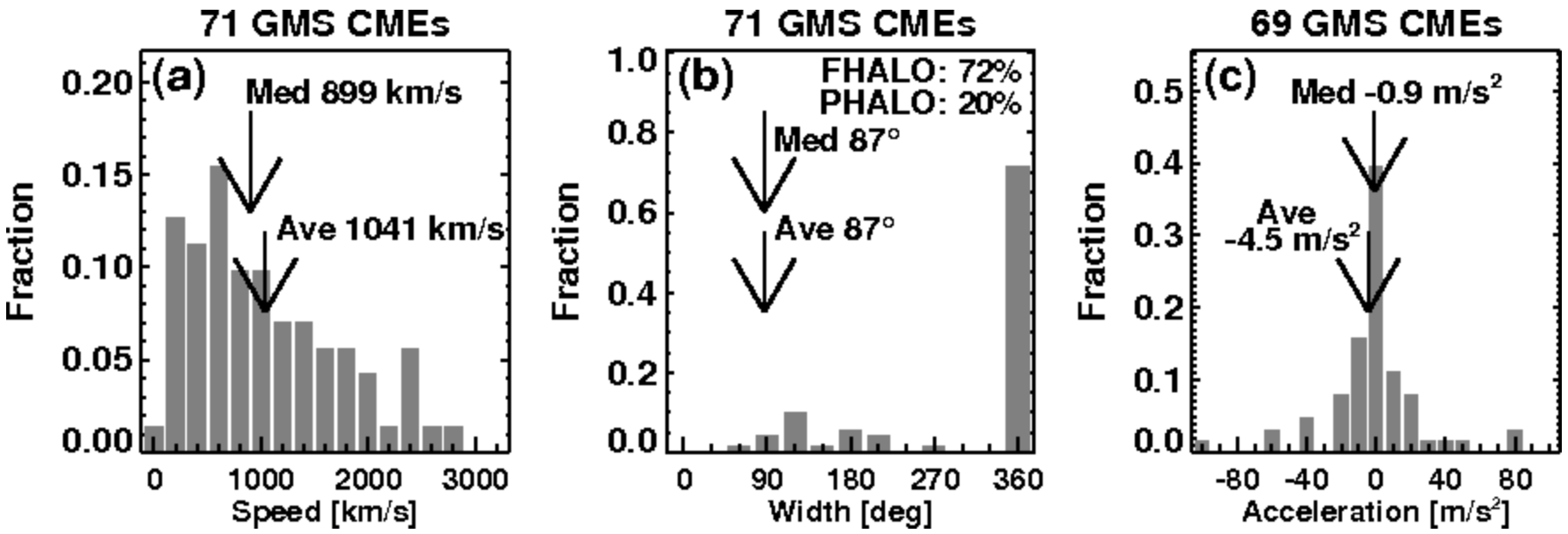


The CMEs are very fast (projected speed ~1041 km/s)

Almost all CMEs are halos or partial halos (92%)

# Solar Source location important for Earth Impact

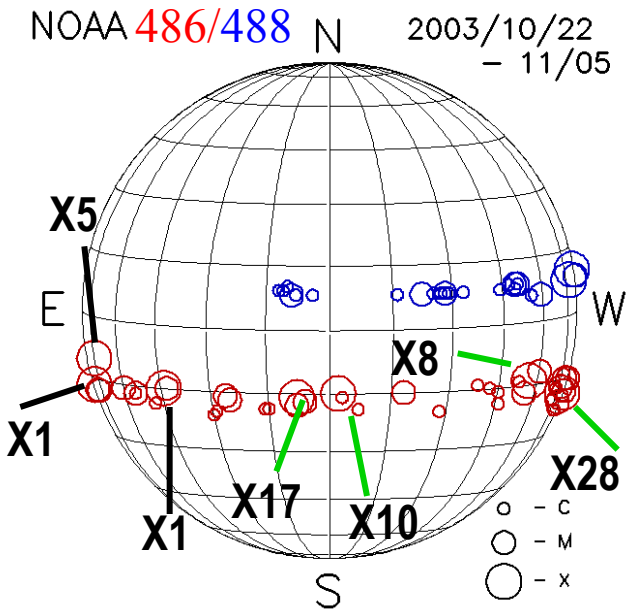


Heliographic coordinates of the CME source location. CMEs occurring near the disk center head directly toward Earth causing storms (e.g. CMEs associated with the X17 and X10 flares)

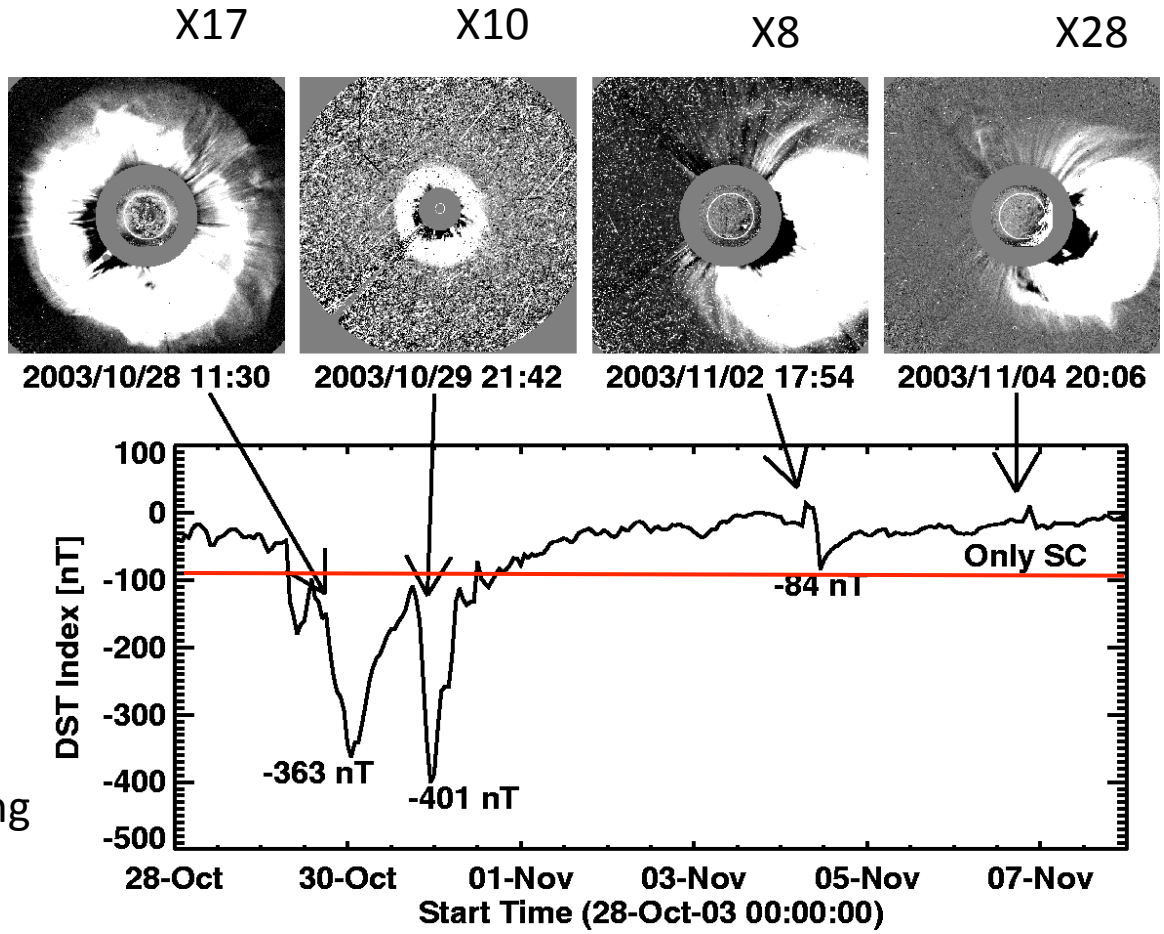


Dst index measures an average horizontal field of the Sun
Storm conditions when Dst< -30 nT
Major storms when Dst < -100 nT

# Geomagnetic Storm and CME parameters

$Dst = -0.01VB_z - 32\ nT$

The high correlation suggests
That V and Bz are the most
Important parameters
( - Bz is absolutely necessary)

V and Bz in the IP medium are related to the CME speed and magnetic content

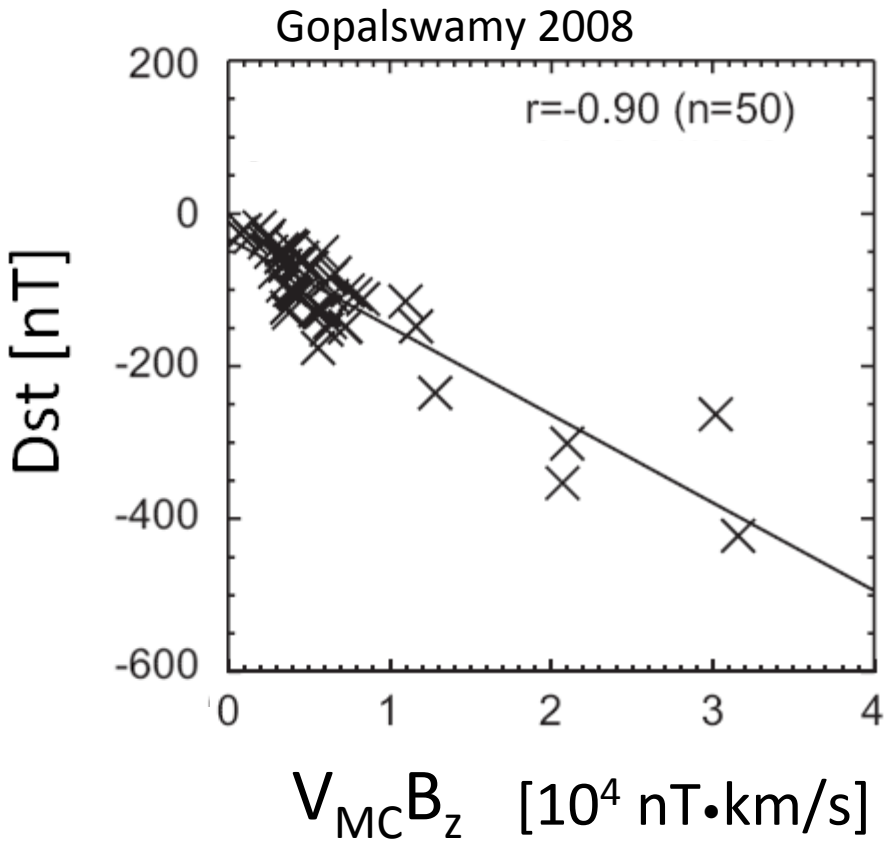


Carrington Event: VBz = 1.6 $10^5$ nT•km/s

V = 2000 km/s, Dst = -1650 nT → Bz = -81 nT

# Origin of V and B

$$Dst = -0.01VB_z - 32 \ nT$$

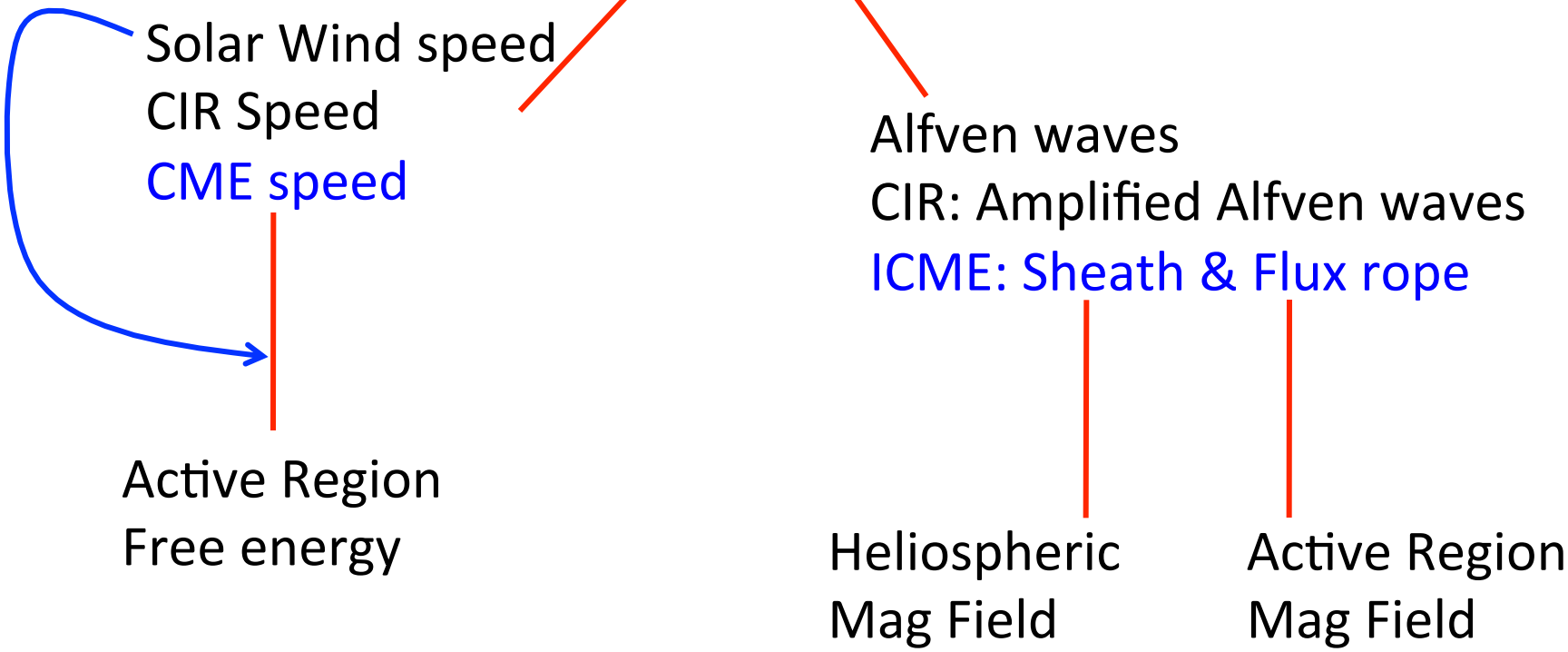

# Geoeffective & SEP-producing CME Sources

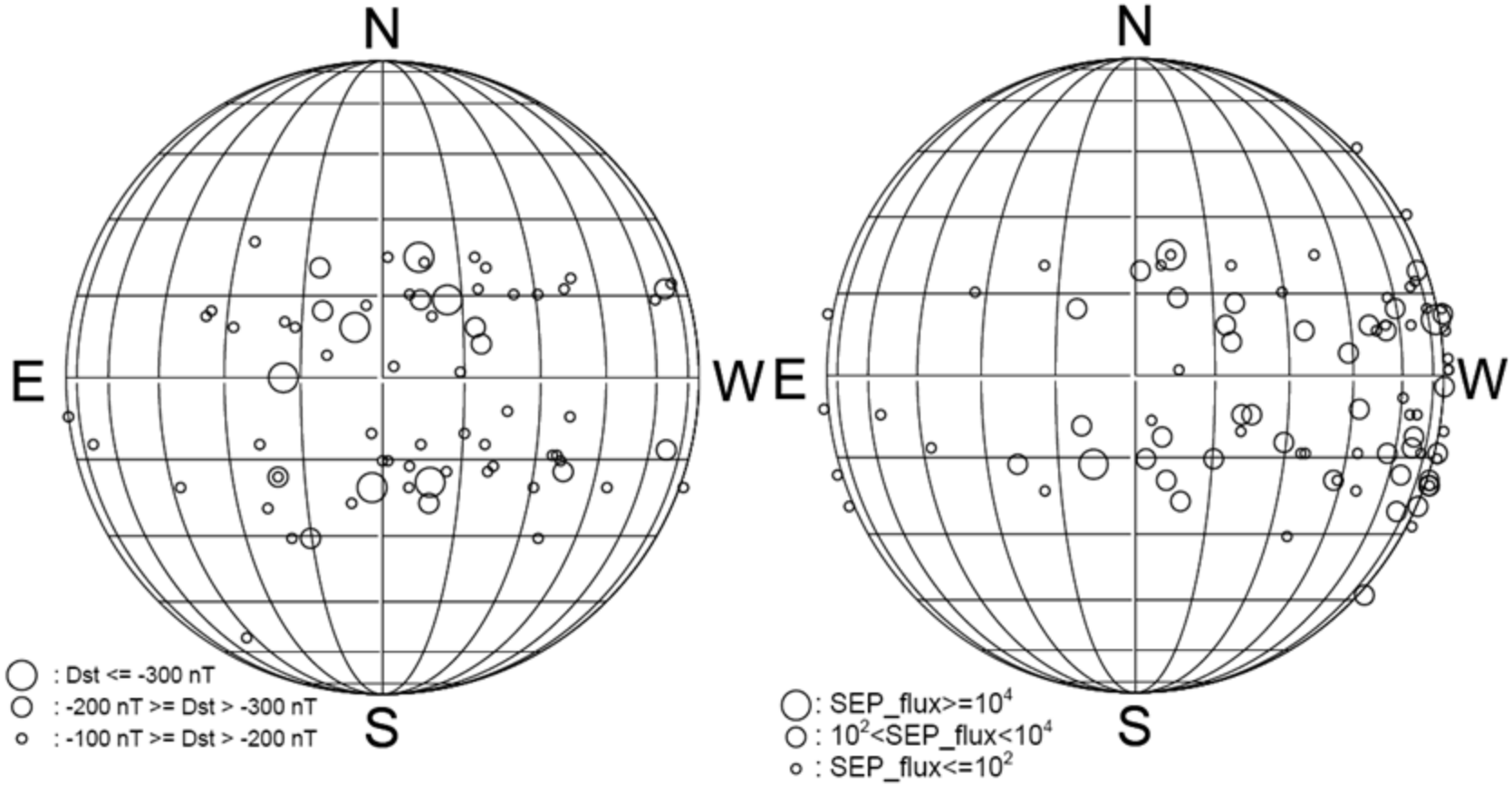


CMEs need to arrive at Earth
CMEs must contain Bz South
Similar to MC and Halo CME sources

CMEs need to drive shocks
Source region needs to be magnetically connected to Earth

Many double-whammy events

# Significant CMEs & their Consequences

Cycle 23 – 24 CMEs from SOHO/LASCO

There seems to be a maximum CME speed

m2 – Metric type II
MC – Magnetic Cloud
EJ – Ejecta
S – Interplanetary shock
GM – Geomagnetic storm
Halo – Halo CMEs
DH – Type II at λ 10-100 meters
SEP – Solar Energetic Particles
GLE – Ground Level Enhancement

Gopalswamy, 2006; 2010

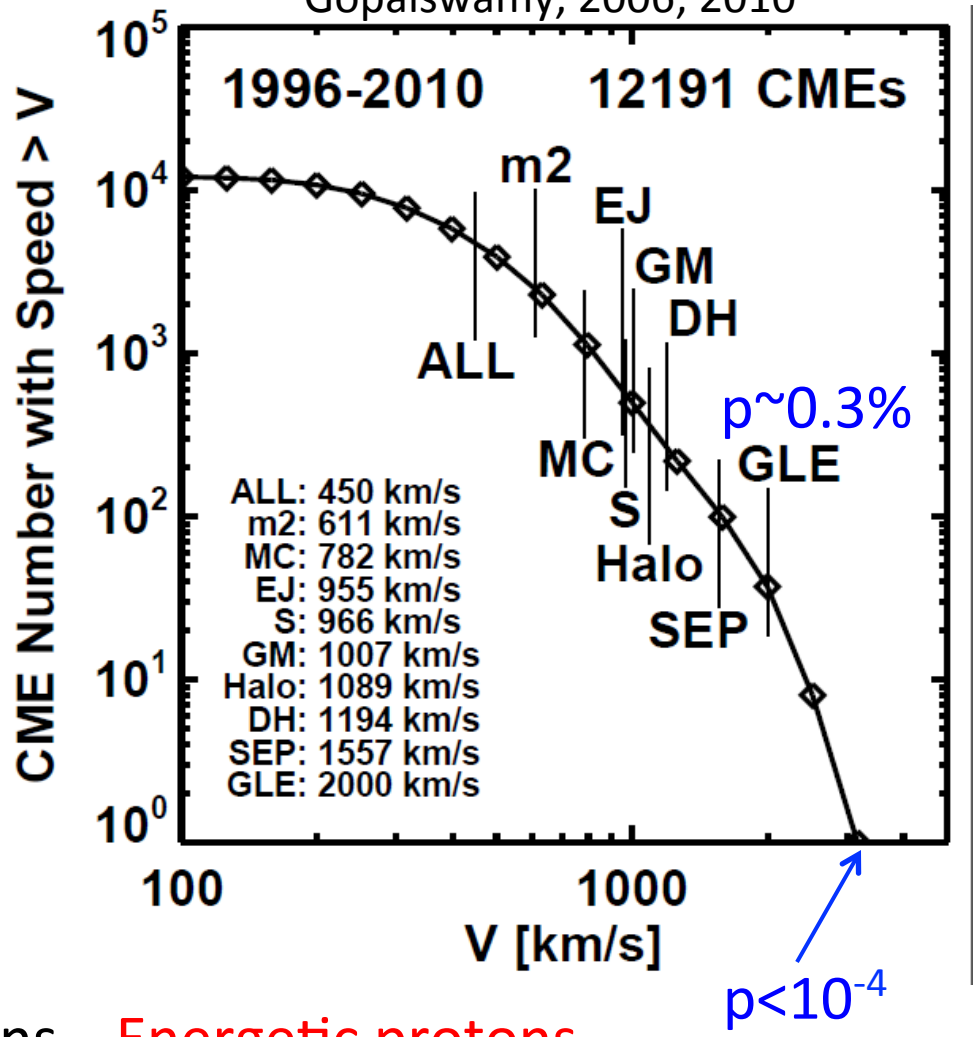


Plasma impact  Energetic electrons  Energetic protons

# Tail of the CME Distribution

| Category | Number of CMEs |
|---|---|
| All identified CMEs | 18000 |
| # CMEs with V ≥ 1000 km/s | 539 |
| # CMEs with V ≥ 1500 km/s | 131 |
| # CMEs with V ≥ 2000 km/s | 39 |
| # CMEs with V ≥ 2500 km/s | 9 |
| # CMEs with V ≥ 3000 km/s | 2 |
| # CMEs with V ≥ 3500 km/s | 1 |
| # CMEs with V ≥ 4000 km/s | 0 |

Exercise: use the search engine on cdaw.gsfc.nasa.gov/CME_list to confirm this

# AR Potential Field Energy ~ Free Energy

- Free Energy ~ Magnetic Potential energy (Mackay et al., 1997)
- Free energy is > Mag PE by a factor 3-4 (Metcalf et al. 2005)

Max potential energy during cycle 23 ~ 4 x $10^{34}$ erg

Max CME KE observed ~ 1.2 x $10^{33}$ erg

CME Speed limit → maximum energy that can be stored depending on A, B

B < 6100 G; A < 5000 msh

→ E ~ $10^{36}$ erg

Livingston et al. 2006; Newton, 1955

(1000, 3675)

$V = 675 \log E_{33} + 1650$

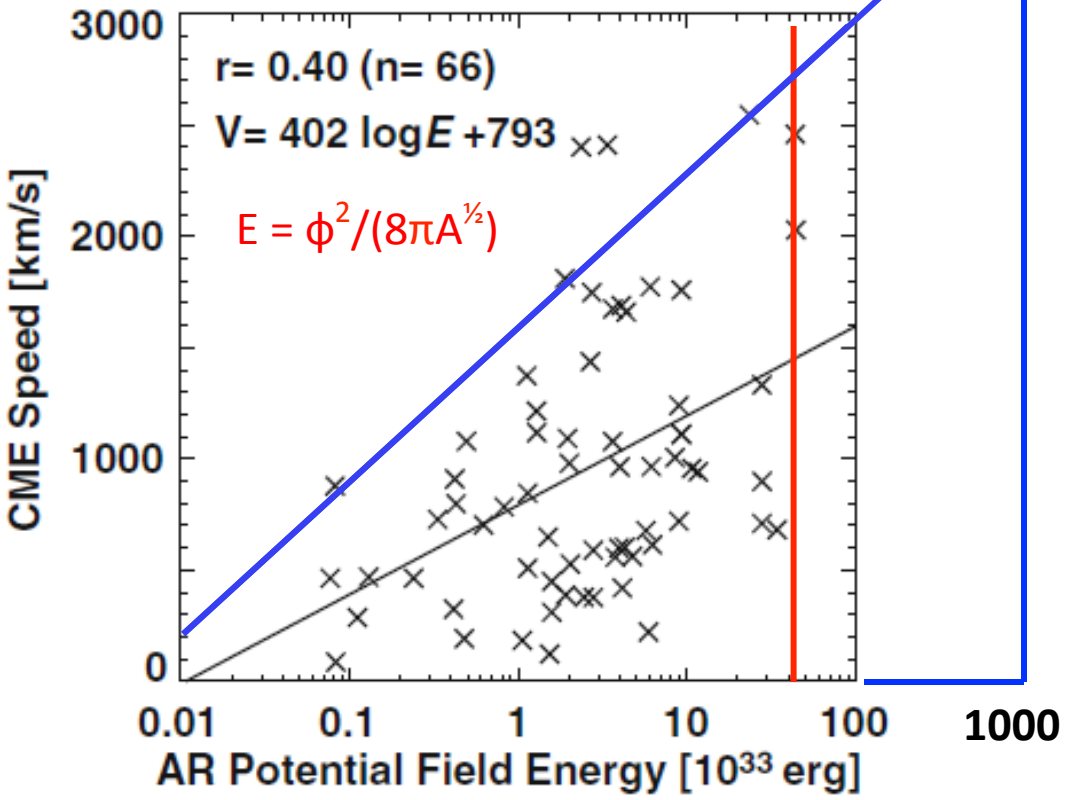


ϕ = AR flux; A = AR area; E = AR Potential energy

Gopalswamy et al., 2010

# Max speed from magnetic Potential Energy (E)

- $V = 675 \log E_{33} + 1650$; $E = \phi^2/(8\pi A^{½})$ $\phi = BA$
- $E \sim 10^{36}$ or $E_{33} = 10^3 \rightarrow V = 3675$ km/s
- Transit time = 11.3 h
- But there is the solar wind → longer transit time ~12.6 h (2005 Jan 20 CME had this speed; transit time was 34 h because the source was at W60)

# CME Interactions

- Non-radial motion of CMEs during the minimum phase
- CME – CME interactions during solar maximum
- CME – Coronal hole interaction during the declining phase
- CMEs tend to align with the heliospheric current sheet: CME rotation

# Non-radial Motion: Toward Equator

NoRH PE: Gopalswamy and Thompson, 2000 JASTP

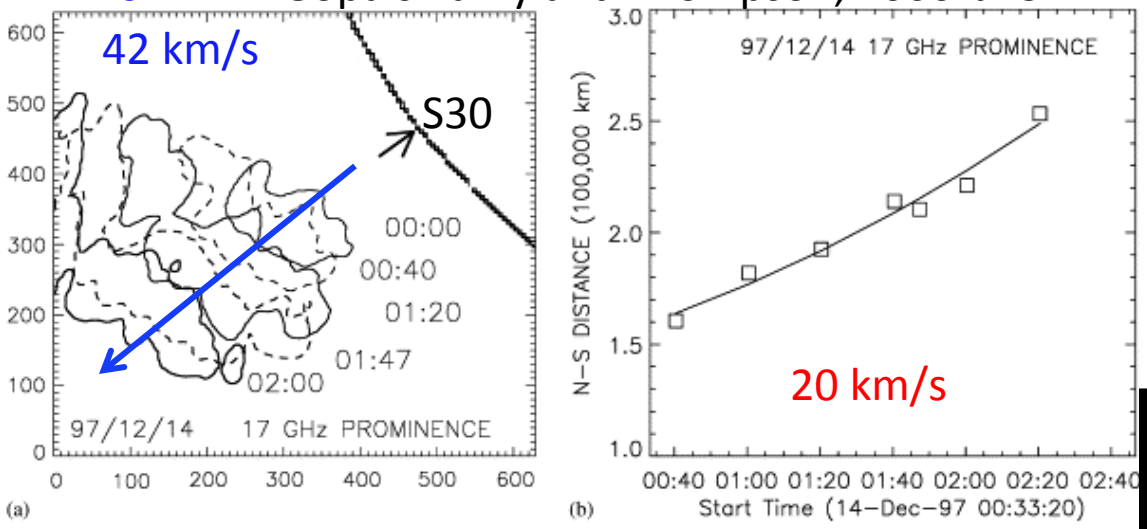


Hildner, 1977
MacQueen et al. 1986
Gopalswamy et al. 2000
Plunkett et al. 2001
Cremades et al. 2004
Gopalswamy et al. 2003,2009
Panasenco et al. 2010
Byrne et al. 2010
Lugaz et al. 2009

Deflection by 30°

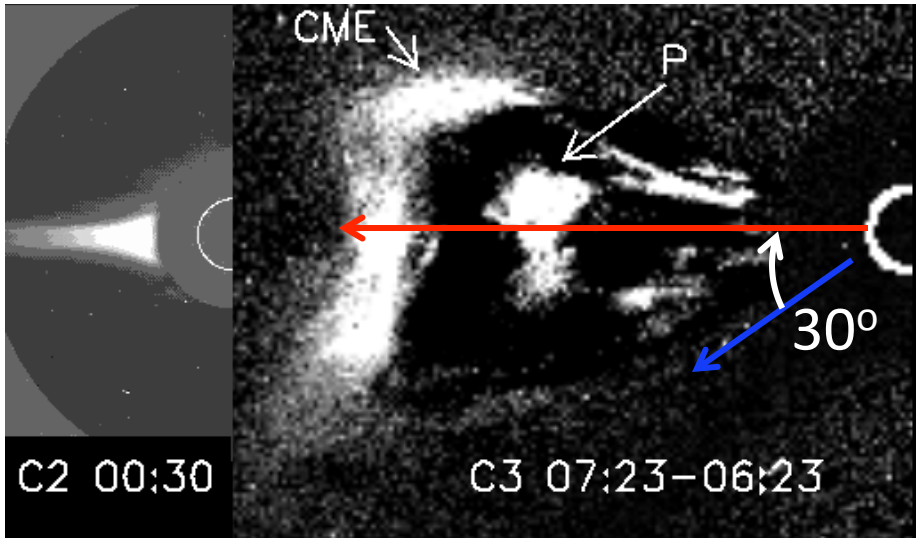


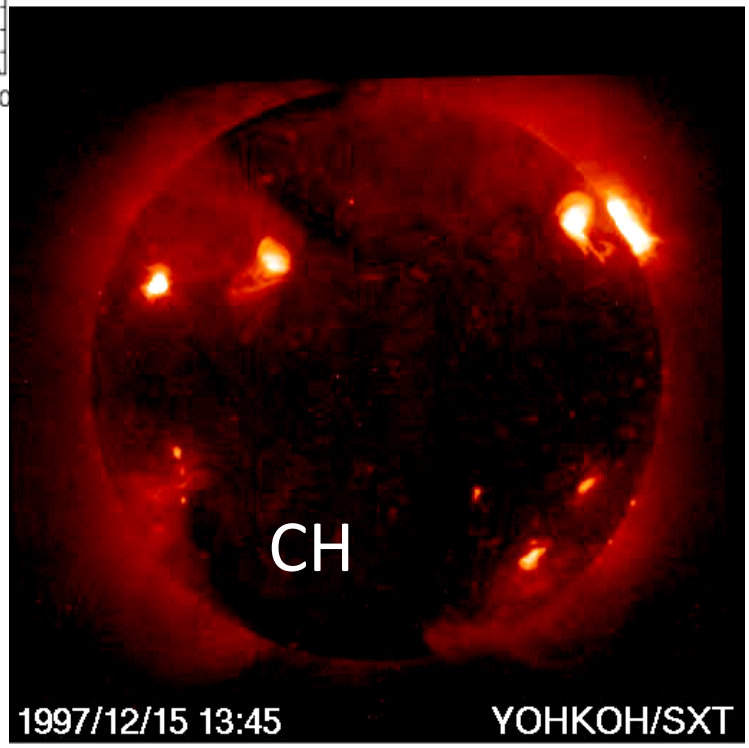

# A Bad Example: 2014 January 7

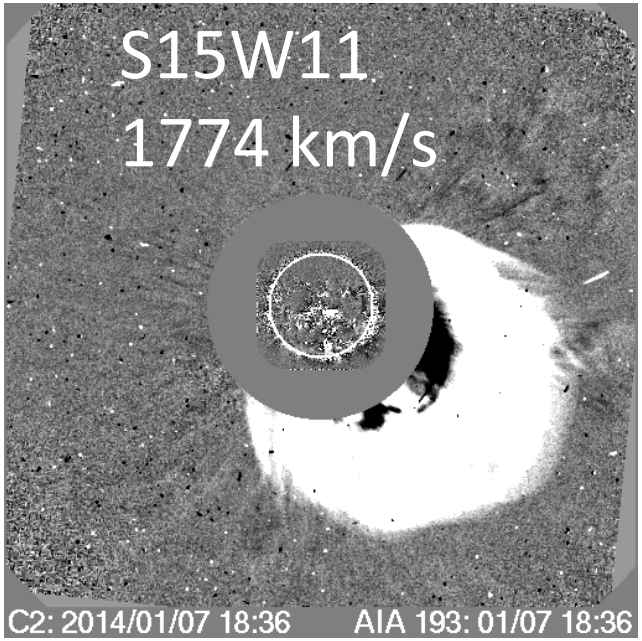


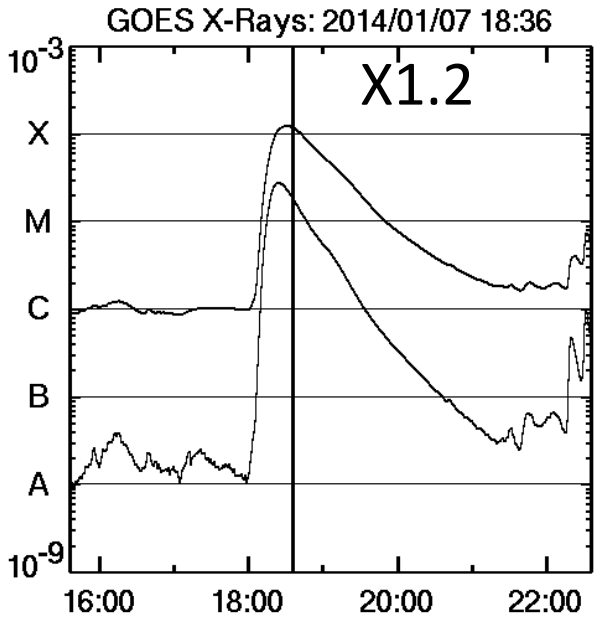


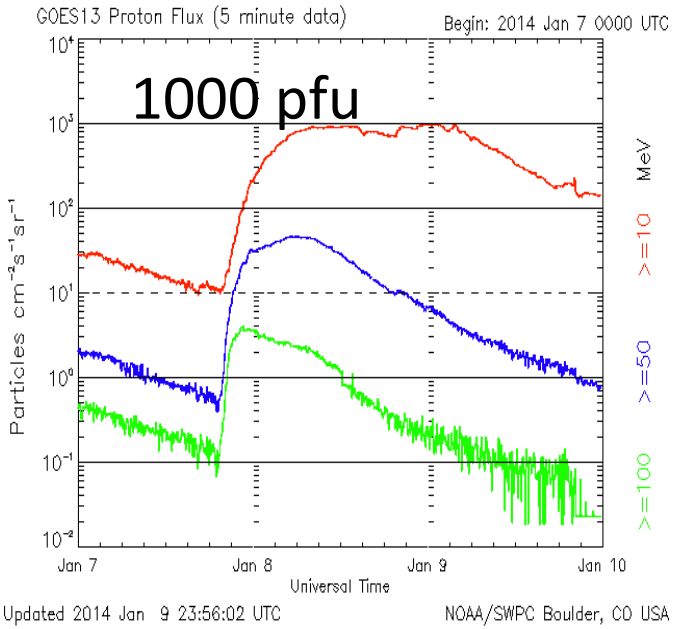


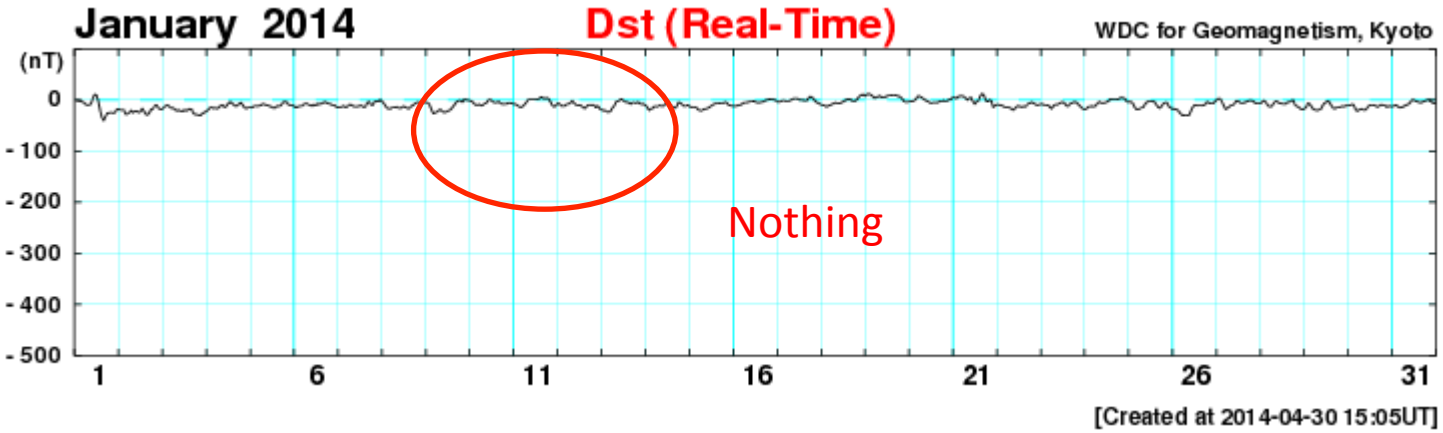

# PE-CME offset

Low prominence eruption rate
North-south asymmetry (more events to the north)
Offset period is also extended, longer in the south

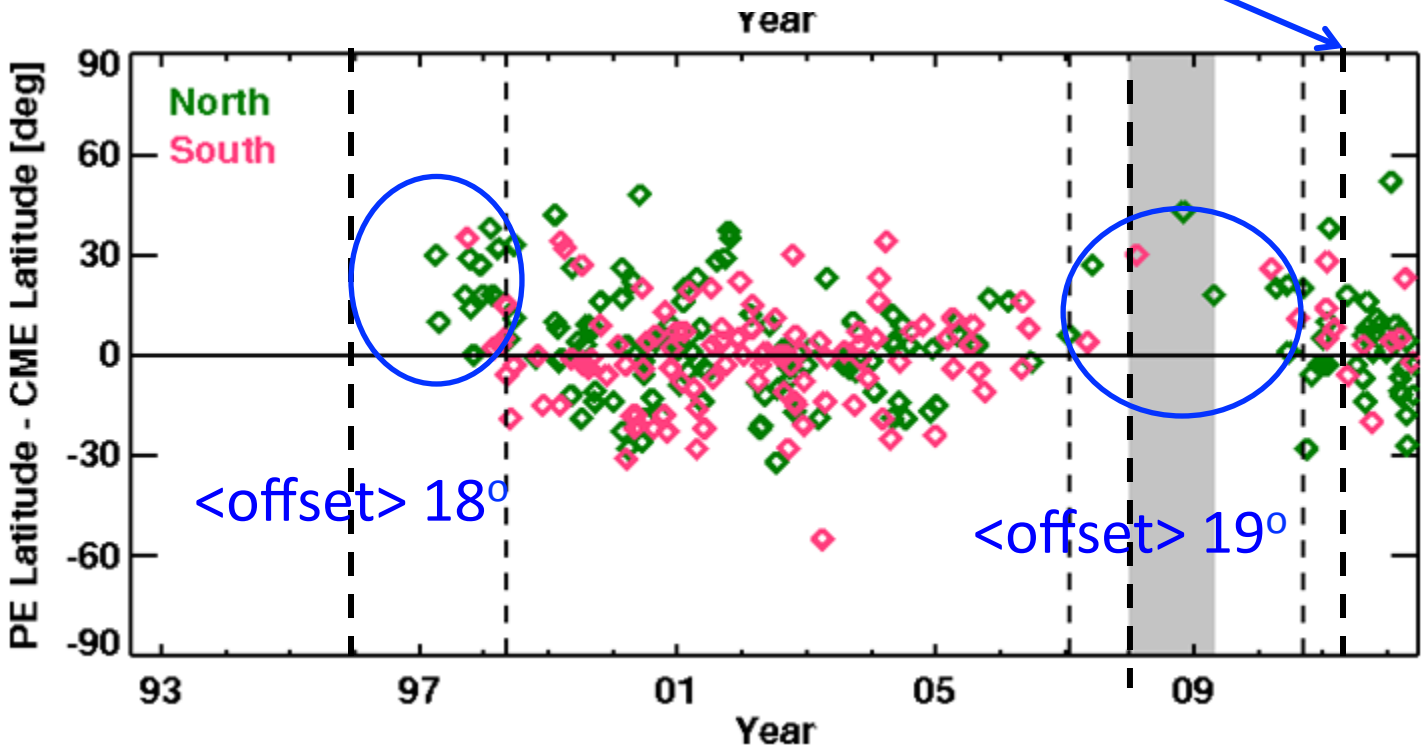

# Consequence of Equatorward Deflection: More Magnetic Clouds during Solar Minimum

| Phase | Lat (N) | Lat (S) | CMD |
|---|---|---|---|
| Rise: | 25.6 | -24.2 | 5.3 |
| Max: | 12.6 | -20.0 | 9.7 |
| Decl: | 8.2 | -13.8 | 1.8 |
| All: | 14.5 | -19.7 | 6.1 |

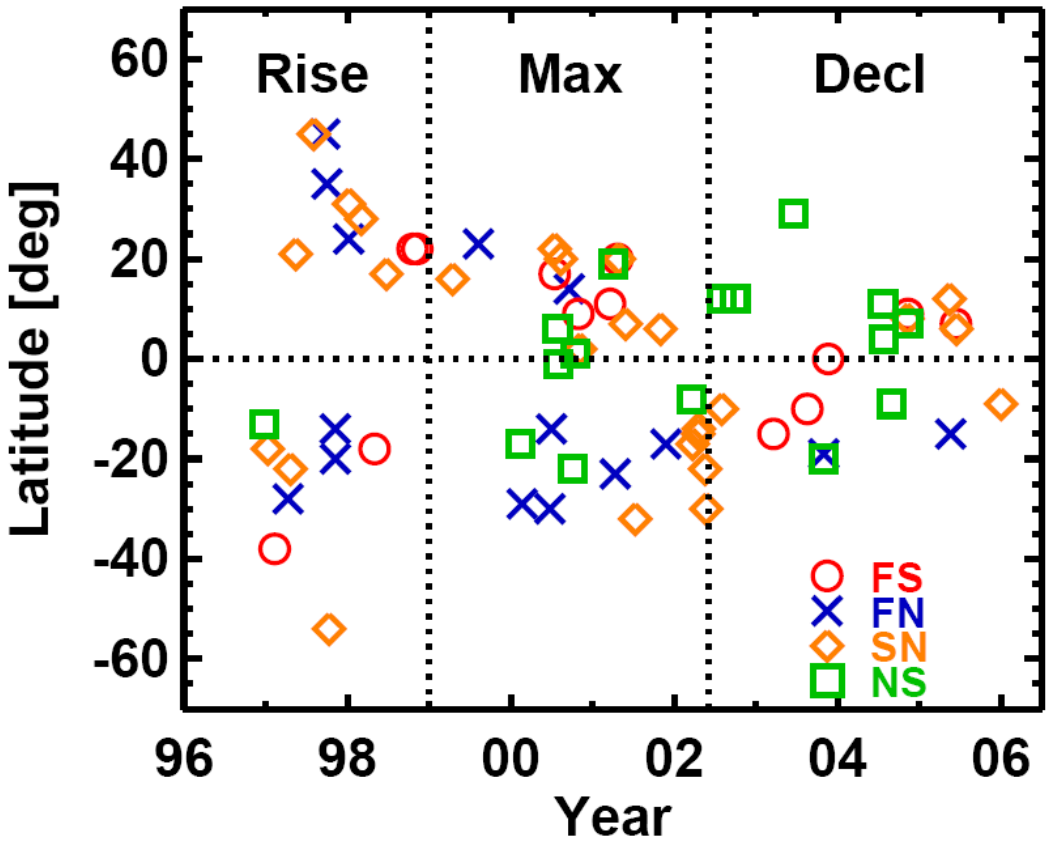


Outstanding question:
Is the deflection due to coronal-hole open field or the global dipolar field?

Gopalswamy, 2006
SSRv

# Why driverless shocks from disk center?

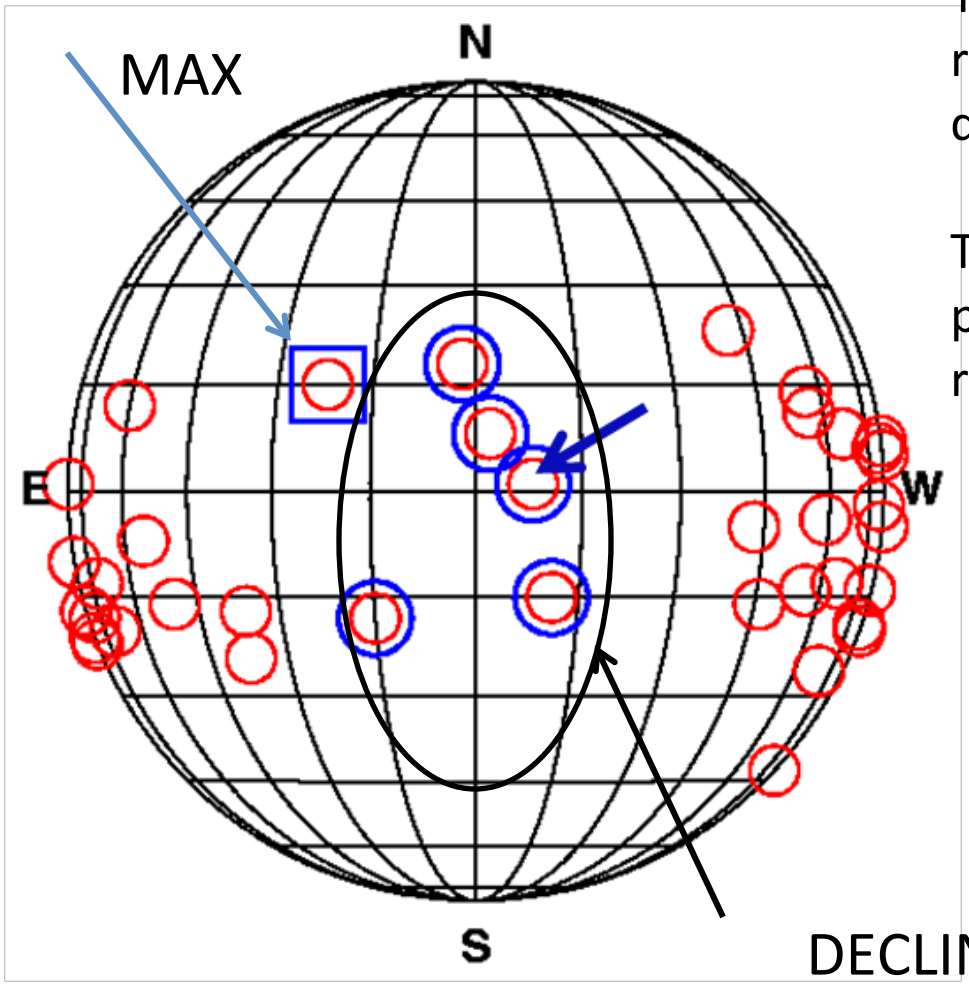


Gopalswamy et al. 2009, JGR

The limb sources are normal (geometrical reason), but the
disk-center sources are anomalous

The anomaly seems to be due to the presence of coronal holes near the source region

# Coronal Hole Influence Parameter

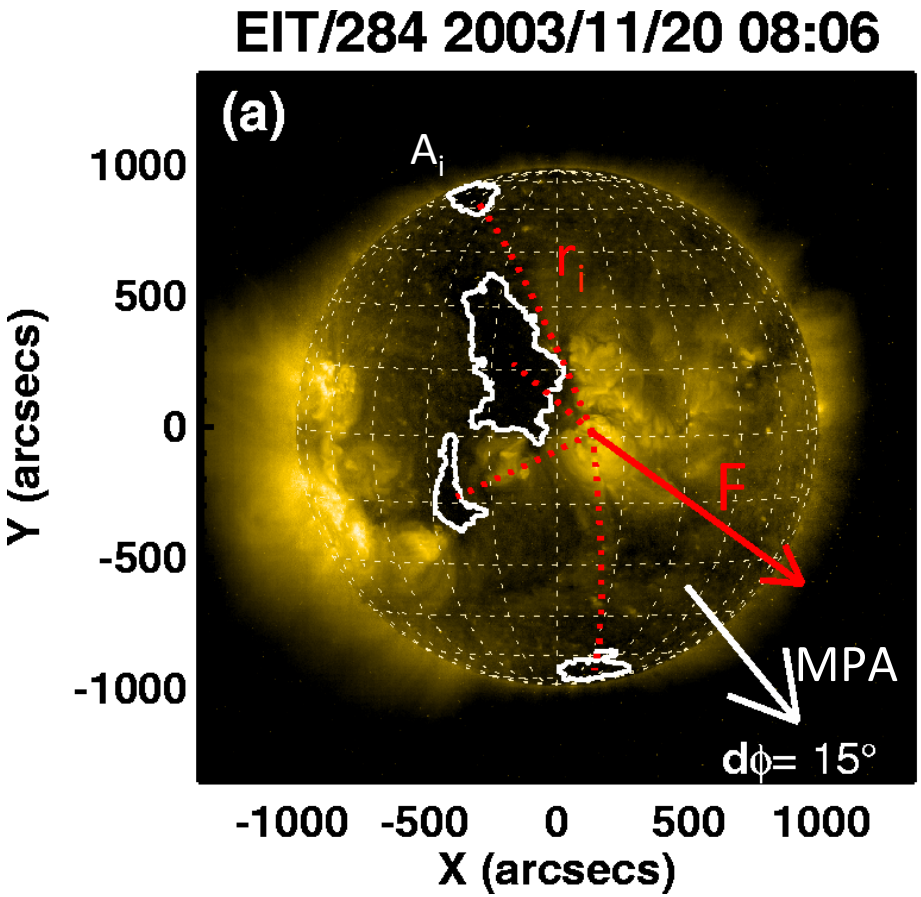


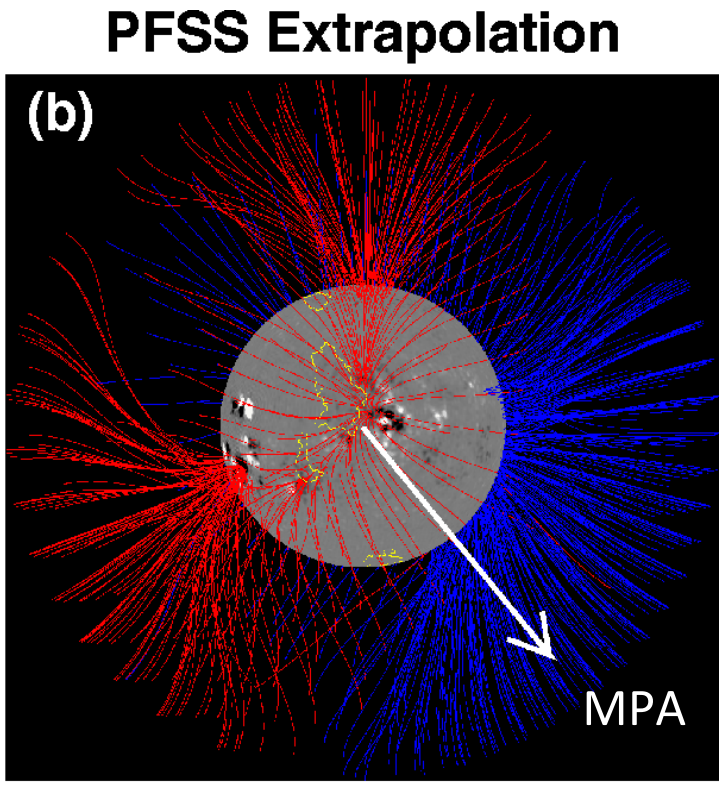


(Open field lines only shown)

$F = \sum f_i \qquad f_i = A_i \langle B_i \rangle / r_i^2$

F = 14 G pointed along the PA (FPA) of 234°.

CME position angle (MPA) aligns with the direction of influence FPA

Gopalswamy et al., 2009 JGR

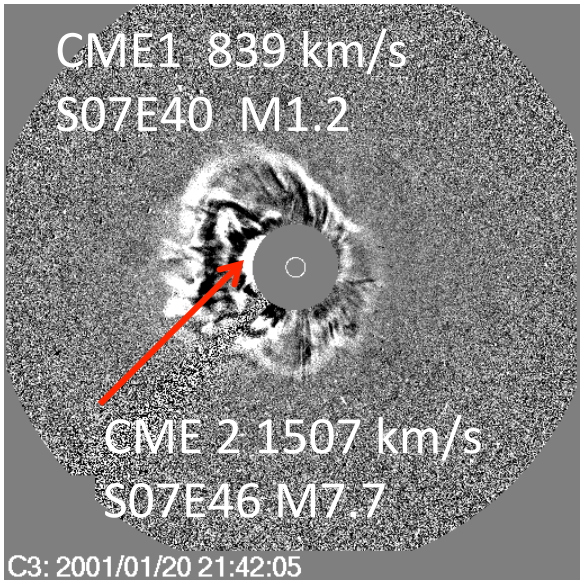


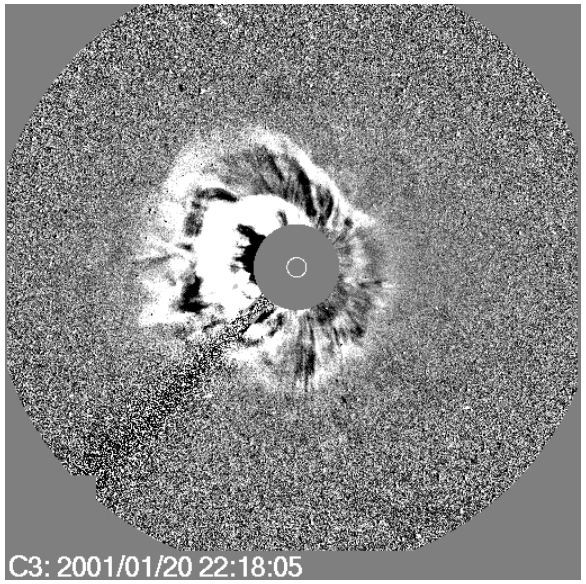


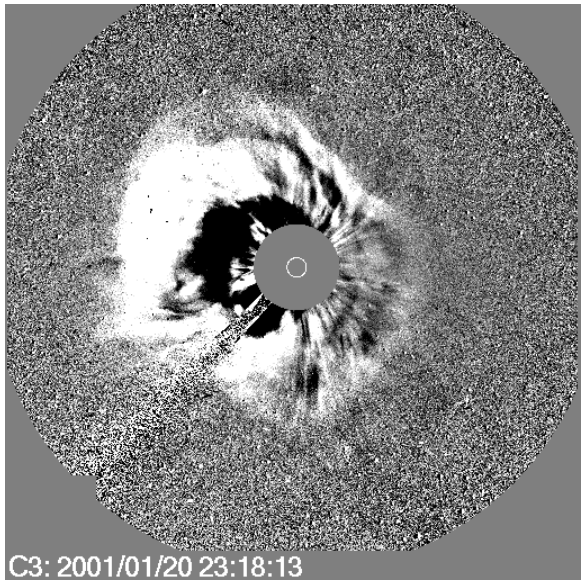


# CME Cannibalism

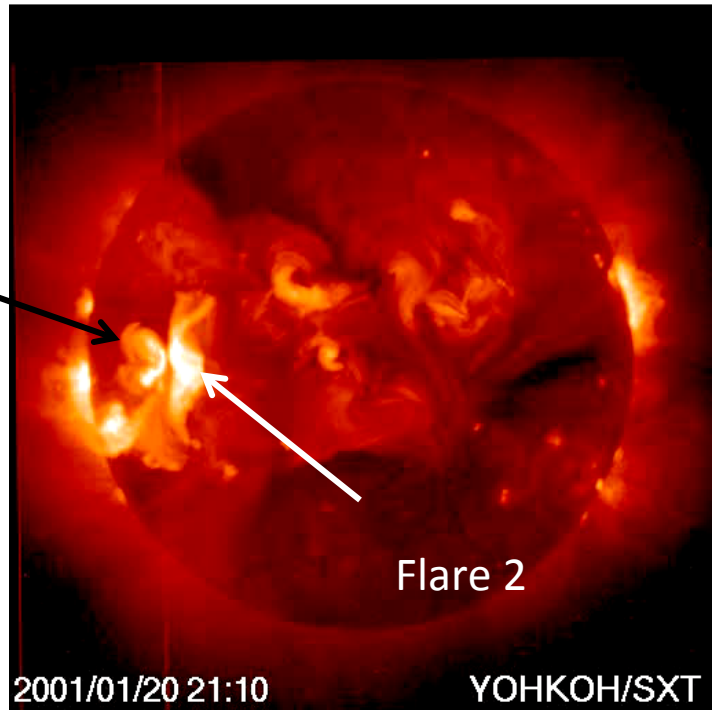


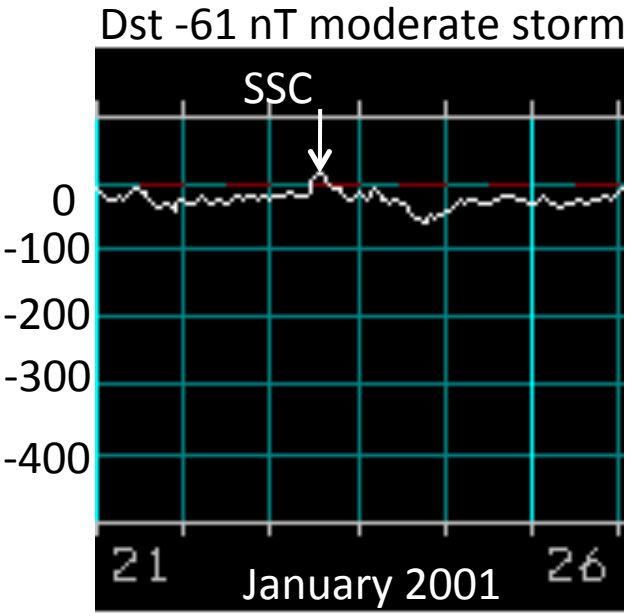


Two CMEs from the same region AR

Single shock

# A Generic Eruption: Summarizes most of the observations discussed

Flare Reconnection leads to CME flux rope formation

CME drives Shock

Shock accelerates electrons and protons

Flare: impulsive SEP events,
Much smaller, high charge states
CME may or may not accompany

The relative contribution from Flare & CME in a given event under debate

flux rope formation by flare reconnection is the injection of hot plasma – high charge states at 1 AU

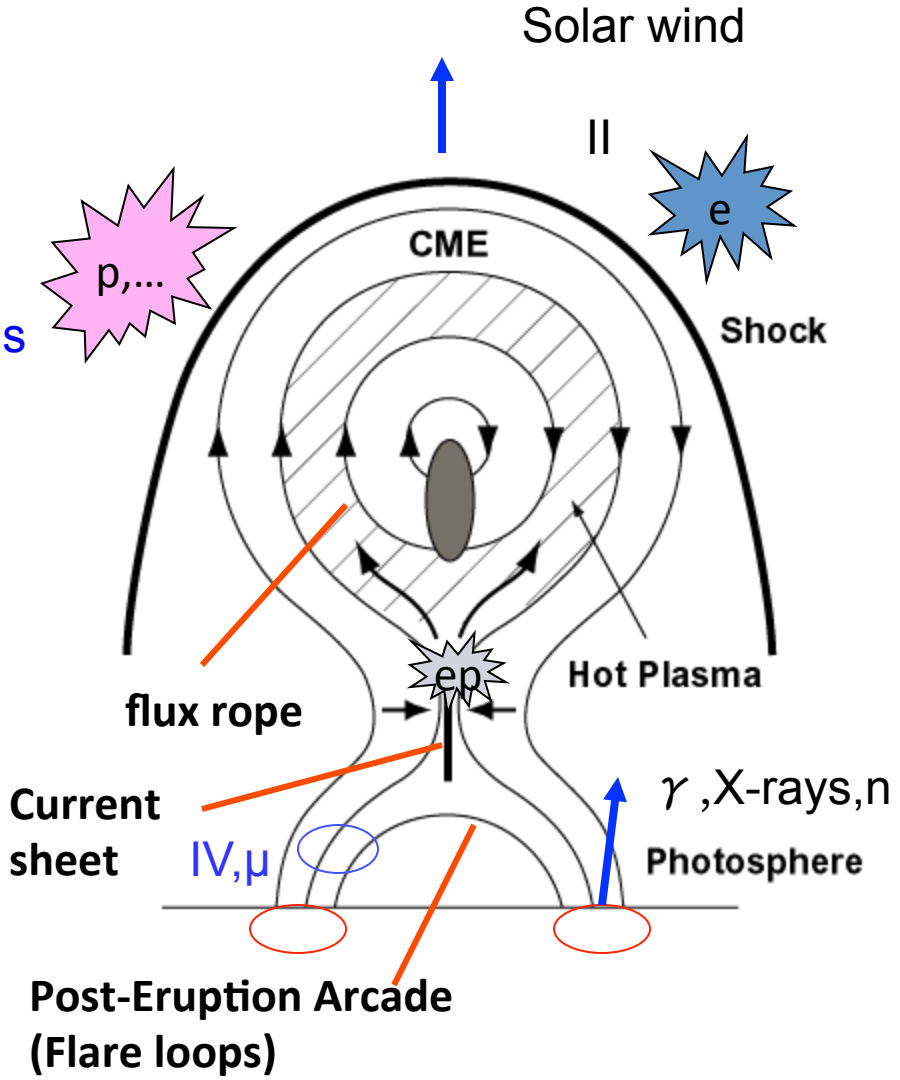

# Summary

- Solar Magnetism and its variability is ultimately responsible for space weather via flares and CMEs
- Flares and CMEs are from closed magnetic regions on the Sun (i.e., bipolar or multipolar) and are part of the same energy release
- Flares cause sudden ionospheric disturbances
- CMEs cause wide-ranging space weather effects: SEPs, geomagnetic storms and the related effects

# References


- Boischot, A., 1957, Comptes Rendus Acad. Sci., Paris, 244, 1326
- Burlaga, L., Sittler, E., Mariani, F., & Schwenn, R., 1981, J. Geophys. Res., 86, 6673
- Forbes, T., 2000, J. Geophys. Res., 105, 23153
- Gold, T, 1962
- Gopalswamy, N., Lara, A., Yashiro, S., Nunes, S., & Howard, R. A., 2003, Solar variability as an input to the Earth's environment, Ed.: A. Wilson. ESA SP-535, Noordwijk: ESA Publications Division, p. 403
- Gosling, J. T., 1993, J. Geophys. Res., 98, 18937
- Sonett et al., 1964, Phys. Rev. Lett

# CMEs and GCR Modulation

Newkirk, Hundhausen, Pizzo, 1981

CMEs play a role in the modulation of galactic cosmic rays (GCRs). Solar cycle dependent cosmic ray modulation can be explained by the presence of CME-related magnetic inhomogeneities in the heliosphere.

Pre-SOHO:
CME rate was not high enough
Min to max variation was too low

# CMEs and GCR Modulation

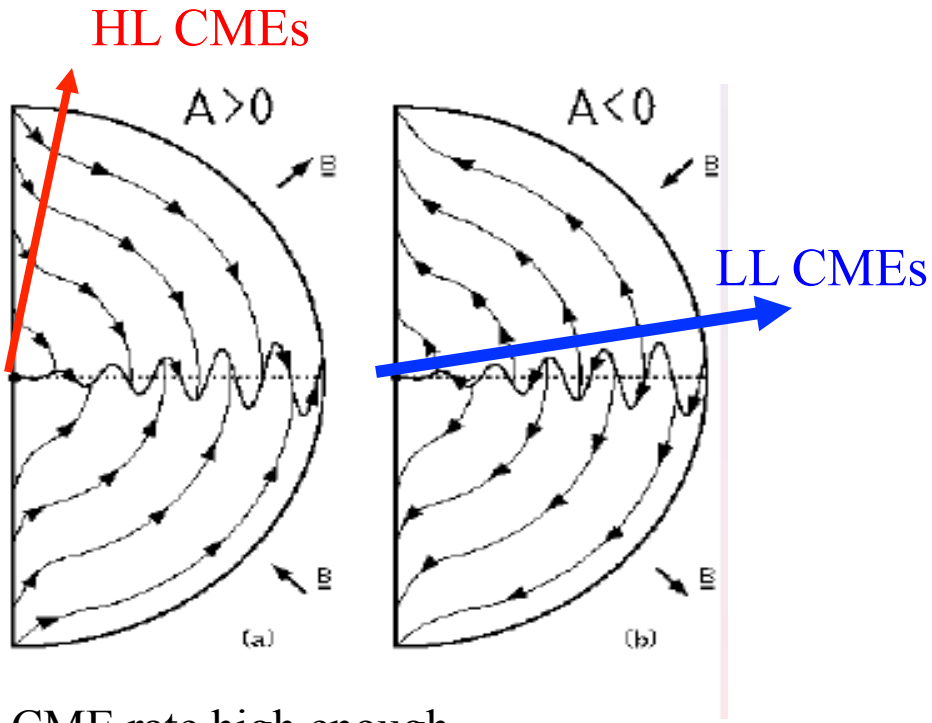


Gopalswamy, 2004; Lara et al. 2005

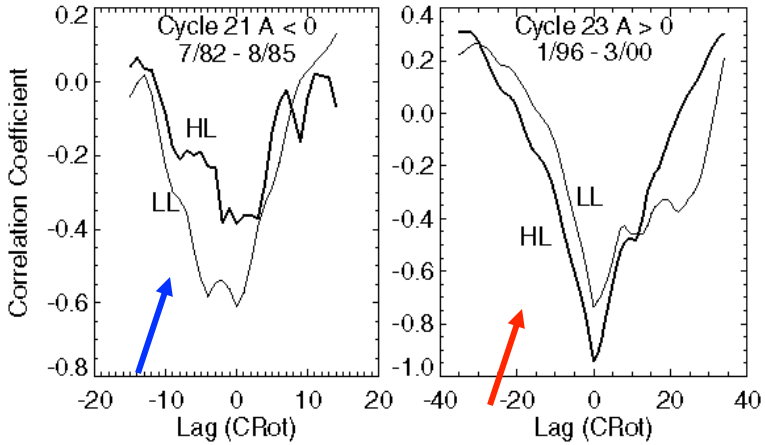


CME rate high enough
Min to max variation high enough
Contribution from High-latitude CMEs
GMIRs did not form during the Oct-Nov 03 storms (Richardson et al. 2005)
See also Cliver et al. 2003
Gazis et al. 2006

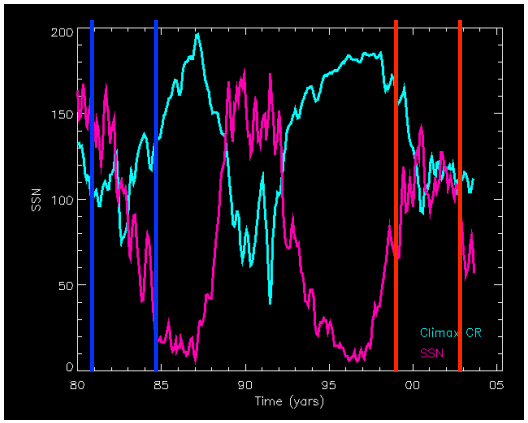

# High Latitude CMEs

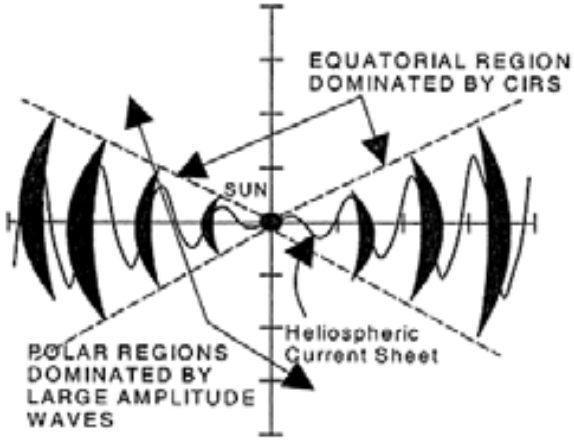


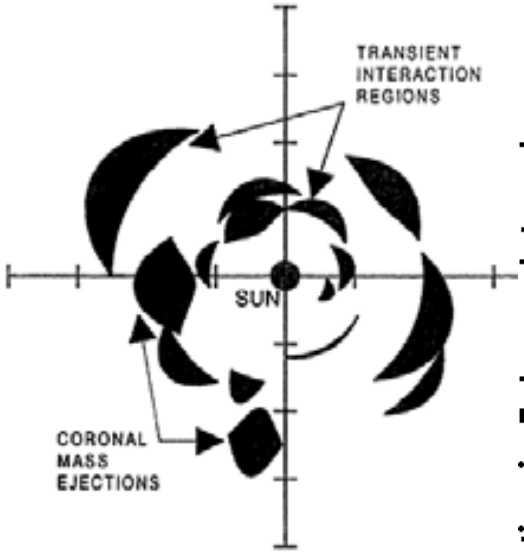


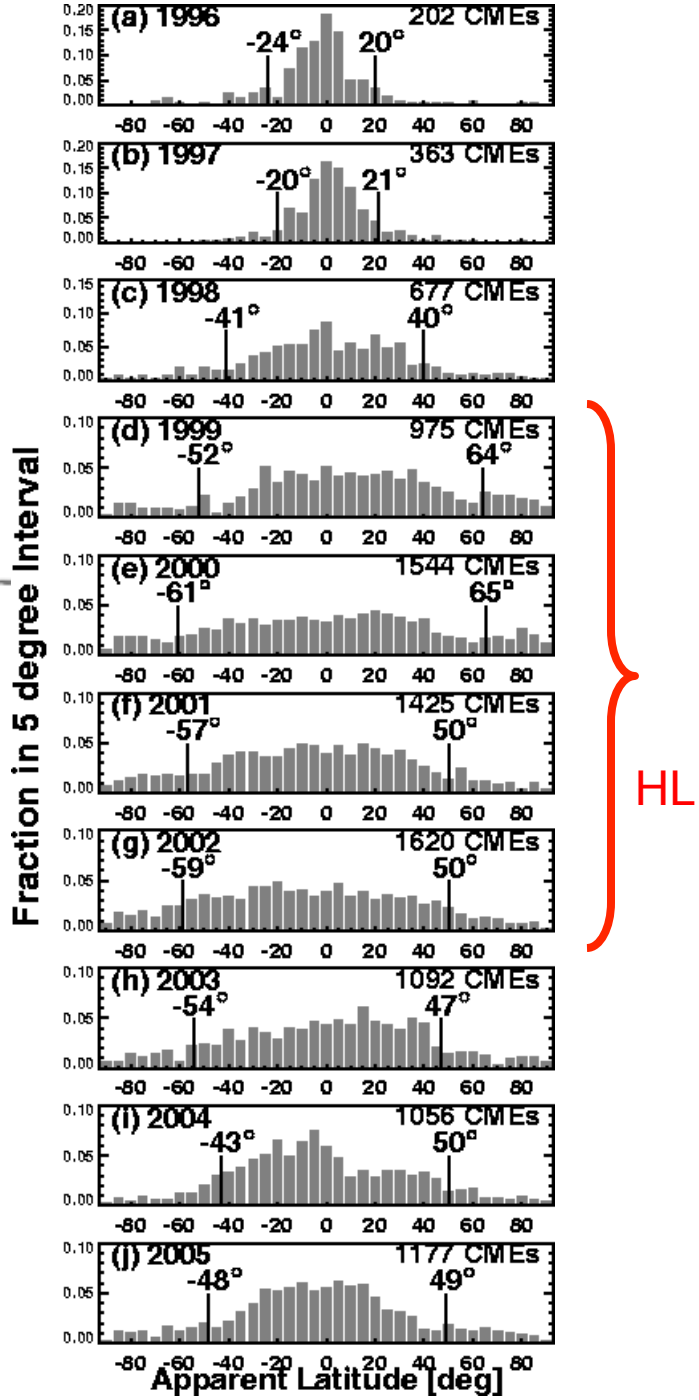


Balogh 2002

Forsyth et al. 2006
Gazis et al.. 2006

Extended from Yashiro et al. 2004

# Difference Image

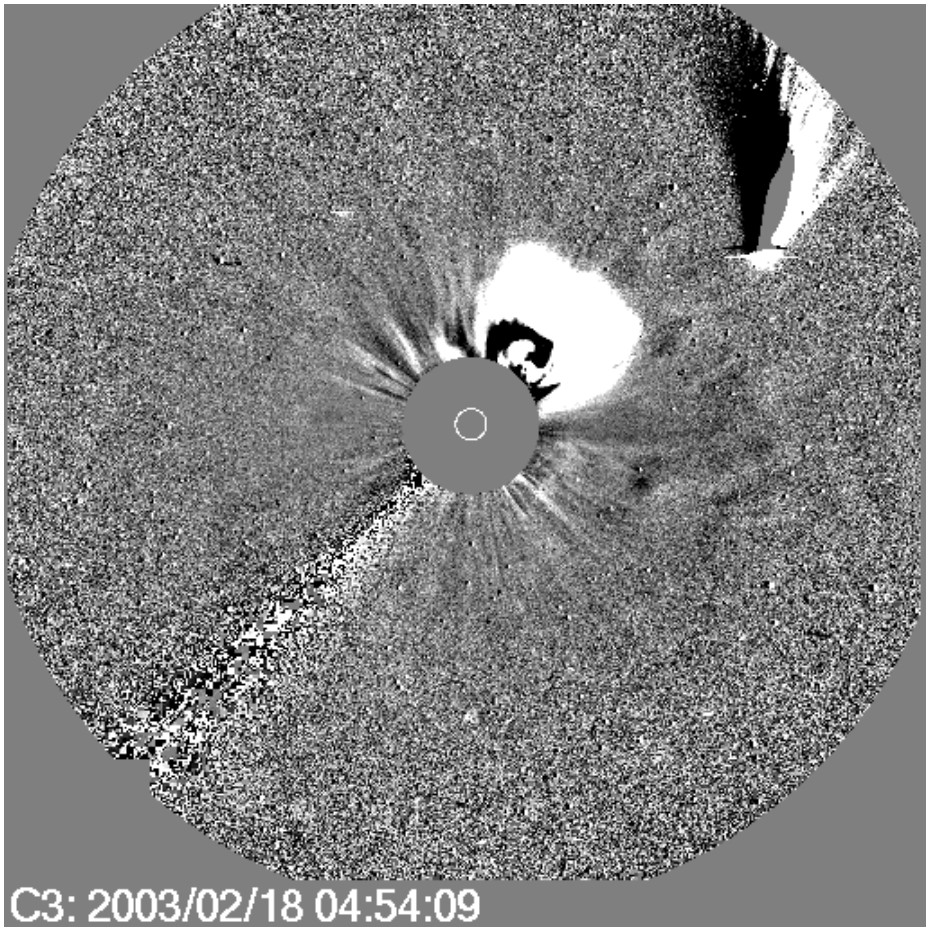


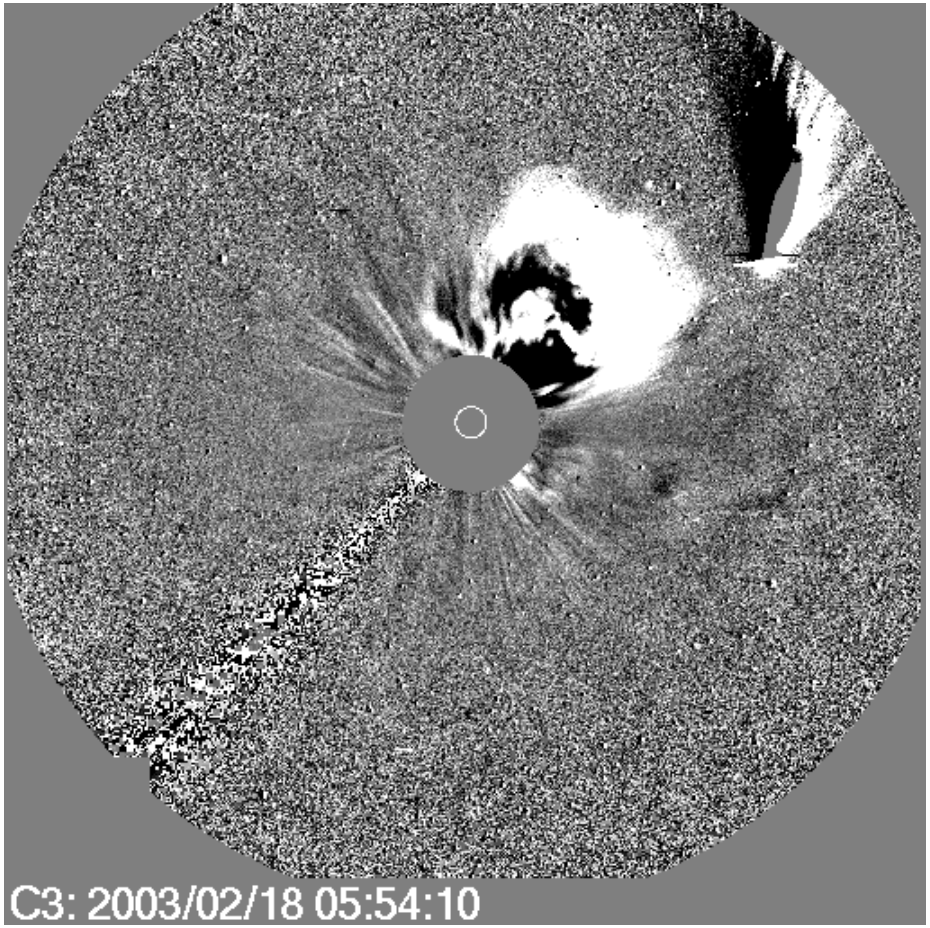

# Magnetic Configuration

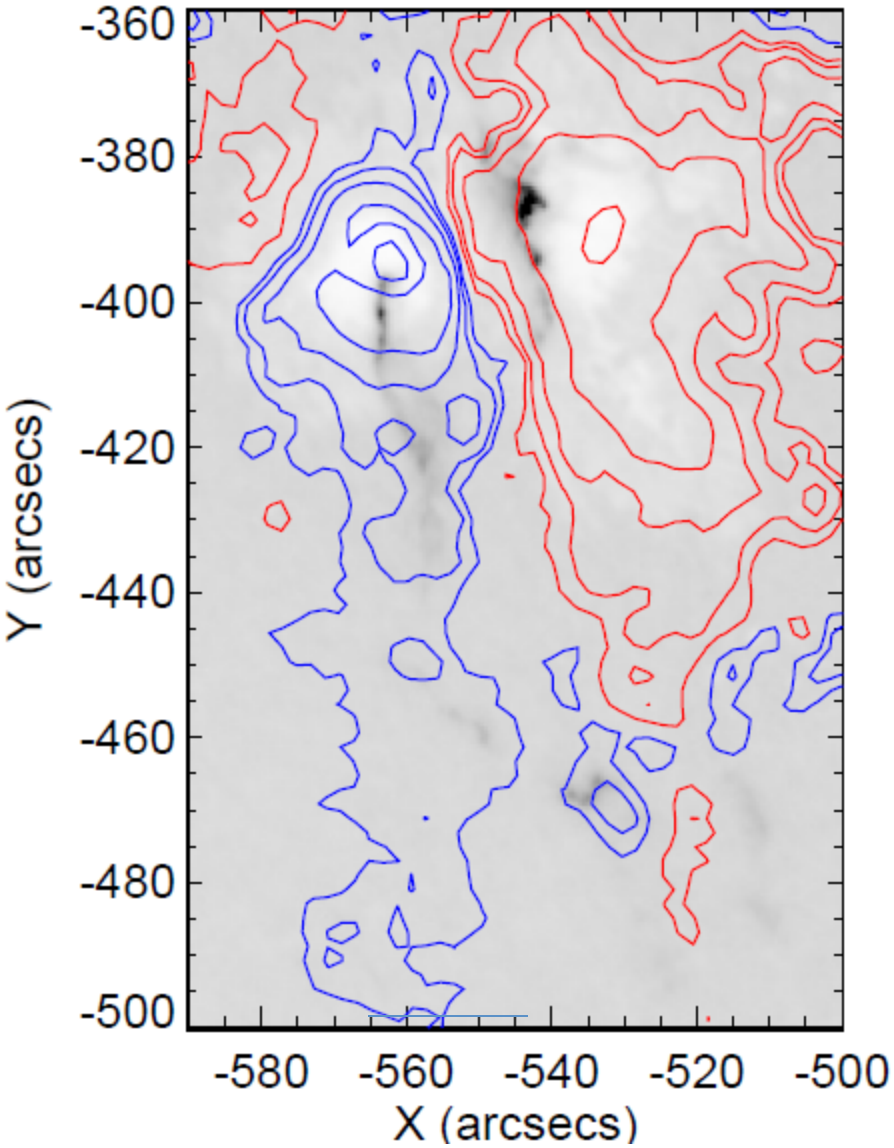


Two-ribbon structure
One ribbon on each polarity
ribbon separation ~20” (1” = 720 km)
Ribbon length ~70”

Similar flare structure observed in chromospheric and coronal layers.

This is in fact due to the energy release in the corona, which is carried to lower atmospheric layers by nonthermal particles

# Time Marks of X-ray Flares

- Start: the first minute, in a sequence of 4 minutes, of steep monotonic increase in 0.1-0.8 nm (1-8 A) X-ray flux
- Max: the minute of the peak x-ray flux
- End: the time when the flux level decays to a point halfway between the maximum flux and the pre-flare background level.
- Details: http://www.swpc.noaa.gov/ftpdir/indices/events/README

# H-alpha Flares and Microwave Flares: Scale comparison

| Flare Area msh (Square degree) | faint | normal | brilliant | radio flux at 5 GHz (sfu) |
|---|---|---|---|---|
| <100 (2.06) | SF | SN | SB | <5 |
| 100-250 (2.06-5.15) | 1F | 1N | 1B | 30-1300 |
| 250-600 (5.15-12.4) | 2F | 2N | 2B | 1300-23000 |
| 600-1200 (12.4-24.7) | 3F | 3N | 3B | 23000 - 30000 |
| >1200 (>24.7) | 4F | 4N | 4B | >30000 |

msh = millionths of solar hemisphere

Imp = log S – 0.5; S radio flux in sfu ($10^{-22}$ $Wm^{-2}Hz^{-1}$); Imp = H-alpha area

Big H-alpha flares also produce large microwave bursts

Both emissions are related to particles accelerated during the flare

# CME-Flare Relationship

- Part of the same process: CSHKP model
- Flares (even X-class) without CMEs, but no CME without flare (if you count weak arcades)
- Eruptive & non-eruptive flares (Munro et al. 1979): good classification
- Prominence eruptions vs. flares: not a good classification
- Active  region and non-AR CMEs?

# Flares with & without CMEs

Yashiro et al. 2006 ApJL

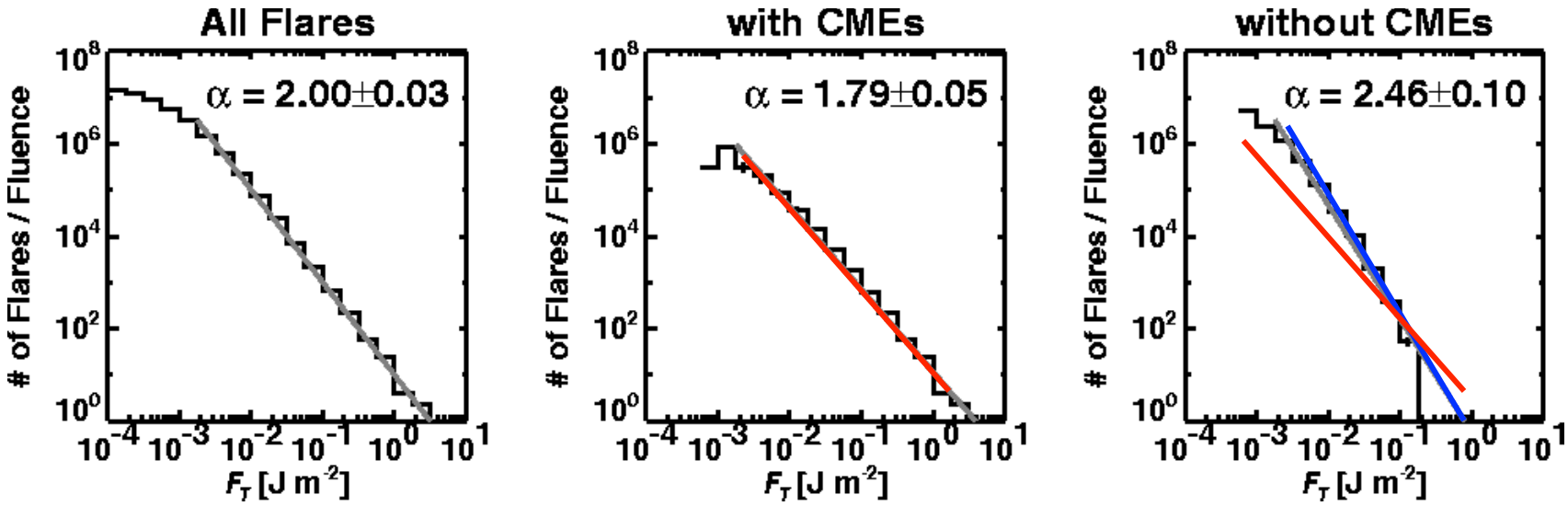


- Flare number (N) distributions obey a power-law of the form: $dN/dX \sim X^{-\alpha}$ where X is a flare parameter (e.g. peak SXR flux)
- $P \sim \int X\, dN/dX \sim X^{-\alpha+2}$
- $\alpha > 2$ → Small X contribute to P (Hudson et al. 1991)
- The larger power-law index for flares without CMEs supports the possibility that nanoflares contribute to coronal heating.
- Consistent with the fact that flares without CMEs are hotter (Kay et al. 2003)

Flare Temp: <Tmax> [MK]: 16.4 (all) 18.7 (w/o CMEs) 11.4 (with CMEs)

# CMEs and Flares: Energy Comparison

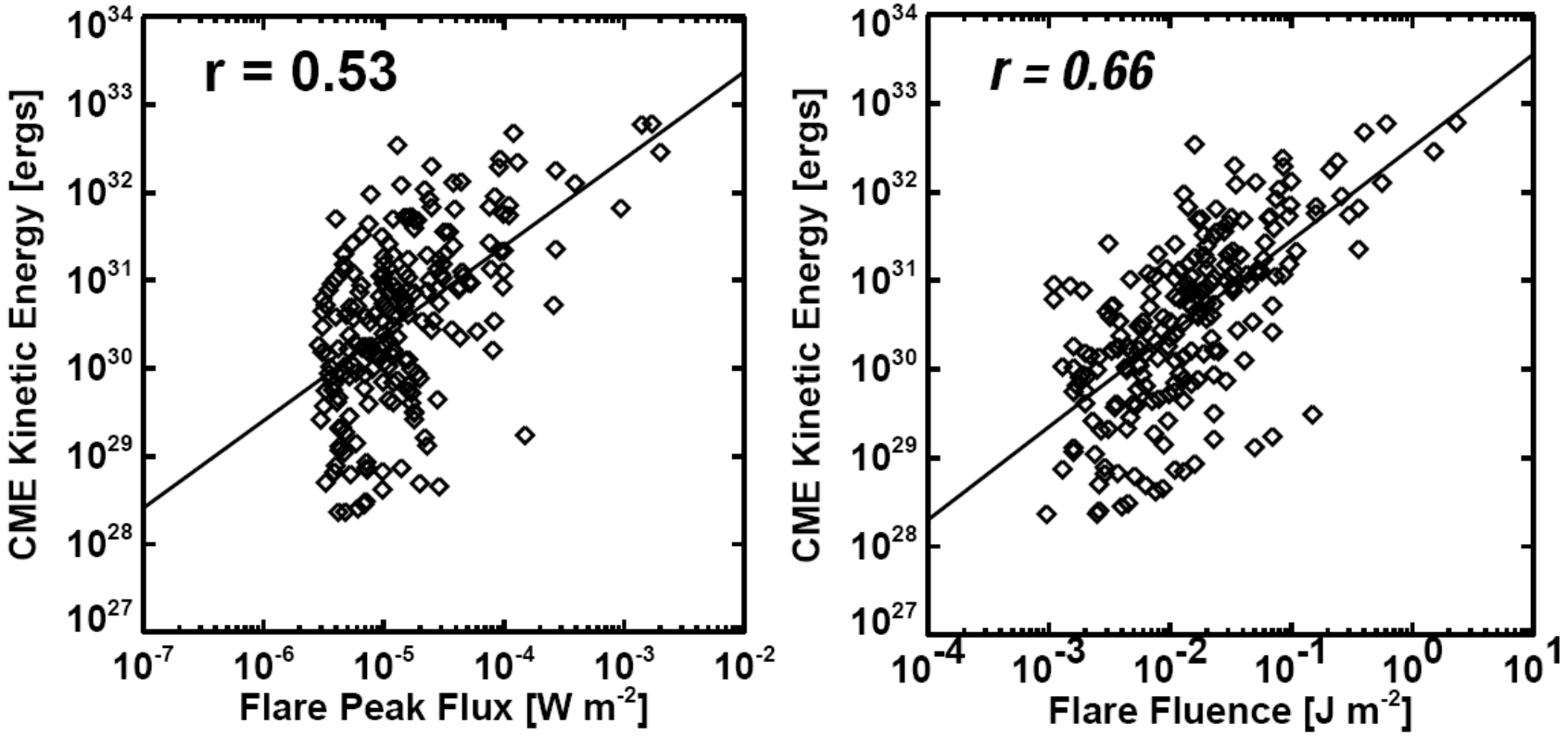


CME kinetic energy and soft X-ray flux/fluence are reasonably correlated showing that they share the same energy release

# Exercises

- Read Ping Images
- Track leading edge of two CMEs
- plot height vs. time
- Fit linear and quadratic fits
- determine speed and acceleration
- Determine the CME width

# Read .png images

- import matplotlib.pyplot
- img1=plt.imread('20011203_120605_lasc2rdf.png')
- ….
- img5=img1=plt.imread('20011203_135415_lasc2rdf.png')
- plt.imshow(img1) # shows image
- use curser to identify the leading edge
- Repeat for all images
- create a data base (h,t)
- plot them
- compare with the given solution
- Compute CME widths using law of cosines

# 2001/12/03 CME

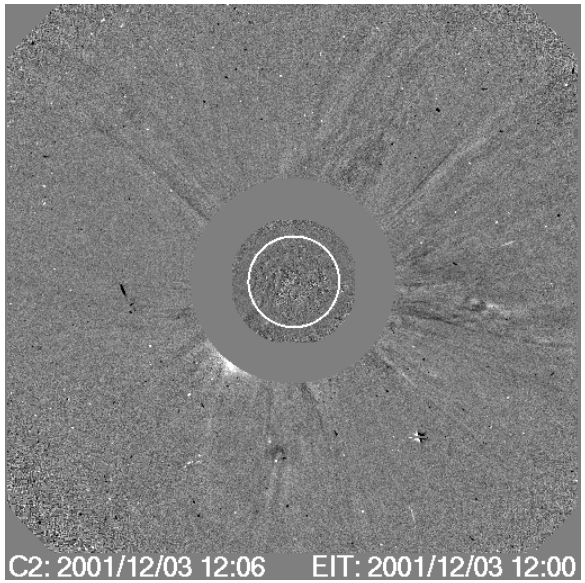


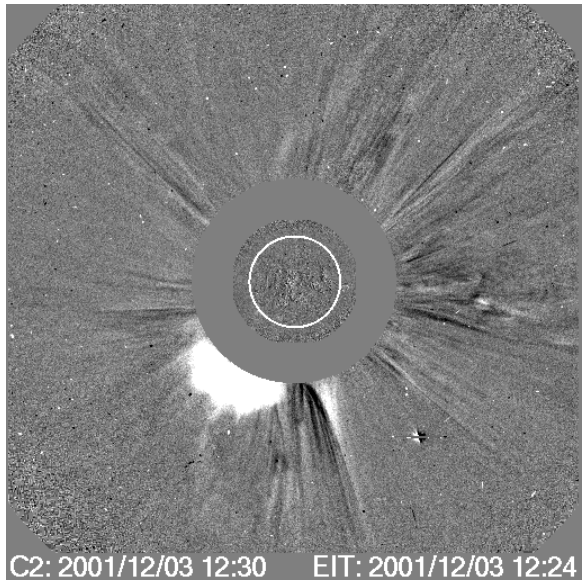


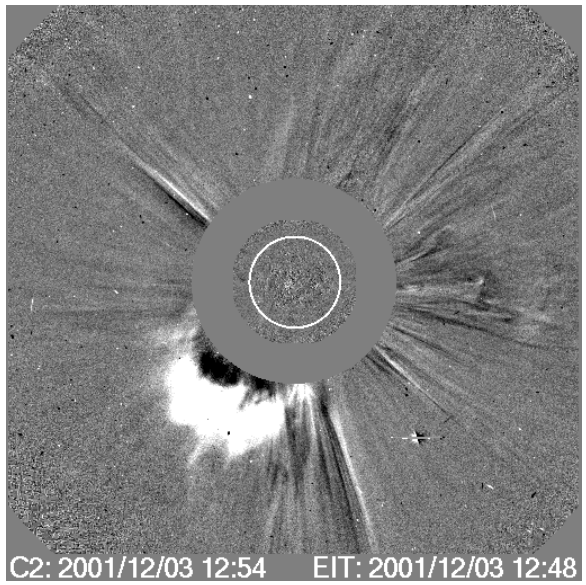


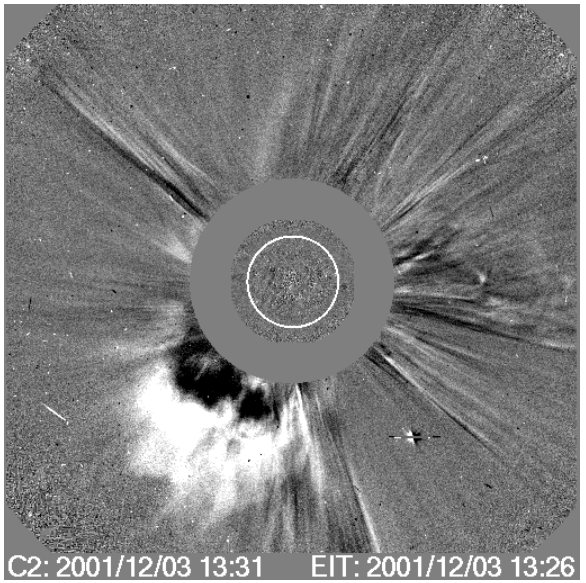


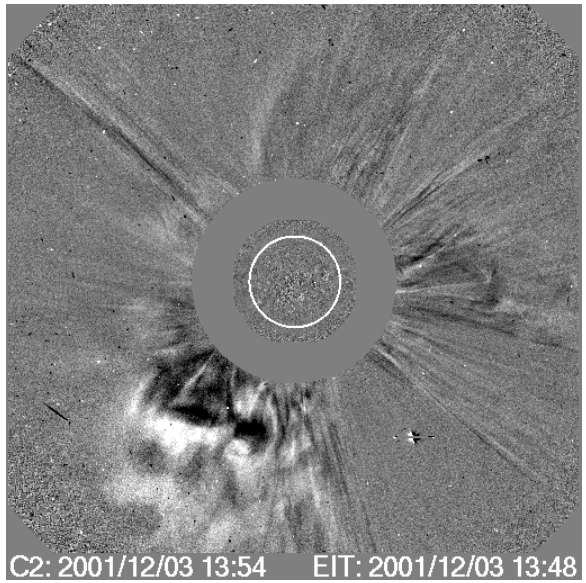

# Plots

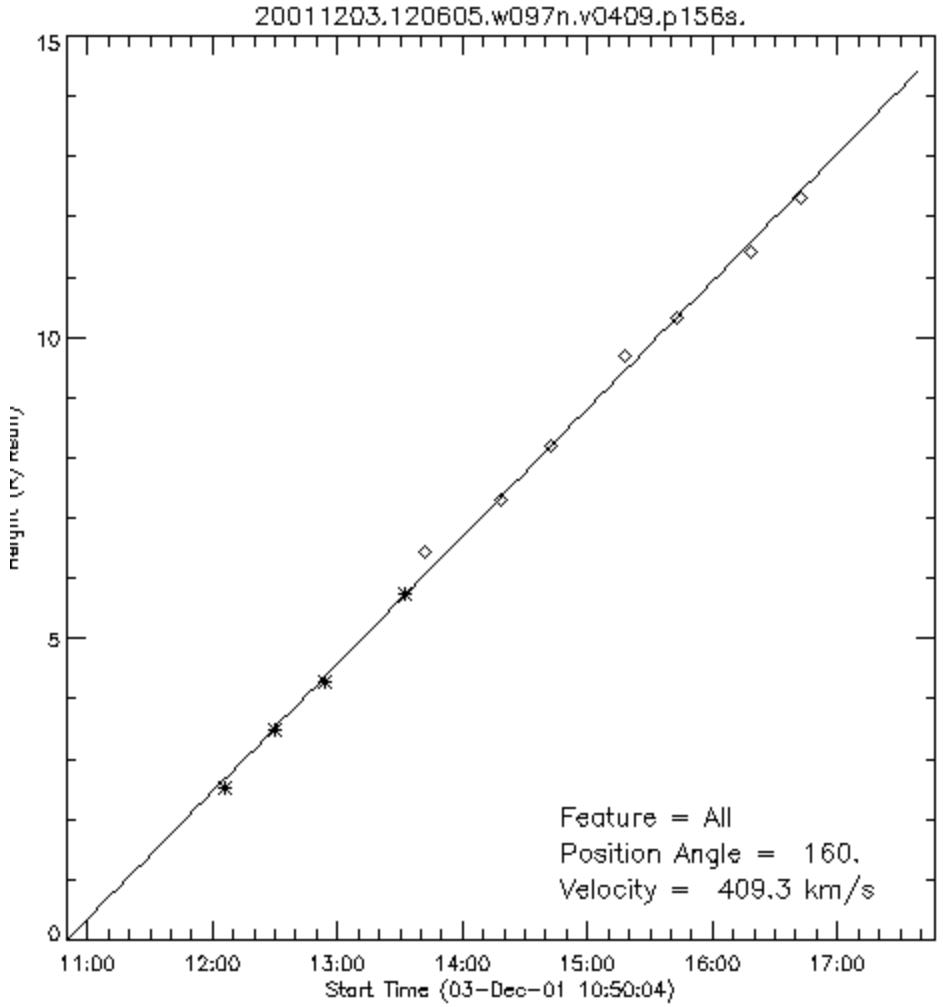
20011203.120605.w097n.v0409.p156s.
Height (R/Rsun)
Start Time (03-Dec-01 10:50:04)
Feature = All
Position Angle = 160.
Velocity = 409.3 km/s

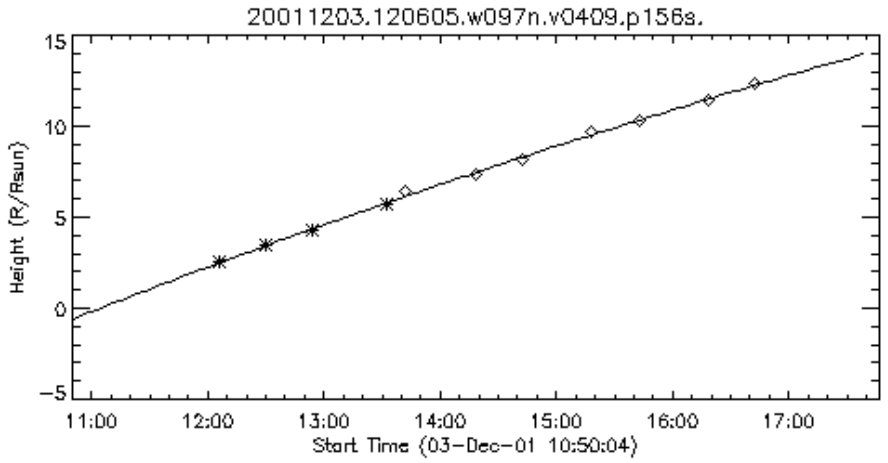
20011203.120605.w097n.v0409.p156s.
Height (R/Rsun)
Start Time (03-Dec-01 10:50:04)

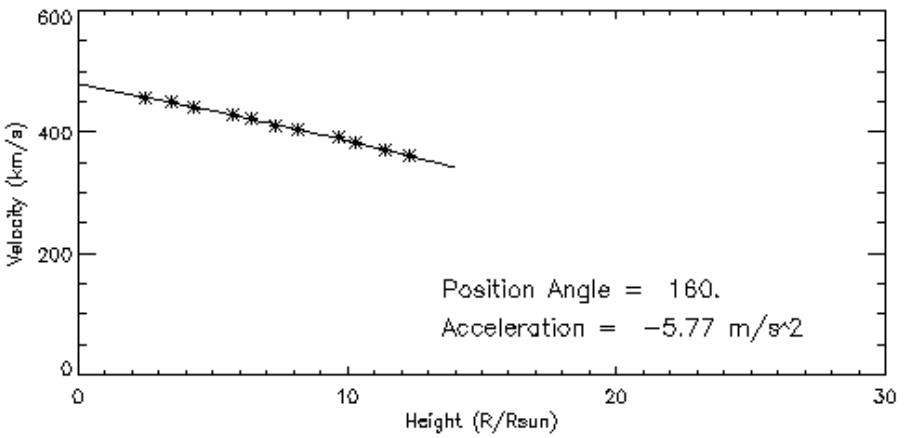
Velocity (km/s)
Height (R/Rsun)
Position Angle = 160.
Acceleration = -5.77 m/s^2

# 2001/12/20 CME

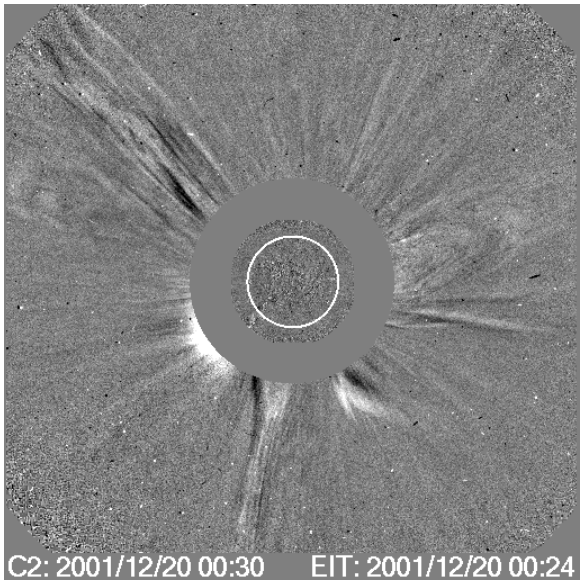


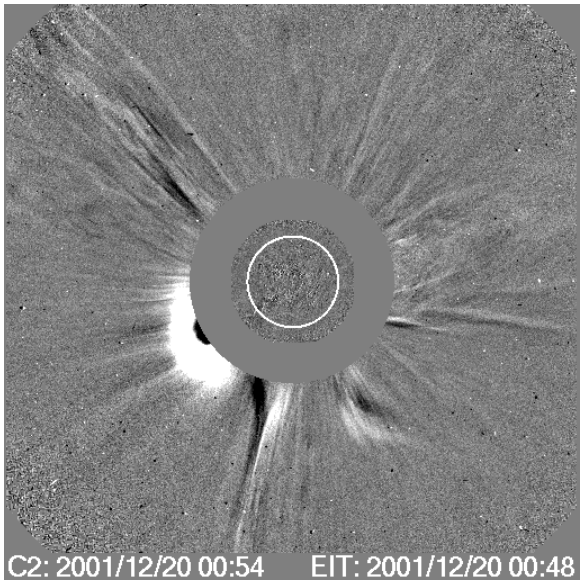


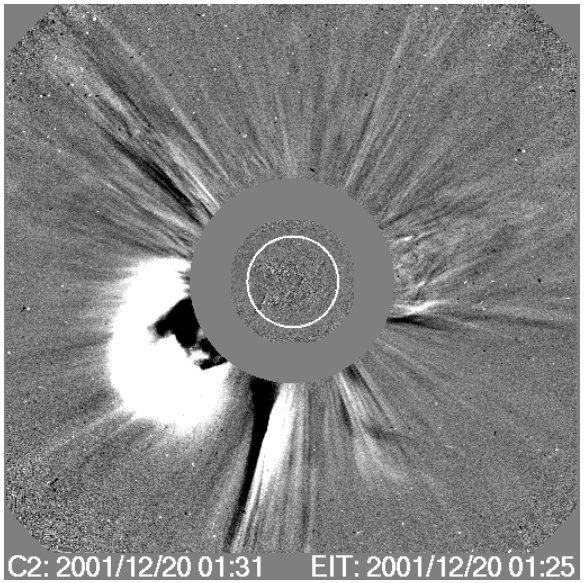


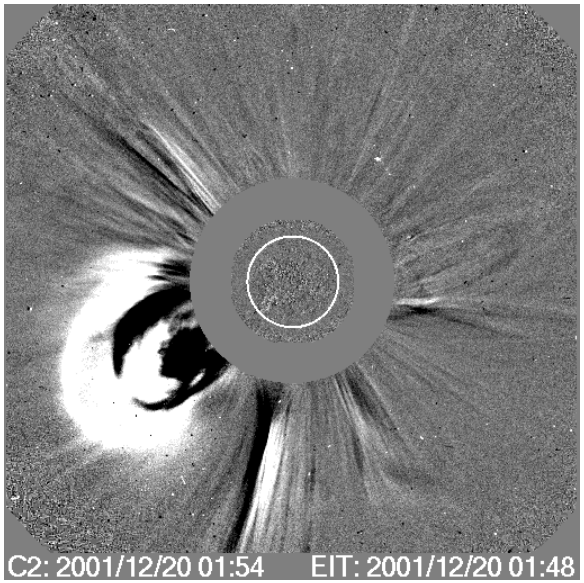


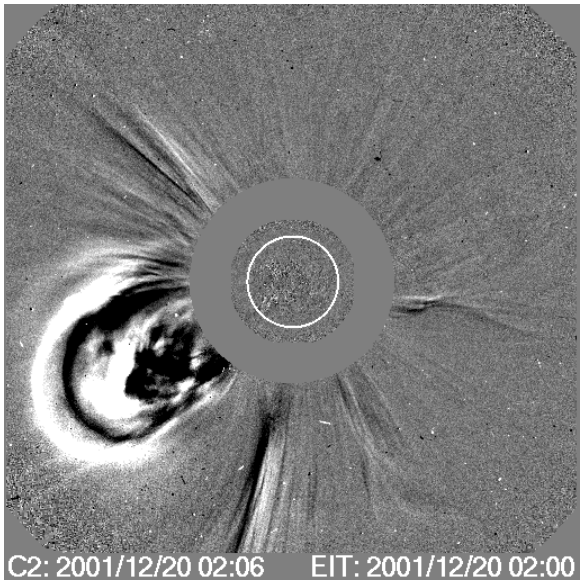

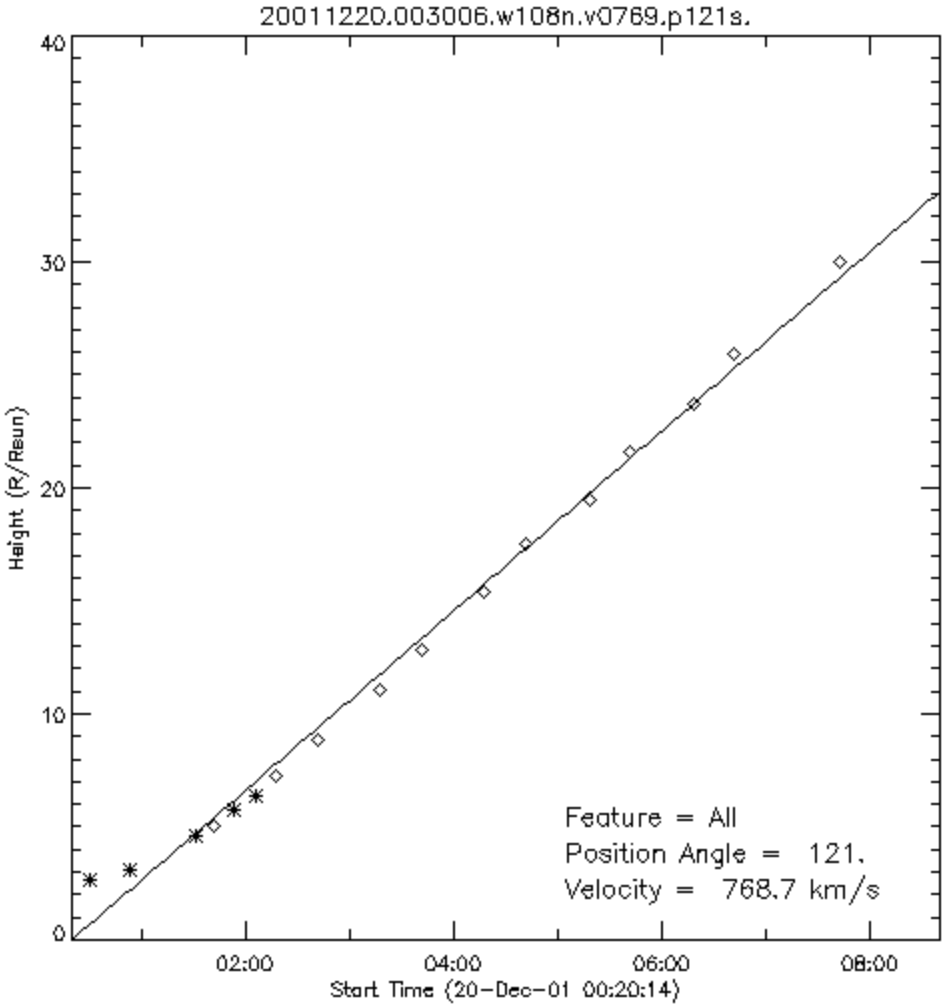
20011220.003006.w108n.v0769.p121s.
Height (R/Rsun)
Start Time (20-Dec-01 00:20:14)
Feature = All
Position Angle = 121.
Velocity = 768.7 km/s

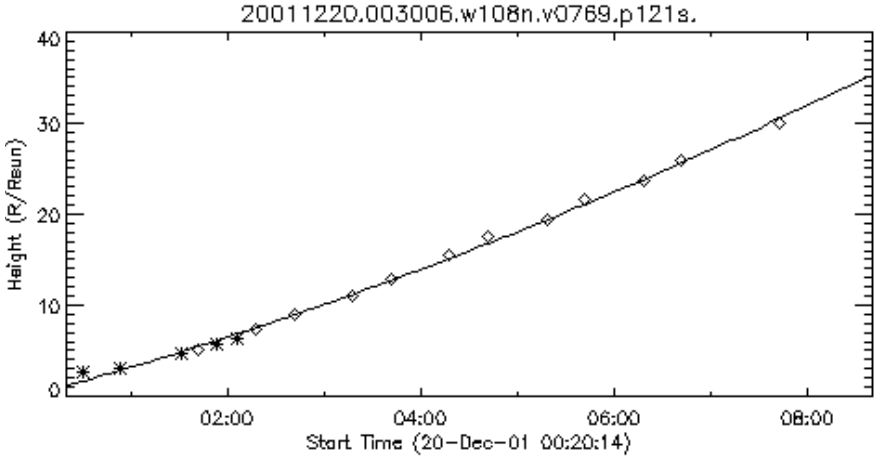
20011220.003006.w108n.v0769.p121s.
Height (R/Rsun)
Start Time (20-Dec-01 00:20:14)

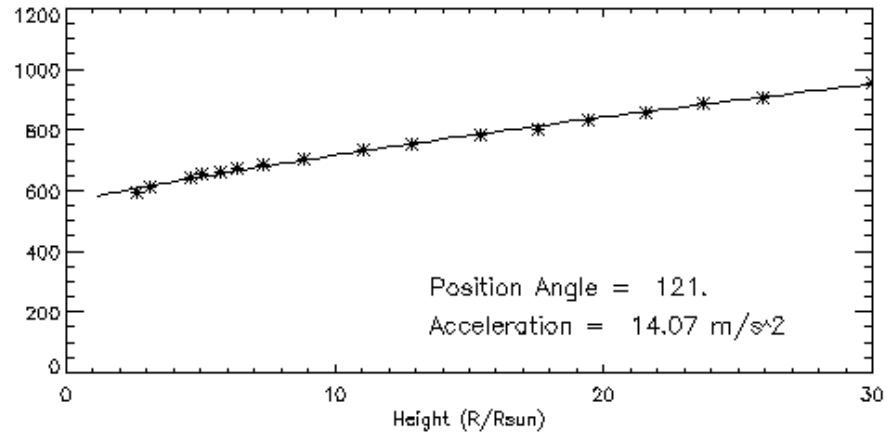
Position Angle = 121.
Acceleration = 14.07 m/s^2
Height (R/Rsun)

# CME Width

CME width

$$\cos(C) = [a^2 + b^2 - c^2]/2ab$$

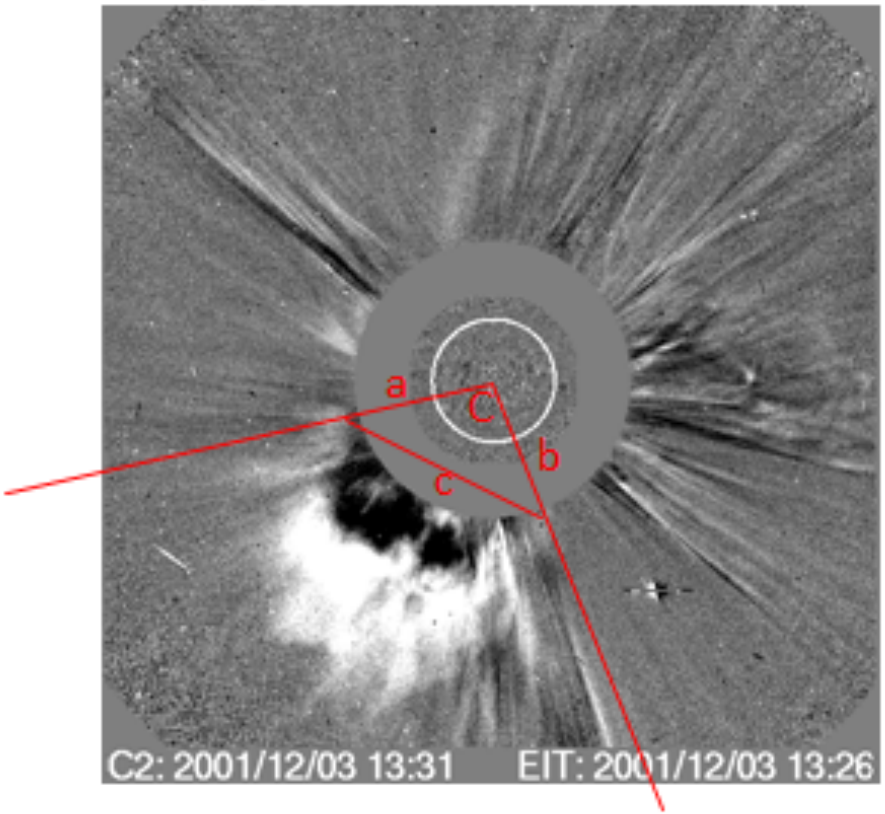


2001/12/03 CME
W = 97°

2001/12/20 CME
W = 108°